Ana Teresa Mataloto Rebocho

Bachelor Degree in Biochemistry

Development of films based on bacterial biopolyesters produced from apple pulp waste

Dissertation for the degree of Master in Biotechnology

Supervisor: Doctor Filomena Freitas, Senior Researcher, UCIBIO, FCT-UNL
Co-Supervisor: Doctor Luísa A. Neves, Assistant Researcher, LAQV, FCT-UNL

Jury
President: Professor Susana Filipe Barreiros
Examiner: Doctor Joana Oliveira Pais
Vogal: Doctor Maria Filomena Andrade de Freitas

FACULDADE DE CIÊNCIAS E TECNOLOGIA
UNIVERSIDADE NOVA DE LISBOA

September, 2018

Ana Teresa Mataloto Rebocho

Bachelor Degree in Biochemistry

Development of films based on bacterial biopolyesters produced from apple pulp waste

Dissertation for the degree of Master in Biotechnology

Supervisor: Doctor Filomena Freitas, Senior Researcher, UCIBIO, FCT-UNL
Co-Supervisor: Doctor Luísa A. Neves, Assistant Researcher, LAQV, FCT-UNL

Jury
President: Professor Susana Filipe Barreiros
Examiner: Doctor Joana Oliveira Pais
Vogal: Doctor Maria Filomena Andrade de Freitas

September, 2018

Development of films based on bacterial biopolyesters produced from apple pulp waste

Aos meus Pais

Agradecimentos

Gostaria de agradecer em primeiro lugar às minhas orientadoras, Filomena Freitas e Luísa Neves, por me terem recebido e dado a oportunidade de trabalhar nos seus laboratórios. Agradeço toda a paciência que tiveram comigo, todo o ensinamento, disponibilidade e conselhos, mas acima de tudo por acreditarem em mim.

Agradeço ao Dr. Vítor Alves, do Instituto Superior de Agronomia, por me ter recebido no seu laboratório e pela ajuda e esclarecimentos na realização dos testes mecânicos.

Não posso deixar de agradecer a todo o grupo BioEng e Laboratório de Processos de Membranas pela forma como me receberam, ensinaram e ajudaram, especialmente na parte experimental de todo o projeto. Um especial agradecimento, à Patrícia Freitas, João Pereira, João Morgado, Patrícia Reis, Diana Araújo, Sílvia Baptista, Inês Farinha e Inês Ferreira por me ensinarem todos os fantásticos truques que tornam a vida laboratorial muito mais fácil, pela paciência, conselhos e momentos de descontração que levo comigo!

Ao meu pai e à minha mãe, sem vocês, o vosso apoio e amor, nada disto seria possível. Muito obrigada por nunca me deixarem desistir dos meus sonhos e por estarem ao meu lado neste momento de enorme felicidade!

Não poderia deixar de agradecer à família pelo vosso apoio constante e palavras de incentivo!

E por último, seria impossível não agradecer aos meus amigos. Para aqueles que encontrei na FCT e que ao longo dos últimos anos trouxeram com eles alegria e amizade quando tudo parecia mais difícil. Um enorme obrigado à Ana Catarina Oliveira, Patrícia Serrano, Bruno Pereira e Marta Gomes. Para aqueles que a Universidade de Évora me deu, para os que estão a meu lado desde o início e que desde o primeiro dia estão lá para partilhar as dificuldades, as ajudas, mas acima de tudo a vossa amizade, um enorme obrigado à Ana Casquinha, Vítor Almodôvar, Letícia Fialho, Joana Silva, Juliana Neves, Isabel Calhau, Tiago Rodrigues, Anaïs Silva, João Letras e Vítor Peniche.

Esta vai para todos vocês!

Abstract

The first objective of this thesis was to use apple pulp waste, a leftover from the fruit processing industry, for the cultivation of *Pseudomonas citronellolis* NNRL B-2504, *Cupriavidus necator* DSM 428 and a co-culture using both strains, culminating on the production of medium-chain-length polyhydroxyalkanoates (mcl-PHAs), short-chain-length polyhydroxyalkanoates (scl-PHAs) and a natural biosynthesized blend, respectively. PHAs are biopolyesters with versatile material properties, applicable in several fields.

The soluble fraction of the apple pulp waste, rich in fructose, sucrose and glucose, was used for the batch bioreactor cultivation of *P. citronellolis* and *C. necator*. The first cultivation, *P. citronellolis*, reached a polymer content in the biomass of 30wt.% with a volumetric productivity of 0.61 g/L.day. The polymer was mainly composed of 3-hydroxydecanoate (68%) and 3-hydroxyoctanoate (22%), and had a molecular weight of 3.7×10^5 Da. It presented melting and thermal degradation temperatures of 53 and 296 °C, respectively, and a crystallinity degree of 15%. *C. necator* DSM 428 achieved a volumetric productivity of 1.59 g/L.day, reaching a polymer content 44 wt.% . The homopolymer, P(3HB) was obtained, with a molecular weight of 5.0×10^5 Da and a crystallinity degree of 43%. Moreover, the polymer had melting and thermal degradation temperatures of 179 and 293 °C, respectively. Finally, a third batch production using a co-culture was performed. The production presented a 34 wt.% of polymer content with a volumetric productivity of 0.96 g/L.day. The polymer produced was a physical mixture of mcl-PHA and P(3HB). These results demonstrated that apple pulp waste is a suitable feedstock for the production of different biopolymers with distinct physical-chemical properties.

The aim of the second part of this thesis was to prepare films based on the PHAs produced from apple pulp waste, followed by their characterization, both physical and chemical.

All films presented similar thermal, crystallinity and chemical features when compared to the neat polymer, which indicates that the procedure did not significantly impact on the polymers' characteristics. Gas permeation tests were performed for both oxygen and carbon dioxide. mcl-PHA films presented the best results for both O_2 and CO_2 (1.1×10^{-09} and 5.3×10^{-09} $cm^3.cm/cm^2.s.cmHg$, respectively). The mechanical tests performed for all PHA films revealed that mcl-PHA and blends demonstrated higher deformation until break, and P(3HB) had superior tensile strength.

Keywords: Apple pulp waste, short-chain length polyhydroxyalkanoates (scl-PHA), medium-chain length polyhydroxyalkanoates (mcl-PHA), polymer blends, films.

Resumo

O primeiro objetivo desta tese foi utilizar resíduos de polpa de maçã, excedentes da indústria de processamento de frutas, para o cultivo de *Pseudomonas citronellolis* NNRL B-2504, *Cupriavidus necator* DSM 428 e uma co-cultura utilizando ambas as estirpes, culminando na produção de polihidroxialcanoatos de cadeia média (mcl-PHAs), polihidroxialcanoatos de cadeia curta (scl-PHAs) e uma mistura biossintetizada natural, respetivamente. Os PHAs são biopoliésteres com propriedades de materiais versáteis, aplicáveis em vários campos.

A fração solúvel do resíduo de polpa de maçã, rica em frutose, sacarose e glucose, foi utilizada para o cultivo em batch de *P. citronellolis*, *C. necator*. O primeiro cultivo, *P. citronellolis*, atingiu um teor de polímero na biomassa de 30%, com uma produtividade volumétrica de 0,61 g/L.dia. O polímero era composto principalmente por 3-hidroxidecanoato (68%) e 3-hidroxioctanoato (22%), e tinha um peso molecular de $3{,}7\times10^{5}$ Da. Apresentou temperaturas de fusão e de degradação de 53 e 296 °C, respetivamente, e um grau de cristalinidade de 15%. *C. necator* DSM 428 alcançou uma produtividade volumétrica de 1,59 g/L.dia, atingindo um conteúdo de polímero na biomassa de 44%. Foi obtido um homopolímero, P(3HB), com um peso molecular de $5.0\text{x}10^{5}$ Da e um grau de cristalinidade de 43%. Além disso, o polímero é caracterizado por temperaturas de fusão e de degradação de 179 e 293 ºC, respetivamente. Finalmente, foi realizada uma terceira produção em batch utilizando uma co-cultura. A produção apresentou um teor de polímero em peso de 34% com uma produtividade volumétrica de 0,96 g/L.dia. O polímero produzido foi uma mistura física de mcl-PHA e P(3HB). Estes resultados demonstraram que o resíduo de polpa de maçã é uma matéria-prima adequada para a produção de diferentes biopolímeros com propriedades físico-químicas distintas.

O objetivo da segunda parte desta tese foi preparar filmes baseados nos PHA produzidos por resíduos de polpa de maçã, seguidos da sua caracterização física e química.

Todos os filmes apresentaram semelhantes características térmicas, cristalinas e químicas quando comparados às características do polímero puro, o que indica que o procedimento não teve impacto significativo nas características dos polímeros. Testes de permeação de gases foram ainda realizados para oxigénio e dióxido de carbono. Os filmes de mcl-PHA apresentaram os melhores resultados tanto para o O_2 quanto para o CO_2 (1.1×10^{-09} e 5.3×10^{-09} $cm^3.cm/cm^2.s.cmHg$, respetivamente). Os testes mecânicos realizados para todos os filmes de PHA revelaram que mcl-PHA e blends demonstraram maior deformação até à quebra, e o PHB com maior resistência à tração.

Palavras-chave: Resíduo de polpa de maçã, Polihidroxialcanoatos de cadeia curta, Polihidroxialcanoatos de cadeia média, Mistura de Polímeros, Filmes.

List of Content

Agradecimentos ix

Abstract xi

Resumo xiii

List of Content xv

List of Figures xix

List of Tables xxi

List of Abbreviations xxiii

Chapter 1 1

Introduction and Motivation 1

1. Introduction 3

1.1. Food Industry Waste 3

1.2. Food Processing Wastes 3

1.3. Apple Pomace 4

1.4. Polyhydroxyalkanoates (PHAs) 5

1.5. Downstream Processing For PHA Recovery 7

1.6. Types of PHA and their physical and chemical properties 8

1.6.1. Short-chain-length PHA 8

1.6.2. Medium-chain-length PHA 9

1.6.3. Blends of Polymers 9

1.7. PHAs Applications 10

2. Motivation 11

Chapter 2 13

Production of Polyhydroxyalkanoates using Apple Pulp Waste 13

2.1. Introduction 14

2.2. Methods 16

2.2.1. Waste Apple Pulp Medium 16

2.2.2. Screening Assay 16

2.2.2.1. Microorganisms and Inocula Preparation 16

2.2.2.2. Shake flask Assays ... 16
2.2.3. Bioreactor Assays ... 17
2.2.3.1. Bacterial Strains ... 17
2.2.3.2. Inoculum and Cultivation Medium ... 17
2.2.3.3. Batch Cultivation ... 17
2.2.4. Analytical Techniques ... 18
2.2.4.1. Cellular Growth ... 18
2.2.4.2. Biomass Quantification ... 18
2.2.4.3. Nile Blue Staining ... 18
2.2.4.4. Quantification of sugars ... 18
2.2.4.5. Quantification of total Nitrogen ... 18
2.2.4.6. Quantification of Ammonia ... 19
2.2.5. Calculations ... 19
2.2.6. Biopolymer extraction ... 19
2.2.6.1. PHA extraction and purification ... 19
2.2.6.2. Acetone Fractionation ... 20
2.2.7. Biopolymer characterization ... 20
2.2.7.1. Composition ... 20
2.2.7.2. Fourier Transform Infrared Spectroscopy ... 21
2.2.7.3. Molecular Mass Distribution ... 21
2.2.7.4. Thermal Properties ... 21
2.2.7.5. X-Ray Diffraction ... 22
2.3. Results and Discussion ... 23
2.3.1. Shake Flask Screening Assay ... 23
2.3.2. PHA production from waste apple pulp ... 28
2.3.2.1. Production of mcl-PHA by *P. citronellolis* NRRL B-2504 ... 28
2.3.2.2. Production of PHB by *C. necator* DSM 428 ... 31
2.3.2.3. Co-culture of *P. citronellolis* NRRL B-2504 and *C. necator* DSM 428 ... 34
2.3.3. Polymers Characterization ... 36

2.3.3.1. Composition 36

2.3.3.2. Molecular Mass Distribution 40

2.3.3.3. FTIR 41

2.3.3.4. Thermal properties of the biopolymers 43

2.3.3.5. X-Ray Diffraction 46

2.3.3.6. P(3HB), mcl-PHA and blend comparison 48

2.3. Conclusions 49

Chapter 3 51

Preparation and Characterization of Films based on PHA 51

3.1. Introduction 52

3.2. Methods 54

3.2.1. Films preparation 54

3.2.2. Morphology Characterization 54

3.2.3. Thermal properties Analysis 54

3.2.4. X-Ray Diffraction Analysis 54

3.2.5. FTIR 54

3.2.6. Water contact Angles 55

3.2.7. Swelling in Water 55

3.2.8. Gas permeation 55

3.2.9. Mechanical Properties 56

3.3. Results and Discussion 57

3.3.1. Morphology and Characterization of PHA Films 57

3.3.2. Thermal Properties of PHA films 61

3.3.3. X-Ray Diffraction of PHA Films 62

3.3.4. FTIR of PHA films 63

3.3.5. Swelling and contact angle of PHA films 64

3.3.6. Gas Permeation 67

3.3.7. Mechanical Properties 70

3.4. Conclusions 73

Chapter 4 75

Conclusions and Future Work 75

4.1. Conclusions and Future Work 76

References 79

Appendices 92

List of Figures

Figure 1 - General structure of Polyhydroxyalkanoate (PHA), where R is the side chain of each monomer and n is the number of monomers (28) 6
Figure 2 - Bacterial intracelular PHA granules (130) 6
Figure 3 - Cellular growth profile of the different bacterial strains tested with apple pulp waste as the sole carbon source. 23
Figure 4 - Sugars profile presents in apple pulp waste, namely arabinose, glucose, fructose and sucrose, at the beginning of the shake flask screening assay. 24
Figure 5 - Sugar profiles, namely arabinose, glucose, fructose and sucrose, in the supernatant for each shake flask assay for different bacterial strains tested with apple pulp waste as the sole carbon source. 25
Figure 6 - Visualization of the several bacterial strain cells under the microscope (100x) during different hours of cultivation, under fluorescence after Nile Blue staining. 26
Figure 7 - Cultivation profile of *P. citronellolis* NRRL B-2504 using apple pulp waste as the sole carbon source (concentration of active biomass (○), PHA (●), total nitrogen (◇), ammonia (△), glucose (■), fructose (□) and sucrose (⊗))..... 28
Figure 8 - Cultivation profile of *C. necator* DSM428 using apple pulp waste as the sole carbon source (concentration of active biomass (○), PHA (●), total nitrogen (◇), ammonia (△), glucose (■), fructose (□) and sucrose (⊗))..... 31
Figure 9 - Cultivation profile of the co-culture using apple pulp waste as the sole carbon source (concentration of active biomass (○), PHA (●), total nitrogen (◇), ammonia (△), glucose (■), fructose (□) and sucrose (⊗))..... 34
Figure 10 - Thermogravimetric analysis (TGA) curves of the PHB and mcl-PHA produced by *C. necator* DSM 428 and *P. citronellolis* NRRL B-2504, respectively, and the blend from apple pulp waste..... 43
Figure 11 - X-ray diffractogram of the P(3HB), mcl-PHA and P(3Hb)/mcl-PHA blend produced by *C. necator* DSM 428, *P. citronellolis* NRRL B-2504 and co-culture, respectively, from apple pulp waste..... 47
Figure 12 - mcl-PHA (A), PHB (B) and PHB/mcl-PHA blend (C) films obtained by solvent casting. 57
Figure 13 - PHB/mcl-PHA blend films obtained by solvent casting using chloroform and DMF as solvents showing the PHB precipitated in the films. 57
Figure 14 - Thermogravimetric analysis (TGA) curves of the PHB, mcl-PHA and the blend produced from apple pulp waste. 61
Figure 15 - X-ray diffractogram of mcl-PHA, PHB and Blend films. 62

Figure A - Size exclusion chromatograms (SEC) of the mcl-PHA polymer produced by *P. citronellolis* NRRL B-2504 from apple pulp waste……..93
Figure B - Size exclusion chromatograms (SEC) of the PHB polymer produced by *C. necator* DSM 428 from apple pulp waste. ……..……..93
Figure C - Size exclusion chromatograms (SEC) of the PHB/mcl-PHA polymer produced by a mixed culture fermentation of *P. citronellolis* NRRL B-504 and *C. necator* DSM 428 from apple pulp waste. ……..……94
Figure D - Tensile- deformation curve for *P. citronellolis* mcl-PHA films……...94
Figure E - Tensile- deformation curve for *C. necator* PHB films……..95
Figure F - Tensile- deformation curve for PHB/mcl-PHA blend films……95
Figure G - Tensile-deformation curve for PHB/mcl-PHA film that presented a significant segregation of the polymers presented in the blend……..96

List of Tables

Table 1. Mcl-PHAs produced by *Pseudomonas* sp. using several carbon sources and respective monomeric composition (OOD, olive oil distillate; FFA, free fatty acids; SBF, Saturated Biodiesel Fraction; CPO, Crude Pollock Oil; SPO, sludge palm oil). 14
Table 2. Composition of apple pomace adapted from (11). 15
Table 3. Cell dry weight (g/L) of *P. stuzeri* NRRL B-775, *C. necator* DSM 428, *P. citronellolis* NRRL B-2504 and *P. resinovorans* NRRL B-2649 obtained on the shake flask screening assay. 24
Table 4. Kinetic and stoichiometric parameters for mcl-PHA production by *P. citronellolis* NRRL B-2504 using several wastes and by-products as feedstocks (μ_{max}, maximum specific cell growth rate; CDW, cell dry weight; r_p, volumetric productivity; $Y_{x/s}$, active biomass yield on a substrate; $Y_{p/s}$, polymer yield on a substrate basis; n.a., data not available). 30
Table 5. Kinetic and stoichiometric parameters for PHB production by *C. necator* DMS 428 using several wastes and by-products as feedstocks (μ_{max}, maximum specific cell growth rate; CDW, cell dry weight; r_p, volumetric productivity; $Y_{x/s}$, active biomass yield on a substrate basis; $Y_{p/s}$, polymer yield on a substrate basis (calculated considering the consumption of sugars, glucose and fructose); n.a., data not available)..... 33
Table 6. Kinetic and stoichiometric parameters of the three batch productions by *P. citronellolis* NRRL B-2504, *C. necator* DSM 428 and the co-culture using apple pulp waste (μ_{max}, maximum specific cell growth rate; CDW, cell dry weight; r_p, volumetric productivity; $Y_{x/s}$, active biomass yield on a substrate basis; $Y_{p/s}$, polymer yield on a substrate basis (calculated considering the consumption of sugars, glucose and fructose); n.a., data not available). 35
Table 7. Monomeric composition of the co-culture biomass, polymer obtained and mcl-PHA and PHB that compose the blend produce in the co-culture production using apple pulp waste. 37
Table 8. Physical-chemical properties of the mcl-PHA produced by *P. citronellolis* and other *Pseudomonas* sp. (HHx, 3-hydroxyhexanoate; HO, 3-hydroxyoctanoate; HD, 3-hydroxydecanoate; HDd, 3-hydroxydodecanoate; HTd, 3-hydroxytetradecanoate; Mn, molecular number; Mw, molecular weight; PDI, polydispersity index; n.a., data not available; n.d., not detected). 38
Table 9. Physical-chemical properties of the PHB produced by *C. necator* DSM 428 and other *C. necator* sp. (3HB, 3-hydroxybutyrate; 3HV, 3-hydroxyvalerate; Mn, molecular number; Mw, molecular weight; PDI, polydispersity index; n.a., data not available; n.d., not detected). 39
Table 10. Thermal properties and degree of crystallinity of the mcl-PHA and P(3HB) produced from *P. citronellolis* NRRL B-2504 and *C. necator* DSM 428, respectively, as well as other PHA

obtained from different bacterial strain (T_m, melting temperature; T_{deg}, degradation temperature; X_c, crystallinity fraction; ΔHm, melting enthalpy ; n. a. data not available; n. d., not detected). 45
Table 11. Composition and physical-chemical properties of the polymers obtained from apple pulp waste (HB, 3-hydroxybutyrate; HHx, 3-hydroxyhexanoate; HO, 3-hydroxyoctanoate; HD, 3-hydroxydecanoate; HDd, 3-hydroxydodecanoate; HTd, 3-hydroxytetradecanoate; Mw, molecular weight; PDI, polydispersity index; T_m, melting temperature; T_{deg}, degradation temperature; X_c, crystallinity degree: n.a., data not available; n.d., not detected)..... 48
Table 12. Surface (a, b) and cross-section (c, d) amplified 500x and 5000x, respectively images obtained by Scanning Electron Microscopy (SEM) analysis of the prepared PHA based films. 60
Table 13. Water contact angles for the PHA films prepared with the biopolymers produced from apple pulp waste and comparison with values reported for different materials (PET, polyethylene terephthalate; P(HBHHx), poly(3-hydroxybutyrate-*co*-3-hydroxyhexanoate); PLA, polylactic acid; PP, polypropylene; PHO, poly(hydroxyoctanoate); PHUA, poly(3-hydroxyundecanoate); P(3HB-co-4HB), poly(3-hydroxybutyrate-co-4-hydroxybutyrate); PHBHV, poly(3-hydroxybutyrate-co-3-hydroxyvalerate)). 66
Table 14. Oxygen and carbon dioxide permeability values for PHA films and for different natural and synthetic materials for both gases (PHB, Polyhydroxybutyrate; PHB/PEG, Polyhydroxybutyrate with 5% PEG (Polyethylene Glycol) as plasticizer ; P(HBV5), poly(3-hydroxybutyrate-*co*-3-hydroxyvalerate) with 5% valerate; P(HBHV), poly(3-hydroxybutyrate-*co*-3-hydroxyvalerate; PET, polyethylene terephthalate; LDPE, low-density polyethylene; PLA, Polylactic acid; MC/PEG, methylcellulose and poly(ethylene glycol); n.a., data not available). 67
Table 15. Mechanical properties of films prepared by solvent casting and comparison with other natural and synthetic polymers (PHB, polyhydroxybutyrate; P(HBHV), poly(3-hydroxybutyrate-*co*-3-hydroxyvalerate); P(HBHHx), poly(3-hydroxybutyrate-*co*-3-hydroxyhexanoate); P(3HB4HB), poly(3-hydroxybutyrate-*co*-4-hydroxybutyrate); PHHxHO, poly(3-hydroxyhexanoate-*co*-3-hydroxyoctanoate); PHA-LE, epoxidized PHA from lineseed oil; PLA, Polylactic acid; SBR, styrene butadiene rubber; PP, polypropylene; n.a., data not available). .. 72

List of Abbreviations

3HB	3-hydroxybutyrate
3HD	3-hydroxydecanoate
3HDd	3-hydroxydodecanoate
3HHx	3-hydroxyhexanoate
3HO	3-hydroxyoctanoate
3HTd	3-hydroxytetradecanoate
3HV	3-hydroxyvalerate
4HB	4-hydroxybutyrate
4HV	4-hydroxyvalerate
CDW	cell dry weight (g/L)
DSC	Differential Scanning Calorimetry
FTIR	Fourier Transform Infrared Spectroscopy
GC	Gas Chromatography
GPC	Gel Permeation Chromatography
HPLC	High-Performance Liquid Chromatography
LB	Luria-Bertani
Mcl	medium – chain – length
M_n	number –average molecular weight
MPa	megapascals
M_w	average molecular weight
n. a.	Data Not Available
n.d.	Data Not Detected
OD	Optical density
P(3HB)	Poly(3-hydroxybutyrate)
P(3HB-*co*-4HB)	Poly(3-hydroxybutyrate-*co*-4-hydroxybutyrate)
P(3HB-*co*-4HV)	Poly(3-hydroxybutyrate-*co*-4-hydroxyvalerate)
P(3HB-*co*-4HHx)	Poly(3-hydroxybutyrate-*co*-3-hydroxyhexanoate)
PDI	Polydispersity index
PEG	polyethylene glycol
PHA	PolyHydroxyAlkanoate
PHB	Polyhydroxybutyrate
rpm	rotation per minute
Scl	short-chain-length
SEM	Scanning electron microscopy

$\mathbf{T_{deg}}$	Degradation Temperature
TGA	Thermogravimetric Analysis
$\mathbf{T_m}$	Melting Temperature
$\mathbf{X_c}$	Degree of Crystallinity
XRD	X-ray Diffraction

Chapter 1

Introduction and Motivation

1. Introduction

1.1.Food Industry Waste

Food waste is considered a topic of concern worldwide and occurs throughout several different stages along the food production chain, starting from the harvesting up to industrial manufacturing and processing, to storage, packaging, retail and household. It represents a resource problem but it also holds a vast concern regarding the environmental and economic matter in the modern society (1,2).

In Europe, it is estimated that food processing industry produces about 2.5×10^8 ton per year of by-products and wastes (3,4). For instance, in Italy, approximately 3.3% and 2.6% of agro-food and final products, respectively, from food industry are discarded. This amount of residues implies a substantial environmental burden resulting from the resource consumption and the emission of polluting gases, such as CO_2, and generates a huge amount of solid wastes and by-products (1). For example, several important factors of the Portuguese economy are winery, pulping and biodiesel industries. These fields generate enormous amount of industrial residues, such as, grape skins and wine must (also known as grape pomace), cheese whey, pulping liquors and crude glycerol (a residue from biodiesel production). These residues possess high content that are potentially suitable to be valorised, for instance, cheese whey and crude glycerol were reported in literature to be used for the production of bioplastics and polyhydroxybutyrate (5). Tomato paste processing is another example generating a large amount of wastes and by-products that require proper discard procedures. Is mainly used as animal feed or as soil fertilizers, but another alternative would be the recovery of different value-added products, such as β-carotene, polyphenols and polysaccharides (6).

In the last years, Europe has been preventing the decrease of food waste through several initiatives with different policies that promote integration of food products and resource efficiency. The implementation of such policies aims for a "zero waste" society and "circular economy" by transforming food waste into value-added products and applications, in order to reduce the main costs and negative impacts on the sustainability of the food processing industry (1,7).

1.2. Food Processing Wastes

Food processing industries generate large amounts of vegetable and fruit waste and by-products (20-60 %, w/w, of the fruit and vegetable processed). Those wastes have high contents of suspended solids, and high biochemical (BOD) and chemical oxygen demand (COD), which implicates costs in recovery and treatment. The large amounts generated of such wastes are only partially valorised for spread on land, composting and for fertilizing. The remaining volumes lead to serious management problems since they have significant harmful effects on the sustainability of the food processing industry. The discard of such wastes is mostly done in municipal landfills

due to the high biodegradability of food waste, which leads to leachate and release of methane emissions and occasionally become sources for vectors, pathogenic bacteria and yeast to thrive (1,4,8).

Vegetable and fruit processing by-products, wastes and effluents consist mostly in sugars, along with other macromolecules, such as hemicellulose, lignin, starch, lipids, proteins, fibres, which makes them highly suitable to become cheap abundant substrates for the biotechnological production of value-added compounds, including bioactive molecules (e.g. pharmaceuticals, flavours, vitamins and organics acid), macromolecules (e.g. biopolymers and enzymes) and biofuels (e.g. bioethanol, methane and biohydrogen). Though, prior to their utilization, some might need specific pre-treatments with physical and biological agents followed by specific recovery procedures (3).

The strategy used for the utilization of those residues has been applied for fermentative or non-fermentative product development. In the first case, the fermentative utilization, the food waste residues are used as microbial substrates for the development of a variety of value added products. Regarding the non-fermentative utilization, food wastes are processed for the extraction of the bioactive molecules mentioned above (9).

1.3. Apple Pomace

Apple pomace is considered a leftover (25%-30% of total processed fruits mass) obtained after cider and apple juice processing. Apple pomace is mainly composed of apple peel, core, seed and pulp remains, moreover, contains 80% of moisture and is a rich source of sugars, acids, vitamin C and mineral, which make it quite perishable and, therefore, a potential environmental problem (10,11). Fruits that are not suitable to be directly consumed are processed mainly for juice, jelly and pulp, which generates a great amount of residues (11). The main products of processed apples is their use for apple juice, either as sweet juice or as fermented juice (cider), apple sauce and slices (12). Despite the variety of apples products, the most substantial part of the apple production, around 15 %, is destined to be used for the drinking sector, for juice and ciders (13). The industrial processing of apple juice produces a large amount of wastes, about 75% of apple is utilized for the production of juice while the remaining 25% is the by-product, apple pomace (1).

In 2015, the world production of apples crossed the mark of 70 million metric tons, with the European Union contributed with more than 15 %, while half a million tons of which came from Spain (7).

Thus far, apple pomace has been transformed separately into biofuels, used as substrate for enzymatic processes, to attain chars, extracted for antioxidants, as a source of bioenergy or sorbents for effluent cleaning, etc. On the other hand, the commercial price for biomaterials is

still very high which makes the search for new sustainable and more economic sources of materials an interesting field (7). The possibility of changing the process conditions towards different substances and materials obtained in the multivalorization of apple pomace, makes this approach enormously versatile, towards possible oscillations in the market, as this adds an economic encouragement for the companies to valorise their waste products. For example, the use of food residues, such as apple pulp waste, as a feedstock to produce microbial polymers, namely, polyhydroxyalkanoates, is a sustainable way for their valorisation (3,7).

1.4.Polyhydroxyalkanoates (PHAs)

Materials based on plastic are present in everyday life and their use has grown rapidly over the years, with 150 million tonnes of plastic material being consumed worldwide. The continuous consumption of plastic is expected to continue until 2020. However, the slow rate of degradation represents a serious pollution concern, due to the persistence of plastics in the environment. Therefore, promising alternatives to replace conventional petroleum-derived materials with biodegradable polymers, namely polylactic acid, starch derivatives PHAs, present an additional benefit of being produced from renewable resources (14).

PHAs are a class of biocompatible and biodegradable polymers with properties similar to conventional plastics. As PHAs are biodegradable and immunologically inert, they have encouraged their applications in food packaging and medical fields, for example (15). PHAs possess features that closely resemble some conventional plastics such as polypropylene (PP) and low-density polyethylene (LDPE). Their biocompatibility, non-toxic, crystallinity, stereochemical regularity in repeating units, insolubility in water, high degree of polymerization, physical and mechanical properties transforms them in thermoplastics that can be produced from renewable sources are a highly competitive substitute for plastics (16,17). However, the use of PHA holds a crucial advantage that distinguishes these polymers from petroleum based plastics, which is their ability to biodegradation in natural environments. This feature depends on several factors such as microbial activity of the environment, and the exposed surface area, moisture, temperature, pH and molecular weight (17,18).

PHAs are, by definition, a family of polyesters of several *R*-hydroxyalkanoic acid (HA) monomers (**Figure 1**) that can be synthesized by many gram-positive and gram-negative bacteria in aerobic and anaerobic conditions, as well as some plants. Though, plant cells can only achieve low yields (less than 10% (w/w) of dry weight) of PHA production, opposed to bacterial cells that are able to accumulate levels of PHA as high as 90% (w⁄w) of the dry cell mass (17,19). In most cases, PHA production is triggered when the microorganisms experience a metabolic stress, for instance a limitation of an essential nutrient (e.g., nitrogen, phosphorus or oxygen), electron donor

or acceptor in excess of a suitable carbon source, leading to a natural accumulation by the cells to store carbon and energy, when nutrient supplies are imbalanced (15,20).

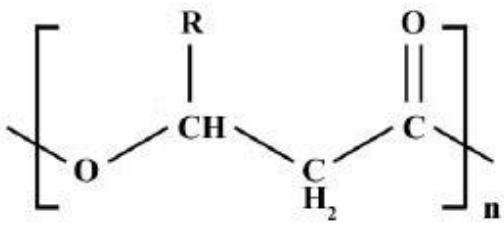

Figure 1 - General structure of Polyhydroxyalkanoate (PHA), where R is the side chain of each monomer and n is the number of monomers (28)

Since PHAs are water insoluble, they are accumulated in the bacterial cytoplasm as intracellular granules (**Figure 2**). They are a product of carbon assimilation and are employed by microorganisms as a form of energy storage to be metabolized when other common energy sources are not available (19–21).

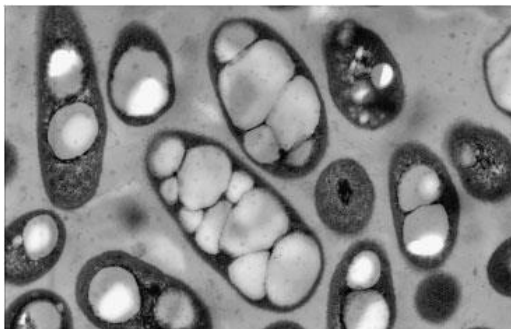

Figure 2 - Bacterial intracelular PHA granules (130)

PHA can be produced by pure or mixed microbial cultures (MMC) (22). PHA production based on mixed cultures do not require the sterilization of the reactor and the fact that these cultures are able to adapt to various complex and cheap waste feedstocks allow a lower production cost, which makes these the major advantages for this production (23). MMC productions involve PHA-accumulating organisms, such as polyphosphate and glycogen accumulating organisms that are selectively enriched during the course of several cultivation cycles in order to accumulate PHA. However, MMC accumulate less than 20% in PHA content, of which the final polymer obtained mostly P(3HB) or copolymers, such as P(3HB-*co*-3HV) or P(3HB-*co*-3HHx) (20,23). MMC are operated under a process designated as Feast and Famine (FF), where the culture growth is restricted due to the alternate substrate availability, compelling the organisms to adapt by using the substrate mainly for polymer storage (24). This represents a disadvantage, since pure cultures can produce PHA while performing the process in a single reactor (20,22,23). Pure cultures, allow a high PHA content (up to 80%) and higher productivities (2.42 g L^{-1} h^{-1} obtained using glucose as carbon source), however, the last one is depending on the biomass concentration reached by

the culture by using feedstocks as carbon sources (25,26). Moreover, the use of a single culture allows to obtain a well-defined composition of polymer (25).

PHA obtained with pure cultures, adopts a two-stage production process, with an inoculum of bacteria being introduced into a sterile solution of nutrients and a suitable carbon source in the growth (first) stage. In the second stage, an essential nutrient is deliberately limited and PHA accumulation takes place (23). Another main advantage presented by pure cultures refers to the substrates, which has been overcoming the need for pure carbon sources since the use of agro-industrial wastes or byproducts has been successfully used for PHA production by these cultures, (e.g. example, sugar cane (5.80 g/L), bagasse (3.90 g/L), wheat bran (4.00 g/L), whey (6.12 g/L) and canola oil (18.27 g/L)) (27). The final characteristics of the polymer depends on the carbon feedstocks fed during accumulation, the metabolic pathways that the bacteria use for the following conversion into precursors, and the substrate specificities of the enzymes involved (22,28).

1.5.Downstream Processing For PHA Recovery

The recovery of PHA from the biomass implies a substantial cost, particularly for large scale of biopolymer fabrication. The fact that PHA is a lipid-like compound intracellular, implies several consequences, when it comes to the recovery of the polymer, since the separation between the PHA in a purified state and the residual biomass, mainly composed by cell genetic material, phospholipids, proteins and peptidoglycans, is considered a difficult step to achieve and depend on a number of factors, such as microbial strain, PHA produced and the final application (16,29,30).

Different approaches have been studied, use of solvents, thermal treatment, chemical, enzymatic or mechanical processes, as pre-treatments to the biomass, previously to the downstream, in order to facilitate PHA extraction and purification by weakening the cell membrane (30). Solvent extraction is usually a common method applied, that is based on the fact that the polymer and the lipids present in the biomass are the only ones that are dissolved. A wide range of organic solvents can be used in this method, such as chloroform, methylene chloride, 1,2-dichloroethane, or the use of acetone, a potential solvent for the extraction of mcl-PHA (29). The following step involves a precipitation using an anti-solvent, for example an alcohol, (e.g. ethanol), or water, with the aim of obtaining a pure PHA with low impact on its molar mass (29,30). The main disadvantage presented by this extraction method is the use of halogenated solvents as well as the amount of volume needed for the precipitation step (29,30). As for the other methods (chemical, enzymatic or mechanical), they are applied at industrial scale, by removing all parts of the cells, through solubilisation, except the polymers granules, which are recovered by centrifugation or filtration (29,30).

1.6. Types of PHA and their physical and chemical properties

Depending on the type of microbial species and the growth conditions, namely pH, fermentation conditions, modes of fermentation (batch, fed-batch, continuous) and type and concentration of the carbon source, the structures of PHAs produced can vary according the previous factors affecting the monomer content, length and composition of the side chains, such variation in the polymer makes it possible to tailor PHA production towards a variety of potential applications (19,31).

Regarding the number of carbon atoms in the side chain, the PHAs can be divided in three major groups such as: short-chain-length PHA (scl-PHA), medium-chain-length PHA (mcl-PHA) and long-chain-length PHA (lcl-PHA). The literature regarding lcl-PHA is still very limited and the focus of this thesis will be maintained for both scl-PHA and mcl-PHA (32–34).

1.6.1. Short-chain-length PHA

Short-chain-length PHAs (scl-PHA) are composed by 3 to 5 carbon atoms and can be biosynthesized by several microorganisms including *Cupriavidus necator*, *Pseudomonas fluorescens* and *Gamma proteobacterium*, among others (31,34,35). Scl-PHAs are described as stiff and brittle biomaterials with high degree of crystallinity (50-80%) (31). This last characteristic supports scl-PHAs to be considered very similar to thermoplastic due to the similar crystallinity and properties exhibited relatively to some of the petrochemical-based polymers such as polypropylene (PP) and polyethylene (PE) (32). Regarding the thermal properties, scl-PHAs have high melting (160-177 ºC) and glass transition (-4 to 15 ºC) temperatures, as well as, molecular weight (200 000 – 3 000 000 Da) and polydispersity index in the range of 1.9 to 2.1.

Amongst scl-PHAs, P(3HB), is the most common homopolymer (36). It is highly crystalline due to the stereo regularity in the side chains. However, the high brittleness of crystalline P(3HB) has impact on the material poor mechanical properties, namely, Young's Modulus (~ 400 MPa) and elongation at break (1-6%), compared to petroleum-based materials. For example, polypropylene (PP) presents a Young's Modulus of 1222 MPa and an elongation at break of 375% (19,31,36,37). P(3HB) shows no toxicity towards a variety of cell lines, which include mouse fibroblast, osteoblast and chondrocytes. Moreover, the homopolymer displays excellent biocompability (36). Copolymers can be produced by the incorporation of monomers in P(3HB), like the case of P(3HB-*co*-3HV) or P(3HB-*co*-3HHx) (31). These materials are less stiff and brittle than P(3HB) and also present lower X_c and T_m, depending on percentage of monomer that is incorporated in the polymer (19,31,36). The incorporation of another monomer also impact the copolymers mechanical properties, for example, the addition of 3-hydroxyhexanoate to P(3HB), results in a

copolymer with higher elongation to break (up to 800 %) and flexibility as well as a reduction in the polymer stiffness (19,31,36).

1.6.2. Medium-chain-length PHA

Medium-chain-length PHA (mcl-PHA) is a type of PHA that contains 6 to 14 carbon atoms. These polymers are usually composed by monomers, such as 3-hydroxyhexanoate (3HHx), 3-hydroxyoctanoate (3HO), 3-hydroxydecanoate (3HD), 3-hydroxydodecanoate (3HDd), 3-hydroxytetradecanoate (3HTd). Mcl-PHAs are produced by several strains, mainly of the *Pseudomonas* genera, for example *Pseudomonas putida*, *Pseudomonas chlororaphis*, *Pseudomonas oleovarans*, etc (38–40).

Mcl-PHAs are less crystalline, presenting crystallinity with X_c below 40%, low melting temperatures (T_m) between 40 and 60ºC and low glass transition temperature (T_g) below room temperature, of -50 and -25ºC, when compared to scl-PHAs (30,41,42). By displaying a low *Tg*, mcl-PHA does not become brittle even at temperatures below freezing point, making them potentially interesting as rubber-like biological materials (39).

Duo to the presence of monomers, such as 3HO, 3HD and 3HDd, mcl-PHAs present mechanical properties with improved elastic and flexibility features in contrast to those of scl-PHAs. Mcl-PHAs display high elongation to break (above 100 %) and low tensile strength (up to 10 MPa) (42,43). The characteristics of mcl-PHA bear a resemblance to those of elastomers, latexes and resins (39). Therefore, materials based on mcl-PHAs are considered as suitable candidates for a variety of applications, such as rubbers, smart latexes, adhesives and glues (39,41).

1.6.3. Blends of Polymers

PHAs have been in the focus of a variety development of blends in order to reduce the prices and, simultaneously, improve the performance of PHAs, mostly those of scl-PHA (31). In the last years, a substantial amount of research has been directed for the blending of different polymers with PHA, as well as the changing of polymer processing by the addition of other materials in order to improve the desirable characteristics of polymer end products (44).

Since the intrinsic structure of scl-PHA has limitations in further applications in the packaging, textile, and biomaterial fields, methods such as physical blending chemical structure design combined with processing conditions have been tested to improve the mechanical properties and applicability of scl-PHA (33). Blends of PHA with materials like rubber, poly(ethylene glycol) (PEG), polycaprolactone, poly(vinyl alcohol) (PVA), poly(3-hydroxybutyrate-*co*-3-hydroxyvalerate) (PHBHV) have been reported (31). The use of natural biodegradable polysaccharides, like the case of cellulose and starch have also been tested for blending with PHA (31).

1.7. PHAs Applications

To achieve low value added yet expensive PHA materials produced in large scale, it is important that the applications can generate high value, and the quantity demand should be high (45). The main reason for PHA applications, is due to the excellent features, such as biocompability, no toxicity and similar behaviour to petroleum-based materials (33). PHAs display significant prospects for future applications, mostly, in the packaging, biomedical fields, or source of biofuel (33). For example, the use of PHAs, like the case of scl-PHA, namely PHBHV, as a biodegradable packaging material to be processed into bottles, bags and films, as replacements for petroleum-based polymers to reduce environmental pollution (33). As for the application in biomedical fields, tissue engineering, sutures, wound dressing, scaffolds for regeneration of arterial tissues, heart valves or as implants and micro-carriers for drug delivery, are some of the examples reported for medical applications (15).

2. Motivation

The arousing numbers of food waste has become a concerning topic due to environmental and economic issues. Thereby, the necessity to reuse the by-products and solid wastes has established several strategies to transform food waste into value-added products (1). Apple pomace is a waste obtained from juice processing that still holds an important source of sugars, thus conferring it a high potential to be used as feedstocks in fermentative use to produce microbial polymers, such as PHAs, encouraging the valorisation of waste products (11). PHAs are biosynthesized by a variety of bacteria using different feedstocks as carbon sources (35). PHAs can be divided in groups according their structure and composition, namely, scl-PHA and mcl-PHA (31). These polymers have a set of characteristic properties, such as, thermal, physical and chemical, that makes them suitable for a variety of applications, namely, in the medical field, as patches and drug delivery systems, or for food packaging (39).

The following work was divided in two parts. The first part had the main goal of using *C. necator* and *P. citronellolis* for the production of scl-PHA and mcl-PHA using apple pulp waste as the carbon source. The strain *C. necator* is reported through the literature, as well known producer of PHB (46), on the other hand, *P. citronellolis*, is a bacteria known to produce mcl-PHA using a variety of feedstocks (35). A third production was also accomplished, using for the first time both, *C. necator* and *P. citronellolis*, as a co-culture to produce a blend composed by PHB and mcl-PHA. The polymers produced were recovered from biomass by solvent extraction with chloroform followed by a purification step with ice-cold ethanol.

In the second part of this work, films based on the polymers previously produced, mcl-PHA, PHB and blends were prepared and characterized. Due to their natural biocompability, biodegradability, but brittle and stiff behaviour PHB usually present worse mechanical properties than mcl-PHAs. Therefore, taking advantage of the blend polymer produced by the co-culture, composed of a mixture of PHB and mcl-PHA, the films prepared used the interaction intended to understand if the presence of both biopolymers had impact on each other properties, namely, on gas permeation and mechanical properties.

Chapter 2

Production of Polyhydroxyalkanoates using Apple Pulp Waste

2.1. Introduction

Many bacteria have been reported to produce mcl-PHA and scl-PHA from several agro-food and industrial wastes/by-products, such as, for example, free fatty acids (35), crude pollock oil (32), saturated biodiesel fraction (39,42), sludge palm oil (38), oil deodorizer distillates (47) and fruit wastes (namely, grapes, apricots and cherries) (48). Among the variety of bacteria able to produce mcl-PHA using a wide range of waste residues, species of the Genus *Pseudomonas* have been the most widely studied, including *Pseudomonas chlororaphis*, *P. stutzeri*, *P. resinovorans*, *P. putida*, *P. mediterranea* and *P. citronellolis*. **Table 1** presents their carbon source and final composition.

Table 1. Mcl-PHAs produced by *Pseudomonas* sp. using several carbon sources and respective monomeric composition (OOD, olive oil distillate; FFA, free fatty acids; SBF, Saturated Biodiesel Fraction; CPO, Crude Pollock Oil; SPO, sludge palm oil).

Microorganism	Carbon source	Monomeric Composition	Reference
Pseudomonas chlororaphis	SBF	3HO-3HD-3HHx-3HDd	(39)
Pseudomonas citronellolis	OOD and FFA	3HO-3HD-3HHx-3HDd-3HTd	(35)
	SBF	3HO-3HD-3HHx-3HDd	(42)
Pseudomonas resinovorans	OOD	3HO-3HD-3HHx-3HDd-3HTd	(47)
Pseudomonas putida	CPO	3HO-3HD-3HHx-3HDd-3HTd	(32)
	SPO	3HO-3HD-3HHx-3HDd-3HTd	(38)

P. citronellolis has been described for is potential due to its ability to eliminate recalcitrant hazardous hydrocarbons from spoiled environment, namely alkanes, that are generally less susceptible to biodegradation (42,49). The fact that it holds encouraging for the production of mcl-PHAs, as a result of a range of converted carbon substrates, including feedstocks, it has been attracting interest for this organism (35,42). *P. resinovarans* and *C. necator* are well reported in literature to synthesize PHA from a variety of renewable sources as their carbon sources, such as, olive oil distillate and margarine waste (46,50). Although, not much is known about *P. stutzeri* and is ability to produce PHA using a large variety of waste residues, until now it has only been described to produce mcl-PHA (with a composition similar to those represented in **Table 1**), using glucose (42,51).

Among the several microorganisms known to produce scl-PHA, especially P(3HB), *Cupriavidus necator* is the most widely described strain in the literature. Nonetheless, some strains of *Pseudomonas* sp. are also reported to produce PHB from a variety of carbons substrates, namely *Pseudomonas oleovorans*, *Pseudomonas fluorescens* and *Pseudomonas putida* (17,34). *C. necator* is able to use different carbon sources (pure as well as wastes) and, generally, is the strain that shows very high content in PHA (70 %) (34,46,52).

The necessity to improve the mechanical properties of PHB, in order to have better and more efficient application for this polymer is leading the attention towards the blending between mcl-PHA and scl-PHA (31). A strategy to achieve this blending would be the co-culturing of two or more bacterial strains that have similar growth necessities but would be able to produce different types of PHA from the same substrate (53). This would contribute also for a more efficient conversion of complex carbon substrates into PHA (28). Such procedure is achieved by the cooperative metabolism of the co-culture, where the different microorganisms not only maximize the utilization of various carbon substrates in order to produce PHA but also to enhance the robustness of individual strains through the removal of inhibitory compounds, providing co-culture an advantage over monoculture systems (28). An example of the successful use of such strategy was reported by Ashby et al. (2005), which used a co-culture of genetically modified *P. oleovorans* and *P. putida* strains (by the addition of the P3HB biosynthetic genes) in order to produce a PHB/mcl-PHA blend using alkanoic acids (53).

Apple pomace can be used as substrate for bacteria cultivation for different productions (11). The composition of apple pomace is highly heterogeneous, contains high water content and is mainly composed of insoluble carbohydrates, however, simple sugars, like glucose, fructose, sucrose, as well as small amounts of minerals, proteins and vitamins. The composition of apple pomace is presented in **Table 2**. The values presented on the table vary according to the apple variety used and the type of processing applied for juice extraction (11).

Table 2. Composition of apple pomace adapted from (11).

Composition (w/w %)	
Moisture	79.2 - 80
Proteins	3.7 - 4.1
Lipids	n.d.
Fibers	38.2 – 40.3
Carbohydrates	59.8
Simple sugars	10.8 - 15

In this chapter, waste apple pulp was used as the sole carbon source for the cultivation of different known PHA producers in batch shake flask experiments. Two bacterial strains, namely, *P. citronellolis* NRRL B-2504 and *C. necator* DSM428, were selected for batch bioreactor production of PHA in monoculture experiments and also in a co-culture experiment of the two strains. The polymers produced in the bioreactor experiments were extracted, characterized and used for the preparation of membranes (**Chapter 3**).

2.2. Methods

2.2.1. Waste Apple Pulp Medium

The waste apple pomace used in this work was provided by Sumol + Compal, SA. The waste apple pomace was diluted with deionized water in the ratio of 1:3, as described by Freitas (2017) (131), for viscosity reduction, followed by a centrifugation (7012×*g*, 30 min) in order to recover the sugar-rich supernatant. The insoluble solids were discarded. The supernatant was collected and its pH (pH1100L, VWR pHenomeral™) was set to 7.0 by the addition of a 5 M NaOH solution. The final solution was sterilized by autoclaving at 121 ºC for 30 min, and used for the bacterial cultivation experiments.

2.2.2. Screening Assay

2.2.2.1. Microorganisms and Inocula Preparation

The microorganisms used in this assay were *Pseudomonas stutzeri* NRRL B-775, *Pseudomonas resinovorans* NRRL B-2649, *Pseudomonas citronellolis* NRRL B-2504 and *Cupriavidus necator* DSM428. All the bacterial strains were preserved in glycerol (20%, v/v), as a cryoprotectant agent, at -80 ºC. The reactivation of the cultures was performed by plating a sample of the cryopreserved vials in CHROMagar™ Orientation plates and incubation at 30 ˚C, during 48 h. Subsequently, a single colony of each culture was inoculated into 50 mL liquid Luria Bertani (LB) medium (2.0 g/L bacto tryptone; 1.0 g/L yeast extract; 2.0 g/L NaCl), pH 7.0), in 50 mL baffled shake flasks, and incubated in an orbital shaker at 200 rpm and 30 ˚C, for 24 h. These cultures served as pre-inoculum for the shake flask assays.

2.2.2.2. Shake flask Assays

The pre-inoculum (20 mL) of the cultures were used as inoculum for the 200 mL cultivation assays (in 500 mL baffled shake flasks) with waste pulp fruit as the sole substrate. The cultivation medium was composed of waste apple pulp supernatant, prepared as described above (200 mL), supplemented with 4 mL of a mineral solution (composed of $(NH_4)_2HPO_4$, 2.2 g/L; KH_2O_4P, 11.6 g/L; KH_2PO_4, 7.4 g/L), 2 mL of a 100 mM $MgSO_4$ solution and 2 mL of a micronutrients solution that was diluted 1:10.

The micronutrients solution contained the following (per liter of 1 N HCl): $FeSO_4.7H2O$, 2.78 g; $MnCl_2.4H_2O$, 1.98 g; $CoSO_4.7H_2O$, 2.81 g; $CaCl_2.2H_2O$, 1.67 g; $CuCl_2.2H_2O$, 0.17 g; $ZnSO_4.7H_2O$, 0.29 g (54). In all shake flask assays, the cultures were incubated in an orbital shaker at 200 rpm and 30 ˚C, for 72 h, during which a daily sample (10 mL) was collected for determination of OD_{600nm}, CDW and sugars quantification.

2.2.3. Bioreactor Assays

2.2.3.1.Bacterial Strains

The bacterial strains used in these assays were *Pseudomonas citronellolis* NRRL B-2504 and *Cupriavidus necator* DSM428. The cultures were reactivated by inoculation in CHROMagar™ Orientation plates with a sample of the cryopreserved bacteria and incubated at 30 ˚C for 48 h.

2.2.3.2.Inoculum and Cultivation Medium

A pre-inoculum was prepared by inoculating a single colony isolated from the CHROMagar™ Orientation plates into 100 mL liquid Luria Bertani (LB) medium (bacto tryptone, 10 g/L; yeast extract, 5.0 g/L; NaCl, 10 g/L, pH 7.0), in 250 mL baffled shake flasks, and incubated in an orbital shaker at 200 rpm and 30 ˚C, for 24 h. Such cultures served as pre-inocula for the bioreactor experiments. The inoculum was prepared by transferring 4×20 mL of the pre-inoculum to four 500 mL baffled shake flasks with 200 mL of LB medium. The shake flasks were kept in the orbital shaker, at 30 °C and 200 rpm, for another 24 h.

2.2.3.3.Batch Cultivation

Batch cultivations of monocultures of *P. citronellolis* and *C.necator*, and the co-culture of both strains were performed in a 10 L BioStat®B-Plus bioreactor (Sartorius, Germany) with a starting volume of 9.5 L. The cultivation medium was composed of 8.5 L of waste apple pulp supernatant prepared as described above, supplemented with 1 L of a mineral solution (composed of $(NH_4)_2HPO_4$, 11 g/L; KH_2O_4P, 58 g/L; KH_2PO_4, 37 g/L), 100 mL of 100 mM $MgSO_4$ solution and 10 mL of the micronutrients solution (with the composition described above). A 10% (v/v) inoculum (800 mL) was used.

The bioreactor was operated under a batch mode during 48 h. The temperature and the pH were controlled at 30 ± 0.1 ˚C and 7.0 ± 0.1, respectively. The pH was controlled by the automatic addition of 5 M NaOH or 2 M HCl.

A constant air flow rate (4 SLPM, standard liters per minute) was kept during all experiments. The dissolved oxygen concentration (DO) was controlled at 30% of the air saturation by automatically adjusting the stirring speed between 300 and 800 rpm. Foam formation was automatically suppressed by addition of Antifoam A (Sigma-Aldrich). Samples were periodically taken from the bioreactor for quantification of the cell dry weight, PHA content in the biomass, ammonia and sugars concentration.

2.2.4. Analytical Techniques

2.2.4.1. Cellular Growth

Cellular growth was monitored during the experiment by measuring the optical density of the cultivation broth at 600 nm (OD_{600}nm) with a dilution necessary for the OD_{600} to be below 0.3 with deionised water as zero reference. All measurements were done in duplicate.

2.2.4.2. Biomass Quantification

The cell dry weight (CDW) was determined by gravimetry. The samples were centrifuged (10956×g, 15 min, 4 ºC) and the cell pellets were washed once by resuspension in deionized water and centrifuged. The washed pellets were lyophilized (ScanVac CoolSafeTM, LaboGene) at -110 ˚C for 48 h. The CDW was obtained by weighing the lyophilized cell pellets. All samples were done in triplicate.

2.2.4.3. Nile Blue Staining

In an Eppendorf tube, 0.5 µL of Nile Blue was added to 0.5 mL cultivation broth sample, covered with aluminium foil and placed in an oven at 70 ° C for 10 minutes. After this time, slides were prepared which were observed under the microscope (Olympus BX51 epifluorescence) under contrast light and fluorescent light, with a magnification of 100x.

2.2.4.4. Quantification of sugars

The sugars quantification in the supernatant samples was obtained by high performance liquid chromatography (HPLC), using a VARIAN Metacarb 87H column coupled to a refractive index (RI) detector. The analysis was performed at 50 °C using H_2SO_4 0.01 N, as eluent with a flow rate of 0.6 mL/min. The samples were prepared by diluting the cell-free supernatant, obtained by centrifugation of the cultivation broth, as described above, in a 1:20 proportion with the eluent. The samples were filtered using VWR centrifuge filters (0.2 µm). Moreover, galactose (Sigma-Aldrich, 99%) and a sugar mix (glucose, sucrose, fructose and arabinose) (Sigma-Aldrich, 99%) standards were used at concentrations of 0.0625 - 0.5 g/L.

2.2.4.5. Quantification of total Nitrogen

For the determination of total nitrogen a kit (LCK 388, LATON®) was used with a detection range of 20-100 mg/L. The sample (0.2 mL) was placed into a digestion flask, and a 2.3 ml of solution A and 1 ml of solution B (Koroleff Digestion – Peroxodisulphate) were added. The flasks were put in a HT 200S (HACH® - LANGE) digester for 15 min at 100 ºC. After cooling to room temperature, a Microcap capsule was added to the solution followed by vigorous stirring until the

capsule dissolves completely. A 0.5 mL of the digested solution was transferred to a new vial, which was later added, 0.2 mL of solution D (Photometric Detection with 2,6-Dimethylphenol) and quickly stirred. After 15 min the absorbance was read in a DR2800 tm spectrophotometer (HACH®).

2.2.4.6. Quantification of Ammonia

The ammonia was determined by colorimetry, as implemented in a flow segmented analyser (Skalar 5100, Skalar Analytical, The Netherlands). Ammonia chloride (Sigma-aldrich) was used as standard at concentration between of 5 and 20 mg/L. The cell-free supernatant was diluted (1:200) in deionized water and analysed.

2.2.5. Calculations

The maximum specific cell growth rate ($\mu_{max,}$ h^{-1}) was determined from the linear regression slope of the exponential phase of Ln X_t versus time, where X_t (g/L) is the active biomass (i.e., cells without PHA) at time *t* (h). The residual biomass was determined by equation 1:

$$X_t = CDW_t - PHA_t \quad (1)$$

where CDW_t (g/L) and PHA_t (g/L) are the cell dry weight and the concentration of polymer at time *t* (h). This concentration is given by the polymer accumulated in the cells (calculated on a dry basis, wt.%).

The volumetric productivity (r_p, g/L·day) was calculated by dividing the final PHA concentration (P, g/L) for the total time of fermentation (Δt, day).

The active biomass yield on substrate basis ($Y_{x/s}$, g_x/g_s) was determined by equation 2:

$$Y_{x/s} = \frac{\Delta X}{\Delta S} \quad (2)$$

where ΔX (g/L) is the active biomass (X) and ΔS (g/L) is the total sugars consumed during the cultivation.

The polymer yield on a substrate basis ($Y_{p/s}$, g_p/g_s) was calculated by equation 3:

$$Y_{p/s} = \frac{\Delta P}{\Delta S} \quad (3)$$

where ΔP (g/L) the PHA produced and ΔS (g/L) is the total sugars consumed during the cultivation.

2.2.6. Biopolymer extraction

2.2.6.1. PHA extraction and purification

At the end of the assays, the cultivation broth was recovered from the bioreactor and centrifuged (13131×*g*, for 20 min). Afterwards, the cell pellets thus obtained were resuspended in deionised

water and centrifuged again under the same conditions. The washed biomass was then lyophilized for 48 hours.

The PHA was extracted from the dried biomass by Soxhlet extraction with chloroform (Sigma-Aldrich, HPLC grade) as solvent (~10 g biomass for 250 mL chloroform), at 80 ˚C, for 48 h. Cell debris were removed by filtration with syringe filters with a pore size of 0.45 µm (GxF, GHPmembrane, PALL) and the polymer was precipitated in ice-cold ethanol (chloroform/ethanol 1:10, v/v). The precipitate was then recovered in a pre-weighted flask and left at room temperature, in a fume hood, for solvent evaporation.

2.2.6.2. Acetone Fractionation

To quantify the content of each type of polymer, scl- and mcl-PHA, in the blend obtained in the co-culture experiment, the method described by Ashby et al. (2005) (53) was used, with some modifications. It consisted in mixing 1 g of the polymer blend with excess acetone (30 mL) in a flask for 24 h at 30 ºC, under constant agitation (in an orbital shaker). The fractions were then separated by centrifugation (10 000 rpm, 10 min, 10 ºC) and the acetone-insoluble (AIS) polymer, P(3HB), was placed into a dry, pre-weighed vial, and let in a fume hood at room temperature, until constant weight. The acetone-soluble (AS) polymer (mcl-PHA) was transferred into a clean, tared pre-weighted vial and left at room temperature, in a fume hood, until complete solvent evaporation.

2.2.7. Biopolymer characterization

2.2.7.1. Composition

The PHA content in the biomass and the polymers' composition were determined by gas chromatography (GC) analysis following the methanolysis method described by Cruz et al. (2016) (47). Hydrolysis was achieved with 2 mL 20% (v/v) sulphuric acid (Sigma-aldrich, HPLC grade) in methanol (Fisher Chemical, HPLC grade) solution and 2 mL of benzoic acid in chloroform (1 g/L) (Sigma-aldrich, HPLC grade). Heptadecanoate (1.0 g/L) acted as internal standard. The hydrolysis was performed at 100 ºC, for 4 h. The procedure was used for dried cells samples (10 mg) and the purified polymers extracted with chloroform (3 mg). After the hydrolysis, 1 mL of deionised water was added in order to separate the organic from the aqueous phase, collected in vials and analysed by GC (430-GC, Bruker) with a Restek column of 60m, 0.53 mmID, 1 µM df, Crossbond, Stabilwax. The injection volume was 2.0 µL, with a running time of 32 min, a constant pressure of 14.50 psi and helium as carrier gas. The heating ramp was 0 to 3 min a rate of 20˚C/min until 100˚C, 3 to 21 min at a rate of 3˚C/min until 155 ˚C and 21 to 32 min at a rate of 20˚C/min until 220˚C. The calibration curve was made using mcl-PHA with 3wt% 3-hydroxyhexanoate (3HHx), 17wt% 3-hydroxyoctanoate (3HO), 57wt% 3-hydroxydecanoate (3HD), 11wt% 3-

hydroxydodecanoate (3HDd) and 12wt% 3-hydroxytetradecanoate (3HTd) in concentrations ranging from 0.1 to 2.0 g/L. P(3HB-co-3HV) (Sigma-Aldrich, 88 mol% 3HB, 12 mol% 3HV) acted as PHB standard in concentrations ranging from 0.4 to 8.0 g/L. Both calibration curves were prepared in benzoic acid in chloroform (1 g/L).

2.2.7.2. Fourier Transform Infrared Spectroscopy

Fourier transform infrared spectroscopy (FTIR) analysis was conducted with a Perkin-Elmer Spectrum two spectrometer. The polymer was directly analysed on the FTIR cells. The spectra were recorded between 400 and 4000 cm^{-1} resolution and 10 scans were conducted at room temperature.

2.2.7.3. Molecular Mass Distribution

A sample (15 mg) of each polymer was dissolved in 3 mL of chloroform, for 18 h at room temperature. Then, the solution was filtered with a glass fibber filter 47 mm (PALL) and analysed by a Size Exclusion Chromatography (SEC) System (Waters Millenium) with support SEC: PLgel 5 µm Guard; Polymer Laboratories; 50×7.5 mm, PLgel 5 µm 104 Å; Polymer Laboratories; 300×7.5 mm, PLgel 5 µm 500 Å; Polymer Laboratories; 300×7.5 mm. Using a temperature of equilibration of 30˚C, with a flow rate of 1 mL/min, degasing and chloroform as the mobile phase. Samples were stored at 4 ˚C before injecting 100 µL in the SEC circuit. A RI detector (Waters 2410) was adopted for polymer detection using the sensitivity 512 and a collect duration of 25 min.

2.2.7.4.Thermal Properties

Differential Scanning Calorimetry (DSC) analysis was performed using a differential scanning calorimeter DSC 131 (Setaram, France). The samples were placed in aluminium crucibles and analysed in the temperature range between -90 and 120 °C, with heating and cooling speeds of 10 °C/min. Thermogravimetric Analysis (TGA) was performed using a thermogravimetric equipment Labsys EVO (Setaram, France). Samples were placed in aluminium crucibles and analysed in the temperature range between 25 and 500 °C, at 10 °C/min. The melting temperature (T_m, ºC) was determined at the minimum of the exothermic peak. The degree of crystallinity (X_c) was calculated by comparing the area of the melting peak (ΔH_m, J/g) with the melting enthalpy of 100% crystalline P(3HB) ($\Delta H_{m100\%}$). The heat of melting of an infinite crystal of P(3HB) was estimated as 146 J/g (46).

$$X_c = \frac{\Delta H_f}{\Delta H_{f,100}} \times 100 \quad (4)$$

2.2.7.5. X-Ray Diffraction

The structural analysis of the samples was performed by X-ray diffraction (XRD) using a X'Pert Pro X-ray diffractometer from PANalytical (Almelo, Netherlands), equipped with an X'Celerator detector, in a Bragg–Brentano geometry with Cu Kα line radiation (λ = 1.5406˚A). The 2θ scans were performed from 10˚ to 90˚, with a step size of 0.03˚.

2.3. Results and Discussion

2.3.1. Shake Flask Screening Assay

The ability of several bacterial strain to accumulate PHA, namely mcl-PHA and PHB, using apple pulp waste as sole substrate was evaluated during a course of a shake flask screening assay. This experiment allowed to recognize the bacteria that performed a better cellular growth alongside with the highest polymer's accumulation.

In this shake flask assay, a group of bacteria known to accumulate PHA, specifically *Pseudomonas resinovarans*, *Pseudomonas citronellolis*, *Pseudomonas stutzeri* and *Cupriavidus necator*, were tested using apple pulp waste as the sole carbon source for the accumulation of PHB and mcl-PHA.

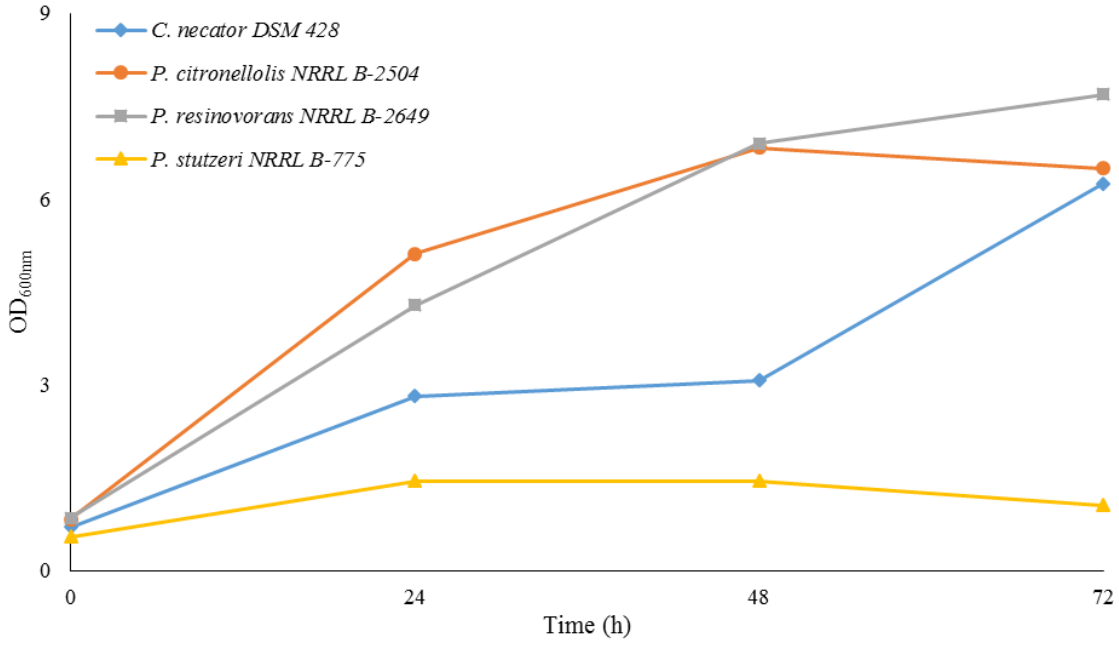

Figure 3 - Cellular growth profile of the different bacterial strains tested with apple pulp waste as the sole carbon source.

The cellular growth profile (**Figure 3**) and gravimetric quantification of the CDW (**Table 3**) of the microorganisms demonstrates that all the strains except *P. stutzeri*, were the growth was very reduced, were able to grow using apple pulp waste as the carbon source on the course of this assay. The gravimetric quantification of CDW allowed to prove that in the end of the assay, *P. resinovorans*, *P. citronellolis* and *C. necator*, all presented higher values of biomass content unlike *P. stutzeri*. In the beginning of the assay, the biomass value was negligible, since the sample analysed by gravimetric quantification of the CDW did not have enough biomass to be demonstrative of the culture, hence it is not presented in **Table 3**.

Table 3. Cell dry weight (g/L) of *P. stuzeri* NRRL B-775, *C. necator* DSM 428, *P. citronellolis* NRRL B-2504 and *P. resinovorans* NRRL B-2649 obtained on the shake flask screening assay.

Time (h)	***P. stuzeri* NRRL B-775**	***C. necator* DSM 428**	***P. citronellolis* NRRL B-2504**	***P. resinovorans* NRRL B-2649**
24	0.48	1.77	2.53	1.75
48	0.62	2.18	5.11	2.68
72	0.67	3.35	5.22	3.37

Within 72 h of the assay, *P. resinovorans* NRRL B-2649 presented the highest cellular growth, as shown by an OD_{600nm} of 7.69 (**Figure 3**). However, it corresponded to only 3.37 g/L of CDW. A value close to the one obtained for *C. necator* DSM 428 (3.35 g/L), but still below the CDW obtained for *P. citronellolis* NRRL B-2504. This bacterium, also reached a very similar growth to that of *P. resinovorans*, an OD_{600nm} of 6.83, and in addition, reached the highest value of CDW, 5.22 g/L, during the 72 h of the assay. *P. stutzeri* revealed to be the microorganism that presented the lowest cellular growth and biomass, respectively, of 1.05 and 0.67 g/L, within 72 h.

The apple pulp waste used as the sole carbon source (**Figure 4**) had a total sugars content of 31.0 g/L, out of which 27.2 g/L were accounted as the monosaccharides fructose (17.9 g/L) and glucose (9.3 g/L). Sucrose was also detected at low concentrations (below 3.4 g/L) and arabinose showed only traces (0.3 g/L) within the apple residue.

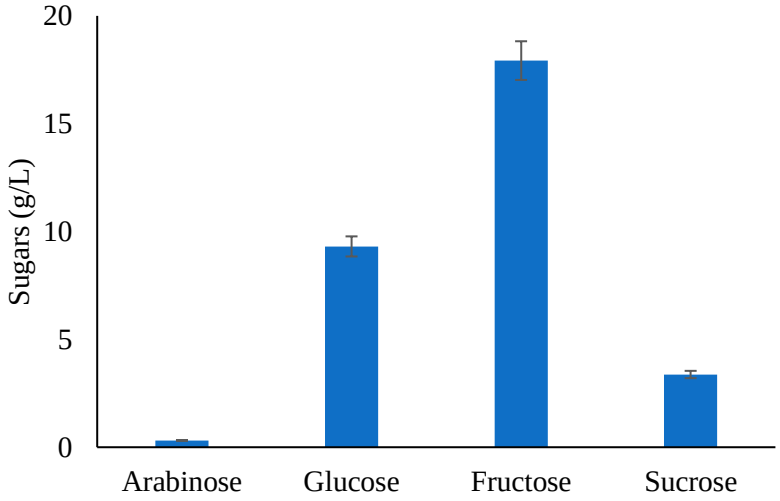

Figure 4 - Sugars profile presents in apple pulp waste, namely arabinose, glucose, fructose and sucrose, at the beginning of the shake flask screening assay.

Figure 5 shows the sugar profile in the supernatant samples, namely, arabinose, glucose, fructose and sucrose, for the 72 h of the assay, for all bacterial strains tested. As it can be seen, *P. stutzeri* does not show a significant decrease in the consumption of any of the sugars, which confirms the practically null cell growth, verified in **Figure 3**. On the other hand, the other *Pseudomonas* strains tested were able to consume most of the available sugars, especially glucose and fructose.

P. citronellolis showed a preference for glucose, which was consumed rapidly (at the end of 48 h it was depleted). The consumption of fructose was slower and occurred, mostly, after the full consumption of glucose. Sucrose appears to have be consumed only after the depletion of glucose too. After 48 h of the cultivation (**Figure 5**), glucose was almost depleted (0.11 g/L) and 5.41 g/L fructose were consumed until the end of the run. Sucrose showed 1.67 g/L of consumption in the last 24 h (**Figure 5**). *P. resinovorans* did not appear to have consumed arabinose or sucrose. Glucose and fructose were consumed simultaneously (3.96 and 5.87 g/L) although the culture was not able to consume to exhaustion all the monosaccharides present in the apple pulp. As for *C. necator*, fructose revealed to be monosaccharide most consumed over the 72 h of cultivation (4.38 g/L). This bacterium is known to growth and produce PHA, specifically PHB, from sugars, namely glucose, fructose and sucrose, present in the orange juice residues as substrate (55). It is interesting to notice that the bacteria revealed a significant growth from 48 h until the end of the assay, which may be related with consumption of fructose, more enhanced in last 24 h of the assay, without having consumed glucose.

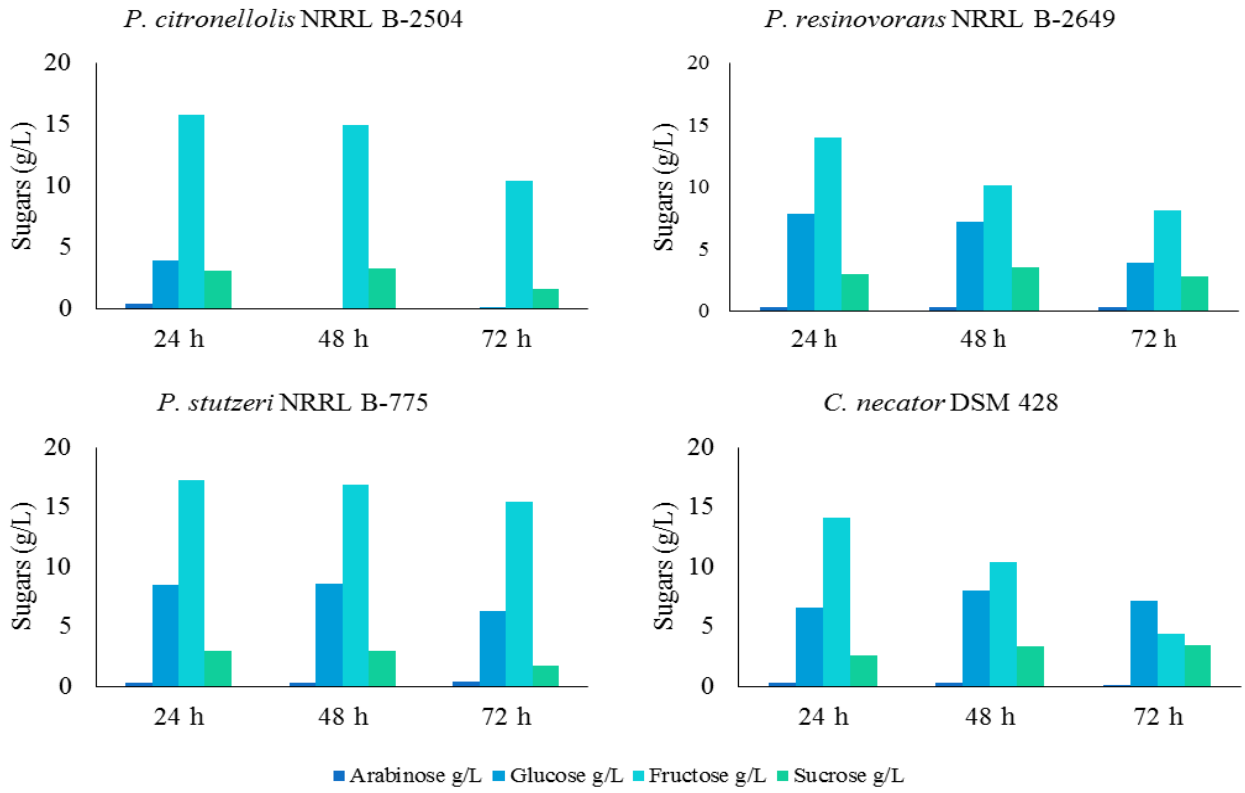

Figure 5 - Sugar profiles, namely arabinose, glucose, fructose and sucrose, in the supernatant for each shake flask assay for different bacterial strains tested with apple pulp waste as the sole carbon source.

To confirm that PHA accumulation was occurring, Nile Blue staining was used upon several samples of the cultivation from the shake flask at 24 h, 48 h and 72 h upon the inoculation (**Figure 6**). The microorganisms were observed under the microscope using fluorescence, which allowed the visualization of the bacteria and the PHA accumulated inside the cells. **Figure 6** show that an increase of the fluorescence was observed, indicating an increase of the PHA inside the cells during the 72 h of the assays. It is also visible that all microorganisms were able to produce PHA however, *C. necator* DSM 428 and *P. citronellolis* NRRL B-2504 seemed to be the bacterial cells with higher PHA accumulation both at 48 h and 72 h.

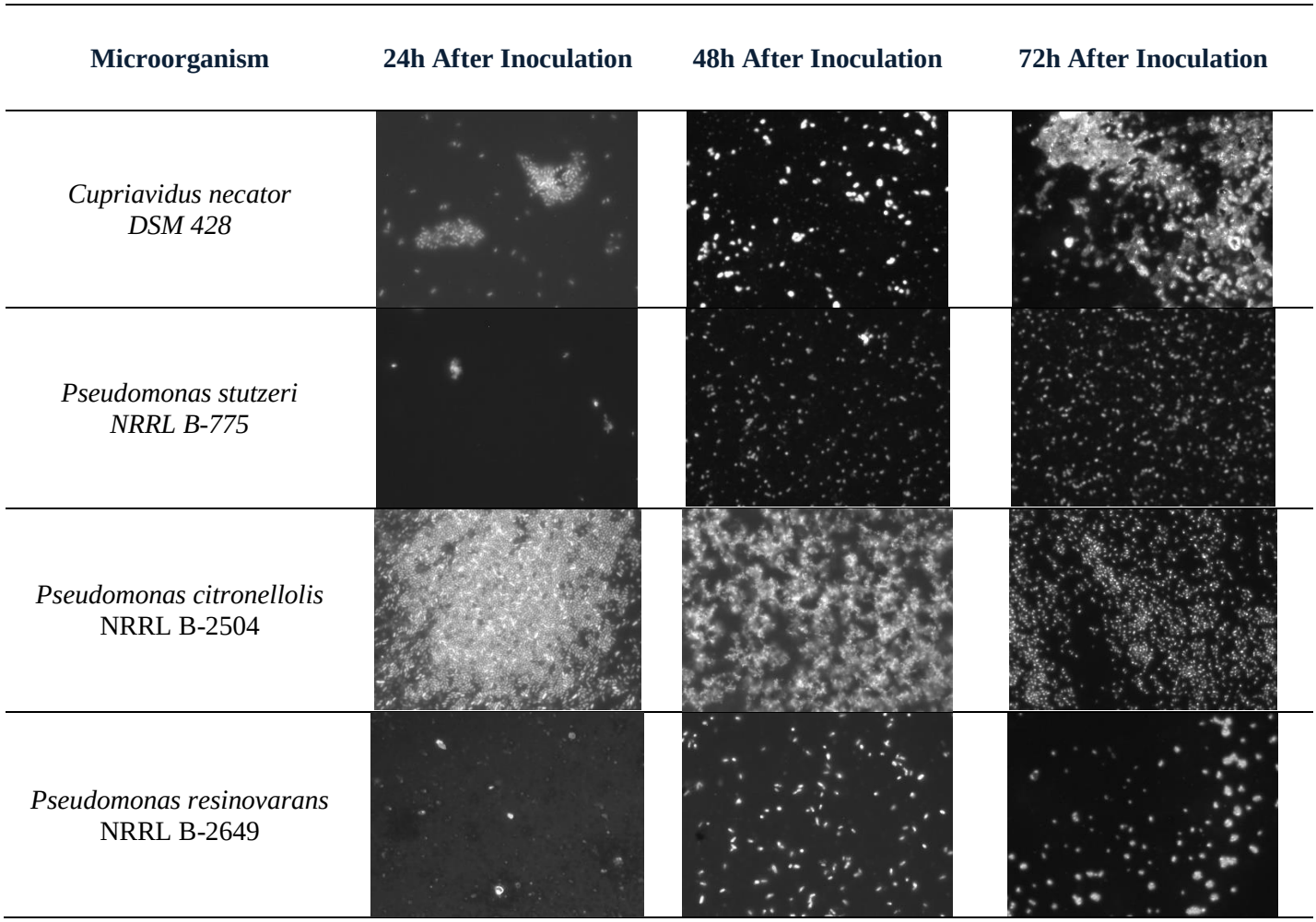

Figure 6 - Visualization of the several bacterial strain cells under the microscope (100x) during different hours of cultivation, under fluorescence after Nile Blue staining.

So far, *P. citronellolis* and *C. necator* have been studied for the production of PHA, namely *P. citronellolis* was reported as a mcl-PHA producer and *C. necator* as a PHB producer, using an extensive range of feedstocks, including saturated biodiesel fractions (42), fatty acids by-product (35), free fatty acids (35), margarine fat waste (46), animal-derived waste (35) and fruit wastes

(e.g., grapes, apricots, cherries, etc.) (48). So, in order to study and comprehend more about these strains and their ability to produce both mcl-PHA and PHB using apple pulp waste, they were selected to proceed with the bioreactor assays for these polymers production.

2.3.2. PHA production from waste apple pulp

In order to characterize mcl-PHA and PHB produced, respectively, by *P. citronellolis* NRRL B-2504 and *C. necator* DSM 428, bioreactor experiments with each bacterium were performed using apple pulp waste as the sole source of carbon. Moreover, a third experiment was performed with a co-culture of both strains. The production using co-cultivation arose because *C. necator* does not use glucose, only the fructose present in the pulp, whereas *P. citronellolis* is preferred by glucose, consuming the fructose more slowly. Thus, with co-cultivation, it was intended to maximize the consumption of both sugars present in the pulp and also to obtain the polymers of each strain in the form of a blend.

2.3.2.1. Production of mcl-PHA by *P. citronellolis* NRRL B-2504

Figure 7 (A and B) presents the cultivation profile of the batch cultivation of *P. citronellolis* using waste apple pulp as the sole substrate.

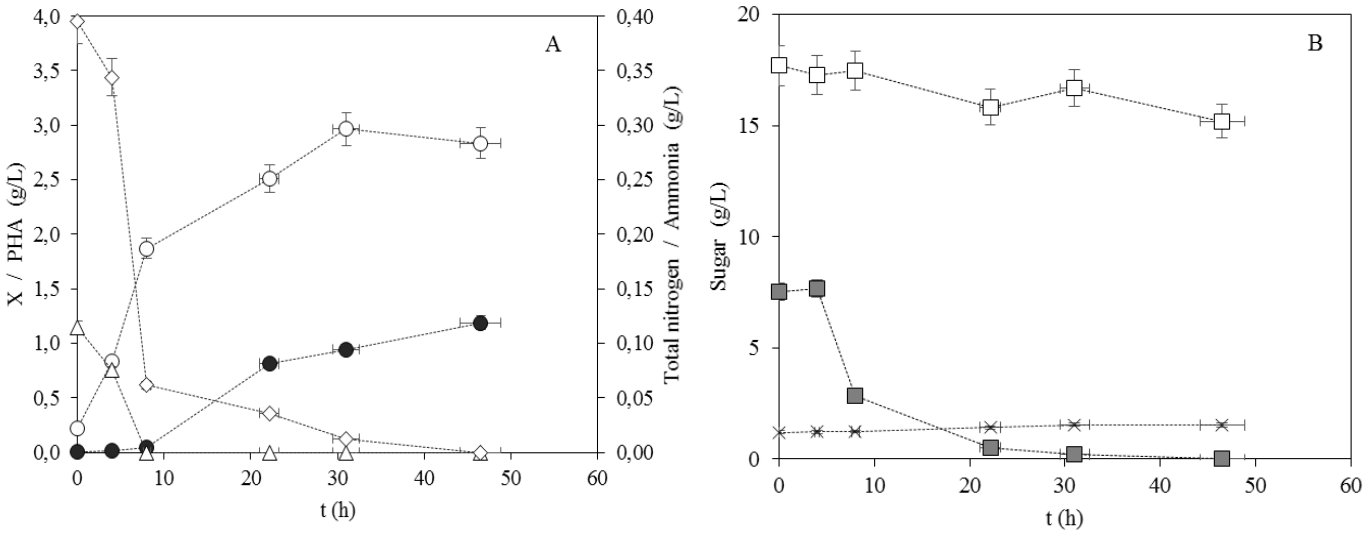

Figure 7 - Cultivation profile of *P. citronellolis* NRRL B-2504 using apple pulp waste as the sole carbon source (concentration of active biomass (○), PHA (●), total nitrogen (◇), ammonia (△), glucose (■), fructose (□) and sucrose (⊗)).

Figure 7 (A) shows a short lag phase, of nearly 2 h, afterwards the cultivation entered in a long growth phase that lasted around 20 h. The culture grew at a specific cell growth rate of 0.24 h^{-1} (**Table 4**) a value considerably higher than the ones reported for cultivation of *P. citronellolis* in a fed-batch bioreactor run using tallow-based biodiesel (0.08-0.10 h^{-1}), thus demonstrating apple pulp waste provided a more suitable feedstock for the culture's cell growth (42). The ammonia levels become very low (0.08 g/L), limiting the growth of the culture, from which PHA concentration increased, while the apple pulp waste sugars concentration (**Figure 7** (B)), mainly

glucose and sucrose decreased. During the exponential phase, when the available ammonia was depleted, an active biomass concentration of 1.9 g/L had been reached within 8 h of cultivation (**Figure 7** (A)). However, there was still nitrogen present in the medium (62 mg/L) (**Figure 7** (A)), which allowed a lower rate of cell growth (0.05 h^{-1}). This nitrogen was present in the apple pulp waste and allowed the culture to attain a maximum active biomass concentration of 2.8 g/L at 31 h of cultivation (**Figure 7** (A)). During the course of the batch fermentation, the polymer production was initiated by the time ammonia was exhausted and the cell growth rate decreased (**Figure 7** (A)). At the end of the assay, was obtained a PHA concentration of 1.2 g/L (**Table 4**). This corresponds to an overall volumetric productivity of 0.61 g/L.day. This value is lower than that reported in the literature of 1.61-2.40 g/L.day, which was obtained in a fed-batch bioreactor cultivation wherein a higher CDW was reached (42). PHA content in the biomass was 30wt.%, higher than the values reported for *P. citronellolis* grown on different substrates, 3-27% and close to those for mcl-PHA produced (15-36wt.%) by different bacteria strain, such as *P. resinovarans* (47) and *P. chlororaphis* (39). The apple pulp waste display a total concentration of 31.0 g/L of sugars, wherein 25.2 g/L represented the monosaccharides fructose (17.7 g/L) and glucose (7.5 g/L). Sucrose was also detected, however, at low concentrations (below 2.0 g/L). Within approximately 20 h of the batch fermentation, glucose was depleted (**Figure 7** (B)). On the other hand, fructose display a low consumption (2.5 g/L) until the end of experiment which ended in not being completely consumed. Oppositely, sucrose was not consumed (**Figure 7** (B)). Considering the monosaccharide sugars, glucose and fructose, in the substrate, there was a 10.0 g/L of total consumption, which corresponds to an active biomass and polymer yield on an apple pulp waste of, 0.27 g_X/g_s and 0.12 g_p/g_s, respectively.

Table 4. Kinetic and stoichiometric parameters for mcl-PHA production by *P. citronellolis* NRRL B-2504 using several wastes and by-products as feedstocks (μ_{max}, maximum specific cell growth rate; CDW, cell dry weight; r_p, volumetric productivity; $Y_{x/s}$, active biomass yield on a substrate; $Y_{p/s}$, polymer yield on a substrate basis; n.a., data not available).

Feedstock	**Cultivation Mode**	μ_{max} **(h^{-1})**	**CDW (g/L)**	**X (g/L)**	**PHA (wt.%)**	**PHA (g/L)**	r_p **(g/L.day)**	$Y_{X/S}$ **(g_X/g_s)**	$Y_{P/S}$ **(g_p/g_s)**	**References**
Apple pulp waste	Batch bioreactor	0.24	4.0	2.8	30	1.2	0.61	0.27	0.12(*)	This study
Tallow-based biodiesel	Fed-batch bioreactor	0.08-0.10	11.2-14.1	8.4-11.2	20-27	2.8-2.9	1.61-2.40	n.a.	n.a.	(42)
Olive oil distillate	Shake flask	n.a.	4.8	4.3	10	0.5	0.19	n.a.	0.08	(35)
Fatty acids by-product	Shake flask	n.a.	3.5	3.4	3	0.1	0.10	n.a.	0.02	(35)
Tallow free fatty acids	Shake flask	n.a.	1.7	1.6	3	0.05	0.02-0.03	n.a.	n.a.	(56)
Margarine waste	Shake flask	n.a.	6.3	5.8	8	0.5	0.17	n.a.	n.a.	(46)

(*) Calculated considering the consumption of sugars, glucose and fructose.

2.3.2.2. Production of PHB by *C. necator* DSM 428

Figure 8 (A and B) represents the cultivation profile of the batch bioreactor cultivation run of *C. necator* DSM 428 with apple pulp waste as the sole substrate.

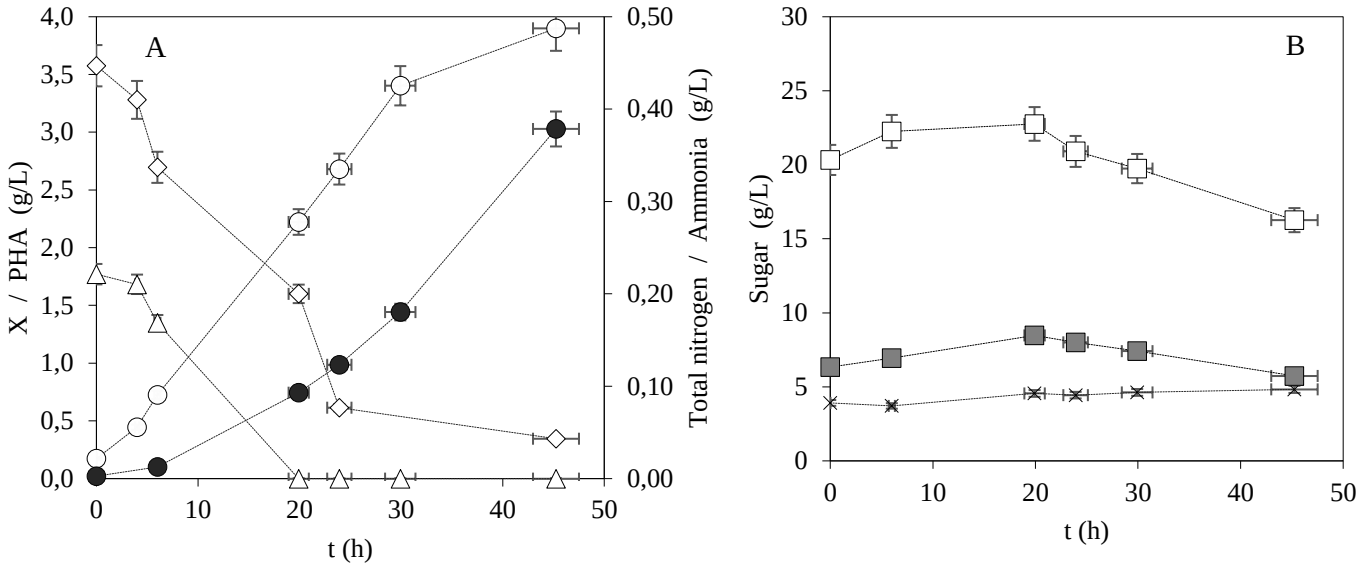

Figure 8 - Cultivation profile of *C. necator* DSM428 using apple pulp waste as the sole carbon source (concentration of active biomass (○), PHA (●), total nitrogen (◇), ammonia (△), glucose (■), fructose (□) and sucrose (⊗)).

The available ammonia was exhausted within 20 h of cultivation, but there was still nitrogen available, as shown by the total nitrogen concentration of 0.20 g/L at that time, thus supporting cell growth until the end of the run, although at a lower rate. Polymer accumulation started around 6 h, attaining a final concentration of 3.03 g/L (**Figure 8** (A)) by the end of the run, corresponding to an overall volumetric productivity of 1.59 gPHA/L.day (**Table 5**). This parameter obtained with apple pulp waste is among the values reported for soybean and jatropha oils (57–59). The PHA content in the biomass reached 44 wt.% at the end of the batch fermentation (45 h). This value is within those obtained, 20 to 53 wt.%, for batch and fed-batch cultivations of *C. necator* using waste oil from rhamnose production (60). *C. necator* was previously tested using cooking oil as the sole carbon source, reaching values of 37 wt.% of polymer content in the biomass, a value lower than that obtained with apple pulp (50). Soy-bean (57,58) and jatropha (59) oils have been reported as substrates for *C. necator* cultivation with significantly higher PHA content in the biomass (72-87 wt.%). However, those runs were performed in fed-batch mode with different cultivation conditions, regarding the feeding and the nitrogen source. For instance, productions with soy-bean oil used ammonium chloride to fed the culture broth to avoid nitrogen depletion, in order to supply enough nitrogen sources for cell growth, whilst, the production with jatropha oil used urea as nitrogen source that allowed to increase CDW and PHB accumulation.

The sugars profile over cultivation time was also analysed (**Figure 8** (B)). The cultivation started with a total sugars content of approximately 31 g/L. The overall sugar consumption was approximately 9 g/L. Fructose stands out as the most consumed monosaccharide (6.50 g/L) followed by glucose which presented a lower consumption (2.74 g/L). Sucrose showed no visible consumption. During the first 20 h after inoculation, the culture did not present sugar consumption, however, presented cell growth. This may be due to the presence of other components, such as nutrients, minerals and some amino acids, which are present in the apple pulp, and contribute to cell growth (11). The same was reported for shake flask production of P(3HB) of the same strain using palm oil pressed juice (OPF juice) containing the same sugars found in apple pulp, namely fructose, sucrose and glucose. In this study, the presence of nutrients, minerals and some amino acids could be used by the bacteria, in this case *C. necator*, as supplementary substrates to growth and simultaneously contribute to the production of P(3HB) (61). It is also important to note that the optimum concentration for the production of PHB is about 9 g/L. High and low concentrations of approximately 40 and 2.5 g/L, respectively, reduce productivity (61). By 20 h, the glucose concentration was below 9 g/L and only thereafter increased significantly, may have influenced the polymer production by the culture.

At the end of the assay, a yield of 0.42 g_x/g_s and 0.34 g_p/g_s for $Y_{x/s}$ and $Y_{p/s}$ (**Table 5**) were achieved, respectively. Previous studies have already reported the use of sucrose, glucose and fructose that is present in orange juice during shake flask cultivations with a different strain, namely *C. necator* H16, than the one used with the apple pulp waste (55). The assays presented a very close $Y_{p/s}$, of 0.39 g_p/g_s and cell growth rate of 0.12 h^{-1} to the apple pulp waste, proving that a different *C. necator* strain is able to produce PHB with fructose and glucose as the carbon source present in apple pulp waste (55).

Table 5. Kinetic and stoichiometric parameters for PHB production by *C. necator* DMS 428 using several wastes and by-products as feedstocks (μ_{max}, maximum specific cell growth rate; CDW, cell dry weight; r_p, volumetric productivity; $Y_{x/s}$, active biomass yield on a substrate basis; $Y_{p/s}$, polymer yield on a substrate basis (calculated considering the consumption of sugars, glucose and fructose); n.a., data not available).

Carbon Source	**Cultivation Mode**	μ_{max} **(h^{-1})**	**CDW (g/L)**	**X (g/L)**	**PHA (wt.%)**	**PHA (g/L)**	r_p **(g/L.day)**	$Y_{X/S}$ **(g_x/g_s)**	$Y_{P/S}$ **(g_p/g_s)**	**References**
Apple pulp waste	Batch bioreactor	0.12	6.93	3.9	44	3.0	1.59	0.42	0.34(*)	This study
Soybean oil	Batch bioreactor Fed-batch bioreactor	n.a.	15 32-126	n.a. n.a.	83 72-81	13 24-96	0.14 0.26-1.40	n.a. n.a.	0.82 0.72-0.85	(57,58)
Jatropha oil	Fed-batch bioreactor	n.a.	13.1	n.a.	87	11.4	0.24	n.a.	0.78	(59)
Waste oil from rhamnose	Batch bioreactor Fed-batch bioreactor	n.a. n.a.	6.3 15.4	n.a. n.a.	20 41	1.24 6.36	0.017 0.088	n.a.	n.a. n.a.	(60)
Margarine waste	Batch bioreactor	0.15	11.2 ±2.26	n.a.	56±2.42	6.4 ±1.50	0.33 ± 0.07	n.a.	0.50 ± 0.15	(46)
Orange Juice	Shake Flask	0.12	9.01	n.a.	82	7.3	n.a.	0.46	0.39	(55)
Spent Coffee Grounds	Fed-Batch bioreactor	0.15	16.7	n.a.	78.4	13.1	4.7	n.a.	0.77	(62)
Fructose/Glucose	Batch bioreactor	n.a.	10.3	n.a.	71	7.3	0.33	n.a.	0.38	(63)

(*) Calculated considering the consumption of sugars, glucose and fructose.

2.3.2.3. Co-culture of *P. citronellolis* NRRL B-2504 and *C. necator* DSM 428

During the shake flask screening assay, it was noticed that *P. citronellolis* NRRL B-2504 and *C. necator* DSM 428 had different uptakes of the sugars present within apple pulp waste. More specifically, *P. citronellolis* demonstrated a preference for glucose, while fructose was consumed only after exhaustion of glucose, whilst *C. necator* showed only consumption of fructose. Therefore, taking advantage of this, a co-culture experiment of *P. citronellolis* and *C. necator* was performed. Moreover, this experiment also allowed to produce a natural PHB/mcl-PHA blend. The same conditions as the ones used for the monoculture cultivation of each strain were used. **Figure 9** (A) and (B) displays the growth profile of the co-culture assay.

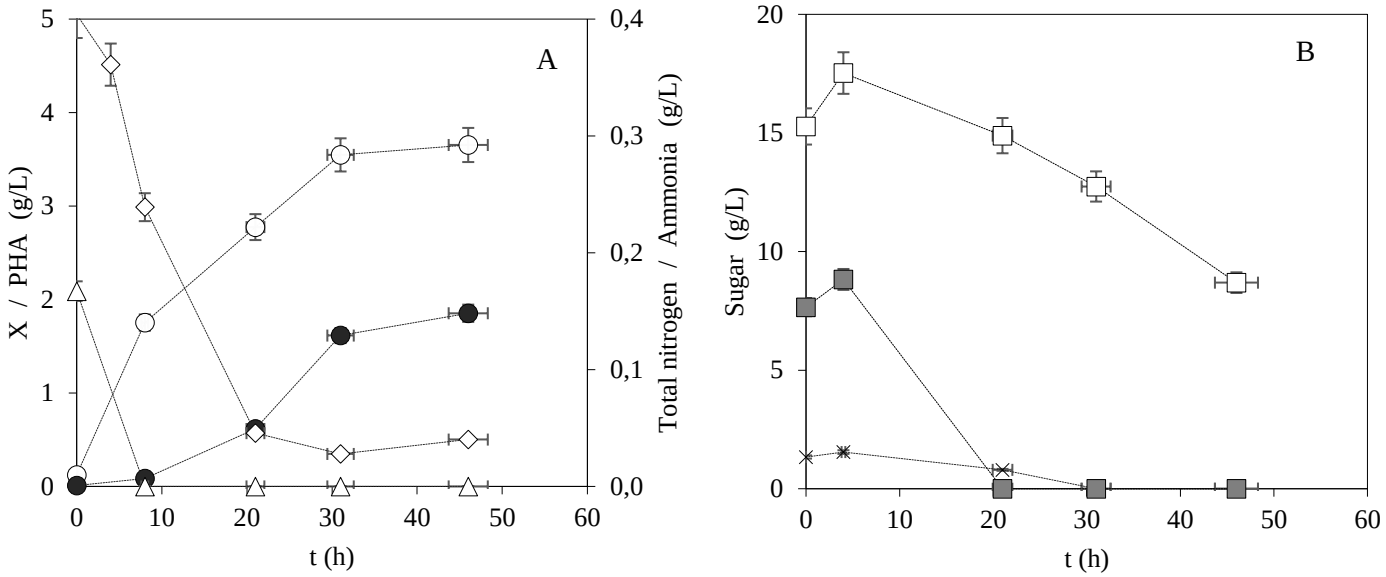

Figure 9 - Cultivation profile of the co-culture using apple pulp waste as the sole carbon source (concentration of active biomass (○), PHA (●), total nitrogen (◇), ammonia (△), glucose (■), fructose (□) and sucrose (⊗)).

Apple pulp waste supported cellular growth (**Figure 9** (A)) and polymer production of both *P. citronellolis* (which produced mcl-PHA) and *C. necator* (which produced P(3HB)). Ammonia became depleted by 8 h into cultivation, but there was still nitrogen available (as shown by the total nitrogen content of 0.24 g/L) (**Figure 9** (A)), which supported cell growth until around 31 h of cultivation, culminating in a CDW of 5.5 g/L. The co-culture presented CDW and active biomass (3.7 g/L) higher than those obtained in the *P. citronellolis* cultivation but above the ones attained in the *C. necator* production (**Table 6**). The polymers' content in the biomass was 34 wt. %. This corresponded to a final production of 1.9 g/L and a volumetric productivity of 0.96 g/L.day (**Table 6**). The initial concentration sugars (sucrose, glucose and fructose) (**Figure 9** (B)) at the beginning of the run was 24.3 g/L, with an uptake of 15.6 g/L by the end of the cultivation.

Sucrose and glucose were totally consumed, and approximately 6.6 g/L of fructose were converted, as it can be seen in **Figure 9** (B). After 4 h of culture, sucrose and glucose were totally consumed. Fructose also showed significant consumption and was the only sugar present at the end of the trial. Similar to *P. citronellolis* production, co-cultivation showed a much higher consumption of sugars, where only glucose was totally consumed and sucrose presented a lower consumption. As regards *C. necator* production, co-cultivation showed a higher sugar consumption, in which fructose was not fully consumed either, and glucose and sucrose showed a high consumption but were not fully consumed at the end of the experiment. At the end of the assay, a yield of 0.23 g_x/g_s and 0.12 g_p/g_s for $Y_{x/s}$ and $Y_{p/s}$ were achieved, respectively (**Table 6**). Similar yields were obtained for the batch production with *P. citronellolis*.

(*) Calculated considering the consumption of sugars, glucose and fructose.

Table 6. Kinetic and stoichiometric parameters of the three batch productions by *P. citronellolis* NRRL B-2504, *C. necator* DSM 428 and the co-culture using apple pulp waste (μ_{max}, maximum specific cell growth rate; CDW, cell dry weight; r_p, volumetric productivity; $Y_{x/s}$, active biomass yield on a substrate basis; $Y_{p/s}$, polymer yield on a substrate basis (calculated considering the consumption of sugars, glucose and fructose); n.a., data not available).

Batch Production	μ_{max} **(h^{-1})**	**CDW (g/L)**	**X (g/L)**	**PHA (wt.%)**	**PHA (g/L)**	r_p **(g/L.day)**	$Y_{X/S}$ **(g_x/g_s)**	$Y_{P/S}$ **(g_p/g_s)**(*)
P. citronellolis NRRL B-2504	0.24	4.02	2.8	30	1.2	0.61	0.27	0.12
C. necator DSM 428	0.12	6.93	3.9	44	3.0	1.59	0.42	0.34
Co-culture of *P. citronellolis* and *C. necator*	0.33	5.51	3.7	34	1.9	0.96	0.23	0.12

The co-culture strategy for the production of PHA blends has been reported by Ashby et al. (53) that demonstrated the production of P(3HB)/mcl-PHA blends with tenable blend ratios by a co-culture of *P. oleovorans* and *P. corrugata* using glycerol as substrate. The cultures required different concentrations of glycerol to achieve the optimal production of polymer. This allowed for a better control of the P(3HB)/mcl-PHA blend ratios. By using this rationale, it was possible to produce P(3HB)/mcl-PHA blends over a range of ratios simply by varying the initial glycerol concentration, the time of inoculation of each organism, and the duration of the fermentations (53).

2.3.3. Polymers Characterization

2.3.3.1. Composition

The polymers produced in the three batch assays using *P. citronellolis* and *C. necator* monocultures, and their co-culture were characterized in order to identify their monomeric composition. The assay using *P. citronellolis* with apple pulp waste produced mcl-PHA, which was mainly composed of 3-hydroxydecanoate (HD), 68 wt% and 3-hydroxyoctanoate (HO), 22 wt% (**Table 8**). It also had minor contents of 3-hydroxydodecanoate (HDd), 5 wt%, and 3-hydroxytetradecanoate (HTd), 4 wt%, while only traces of 3-hydroxyhexanoate (HHx), 1 wt%, were detected. The same monomers were reported for other *mcl*-PHA synthesized by *P. citronellolis* strains (**Table 8**), although their relative content is significantly different. HD and HO were the main monomers, but HD was the dominant component in the *mcl*-PHA produced from apple pulp waste, while both monomers were present in similar amounts or HO had a higher content for the mcl-PHA produced from saturated biodiesel fraction (42), olive oil distillate (35), fatty acids by-product (35) and tallow fatty acids (56). These differences may be related with different substrates. Comparing the mcl-PHA with others produced by other *Pseudomonas* sp., it is clear that the composition of the synthesized polymer is highly dependent, not only from the producing strain, but also from the feedstock used (**Table 8**). For example, productions using *P. mediterranea* CFBP 5447 (43) and *P. stutzeri* 1317 (51,64) resulted in a mcl-PHA with monomer composition similar to the one produced by *P. citronellolis* from apple pulp waste using glycerol or glucose, respectively, as carbon sources.

The polymer produced by *C. necator* DSM 428 (**Table 9**) was a homopolymer composed by 3-hydroxybutyrate (3HB). The composition is very similar to the ones obtained for the same strain using several different feedstocks, such as, used cooking oil (35,50), olive oil distillate (35), fatty acids byproduct (35), spent coffee grounds oil (62) and margarine waste (46), where the polymers obtained from this productions were also homopolymers P(3HB). *P. oleovarans* (**Table 9**) also produced a similar polymer using different feedstocks, namely fatty acids byproducts (35), olive oil distillate (35) and hydrolysed pollock oil (35), which resulted in a P(3HB) homopolymer. Previous studies reported similar results revealed that *C. necator* has a Type I synthase, therefore it is only able to synthesize two monomers, 3HB and 3HV, respectively, and the last one if it uses precursors (35).

The polymer recovered from the biomass produced by co-culturing *P. citronellolis* NRRL B-2504 and *C. necator* DSM 428 was composed of 48 wt% HB, 36 wt% HD, 10 wt% HO, 3 wt% HDd, 3 wt% HTd and traces of HHx (0.5 wt%) (**Table 7**). These results proved that the polymer obtained by the co-culture of *P. citronellolis* and *C. necator* was a random blend with the same monomer composition as the individual polymers of each culture. Hence, both bacteria were able to growth and accumulate polymer. The acetone fractionation allowed to determine the effects the co-culture may have had on the repeat unit compositions of the P(3HB) and mcl-PHA blend

components of the polymer produced. The two polymers in a sample of the blend were separated by fractionation with acetone. The acetone insoluble and acetone soluble fraction for the polymer blend contained P(3HB) and mcl-PHA, respectively. The last one presented the same monomers as the ones that composed the mcl-PHA attained from the production with *P. citronellolis*. Overall, all the mcl-PHAs showed HD and HO as their primarily monomers (**Table 7**). However, exists a considerable difference between the composition of the mcl-PHA component of the blend and the composition found in the polymer blend. As for the P(3HB) obtained, the sample that was recovered was not pure, hence there still some mcl-PHA present in the P(3HB) analysed (**Table 7**).

The separately produced polymers, P (3HB) and mcl-PHA, have a monomeric composition which relates to that obtained with the blend obtained in the co-culture, and vice versa. The same monomers that constitute the mcl-PHA by *P. citronellolis* (HHx-HO-HD-HDd-HTd) are the same as those found in the blend and the mcl-PHA component of the blend, with the HO and HD monomers in the majority. The polymer produced by *C. necator*, again, produced the same type of monomer, 3HB, in the co-culture.

Table 7. Monomeric composition of the co-culture biomass, polymer obtained and mcl-PHA and PHB that compose the blend produce in the co-culture production using apple pulp waste.

Polymer	**Composition (wt %)**						
	HB	**HV**	**HHx**	**HO**	**HD**	**HDd**	**HTd**
Blend	48	0	<1	10	36	3	3
Blend: mcl-PHA	0	0	<1	22	68	4	4
Blend: PHB	54	0	0.3	8	32	3	3

Table 8. Physical-chemical properties of the mcl-PHA produced by *P. citronellolis* and other *Pseudomonas* sp. (HHx, 3-hydroxyhexanoate; HO, 3-hydroxyoctanoate; HD, 3-hydroxydecanoate; HDd, 3-hydroxydodecanoate; HTd, 3-hydroxytetradecanoate; Mn, molecular number; Mw, molecular weight; PDI, polydispersity index; n.a., data not available; n.d., not detected).

Bacteria	**Feedstock**	**Composition (wt%)**					**Mw ($\times 10^5$ Da)**	**Mn ($\times 10^5$ Da)**	**PDI**	**References**
		HHx	**HO**	**HD**	**HDd**	**HTd**				
P. citronellolis NRRL B-2504	Waste apple pulp	1	22	68	5	4	3.7	1.7	2.1	This study
	Saturated biodiesel fraction	5-6	40-46	36-40	7-9	---	0.7-2.0	0.4–0.8	1.9–2.5	(42)
	Olive oil distillate	14	43	32	12	<1	0.3	0.2	1.5	(35)
	Fatty acids by-product	10	36	40	14	<1	n.a.	n.a.	n.a.	(35)
	Tallow fatty acids	10	48	28	10	4	0.9–1.6	0.4–0.7	2.2–2.6	(56)
P. resinovorans NRRL B-2649	Olive oil distillate	19	44	28	9	<1	0.2	0.3	1.5	(35)
		12	48	31	8	<1	0.3	n.a.	1.5	(47)
	Crude Pollock oil	3	27	48	15	7	3.4	1.5	2.2	(32)
P. mediterranea CFBP 5447	Glycerol (99.8%)	4	17	61	6	n.a.	0.5	n.a.	1.3	(43)
	Refined Glycerol (87.5%)	<1	9	67	8	n.a.	0.6	n.a.	1.4	(43)
P. oleovorans ATCC 29347	Octanoic Acid	8	93	-	-	-	3.9	2.1	1.8	(40)
P. putida JCM6160	Glycerol	3	25	51	22	---	0.6	0.4	1.4	(65)
P. stutzeri 1317	Glucose	2	21-22	63-68	8-10	<1	n.a.	n.a.	n.a.	(51,64)

Table 9. Physical-chemical properties of the PHB produced by *C. necator* DSM 428 and other *C. necator* sp. (3HB, 3-hydroxybutyrate; 3HV, 3-hydroxyvalerate; Mn, molecular number; Mw, molecular weight; PDI, polydispersity index; n.a., data not available; n.d., not detected).

Bacteria	**Feedstock**	**Composition (wt%)**	**Mw ($\times 10^5$ Da)**	**Mn ($\times 10^5$ Da)**	**PDI**	**References**
		3HB				
C. necator DSM 428	Apple pulp waste	100	5.0	2.5	2.0	This study
	Used Cooking oil	100	1.7	1.1	1.5	(35)
	Olive oil distillate	100	1.6	1.0	1.6	(35)
	Fatty Acids Byproduct	100	1.6	0.8	2.0	(35)
	Spent coffee grounds oil	100	2.3	1.9	1.2	(62)
	Used Cooking oil	100	2.6	1.6	1.6	(50)
	Margarine Waste	100	n.a.	n.a.	n.a.	(46)
	Chricory Roots	100	4.6	n.a.	1.8	(66)
C. necator NRRL B-4383	Used cooking oil	100	1.8	0.9	2.0	(35)
	Olive oil distillate	100	1.7	0.6	2.8	(35)
	Fatty Acids Byproduct	100	1.0	0.4	2.5	(35)
C. necator DSM 545	Chricory Roots	100	5.1	n.a.	1.3	(66)
C. necator 531	Chricory Roots	100	3.7	n.a.	1.9	(66)
C. necator H16	Waste Sesame Oil	100	5.5	n.a.	1.1	(67)
	Fructose	n.a.	13.2	n.a.	2.0	(67)
P. oleovorans NRRL B-14682	Fatty Acids Byproduct	100	2.9	2.0	1.5	(35)
	Olive oil distillate	100	2.2	1.4	1.6	(35)
	Hydrolized Pollock Oil	100	3.9	1.9	2.0	(35)

2.3.3.2. Molecular Mass Distribution

The SEC chromatogram (**Figure A** in Appendices) highlights that the mcl-PHA synthesized by *P. citronellolis* exhibited a large peak with the presence of a smaller one located on the lower molecular weight side. The polymer had an average molecular weight (M_w) of 3.7×10^5 Da, with a polydispersity index (PDI) of 2.1 (**Table 8**). The Mw obtained was higher than the values attained for the mcl-PHA from the same strain using different carbon sources, such as saturated biodiesel fraction (0.7×10^5-2.0×10^5 Da) (42), olive oil distillate (0.3×10^5 Da) (35) and tallow fatty acids (0.9×10^5-1.6×10^5 Da) (56), a characteristic that can be reflected by the polymers composition and properties (35,42,56). The observed differences may be due to the different production conditions, specifically, the composition of the substrate, cultivation mode and the stage of growth when the cells were harvested (56).

The average molecular weight of the polymer recovered from *C. necator* biomass by chloroform extraction was 5.0 x 10^5 Da (**Table 9)** (SEC chromatogram in Appendices, **Figure B**). This value is a very high value compared to those reported for P(3HB) synthesized by the same strain ($1.6\text{x}10^5$ Da -$2.6\text{x}10^5$ Da) and *C. necator* NRRL B-4383 ($1.0\text{x}10^5$ Da -$1.8\text{x}10^5$ Da) (**Table 9**) grown on other feedstocks, namely, used cooking oil (35,50), olive oil distillate (35), spent coffee grounds oil (62), fatty acids byproducts (35). A similar value was reported for the PHB produced by *C. necator* DSM 545 using waste sesame oil as carbon sources (5.1 x 10^5 Da) (66). However, the polymer presented a smaller polydispersity index, of 1.3, than the P(3HB) obtained by *C. necator* DSM 428 using apple pulp waste, of 2.0 (**Table 9**). The same happens with PHB produced by *C. necator* H16 using sesame oil, that produced a polymer with a similar Mw ($5.5\text{x}10^5$ Da) but a lower PDI (1.1) (67). This may occur due to the difference of the extraction process that impacted the polymers macromolecules (68).

The PHB/mcl-PHA blend exhibited an average molecular weight of 4.3×10^5 Da with a polydispersity index of 2.2. Regarding the molecular weight and PDI obtained for the monocultures of *P. citronellolis* and *C. necator*, the blend attained a value for the molecular weight higher than the one obtained for the mcl-PHA and closer to the PHB. The molecular weight value obtained for the blend is almost a mean between the values obtained for mcl-PHA and P(3HB). The SEC chromatogram (**Figure C** in Appendices) shows only one peak which means that both polymers, mcl-PHA and P (3HB) have Mw of the same order of magnitude.

2.3.3.3. FTIR

The FTIR spectra (**Figure 10**) for both the *mcl*-PHA produced by *P. citronellolis* and PHB produced by *C. necator* from waste apple pulp show an intense absorption peak at 1727 cm^{-1} corresponding to the stretching band of the ester carbonyl group ($C = O$), which is also a characteristic of the crystalline phase (69). This band is the strongest peak in the spectra, corresponding to a characteristic band of PHA. Regarding, the mcl-PHA FTIR spectrum (**Figure 10** (a)), near 2961-2854 cm^{-1} three peaks can be identified that can be attributed to the asymmetric methyl group (the peak at 2961 cm^{-1}), to the stretching vibration due to asymmetric CH_2 of the lateral monomeric chains (the peak at 2924 cm^{-1}) (70) and to the symmetrical methyl group (the peak at 2854 cm^{-1}) (**Figure 10** (a)). Between 1000 and 1500 cm^{-1}, a group of peaks is detected, indicating the presence of numerous characteristic structures within *mcl*-PHA. For instance, the peak at 1260 cm^{-1} corresponds to asymmetric C-O-C stretching vibration. The region between 1010 and 1161 cm^{-1} shows series of absorption bands, which can be assigned to C-O and C-C stretching vibration in the amorphous phase of the *mcl*-PHA (69,71). The band nearby 802 cm^{-1} is attributed to the CH_2 bonds in the side-chain of the polymer (28,72,73).

Concerning the P(3HB) FTIR spectra (**Figure 10** (b)), the weakest band in the spectra is relatively to the methylene C-H elongation vibration near 2900 cm^{-1} (74). Literature had previously reported that this vibration was stronger for mcl-PHA and weaker regarding PHB (73). FTIR is also used to evaluate the crystallinity of PHB, the band at 1721 cm^{-1} is attributed to the stretching vibration of the crystalline carbonyl group (71,74). The bands between 1057 and 1278 cm^{-1} are related to the degree of crystallinity, with 1057 cm^{-1} peak related to C-O bonds (74,75).

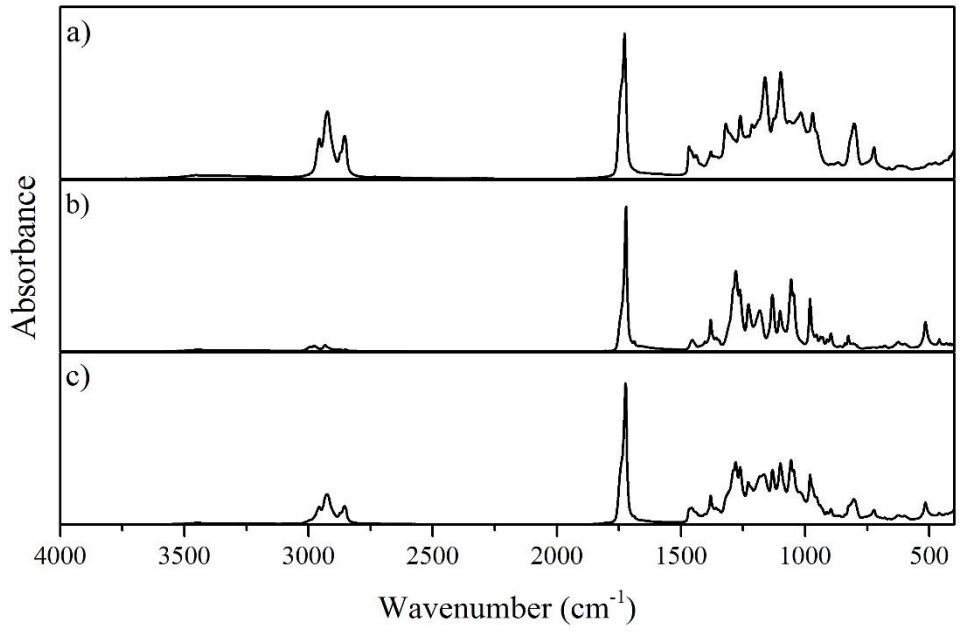

Figure 10 - FTIR-ATR spectra of the mcl-PHA produced by *P. citronellolis* (a), PHB produced by *C. necator* (b) and PHB/mcl-PHA produced in a co-culture (c) from apple pulp waste.

The peaks obtained in the FTIR spectra for the P(3HB) produced by *C. necator* are very close to those reported in the literature wherein the main bands found in the PHB spectrum (**Figure 10** (b)) are attributed to C-C coupling with CH_3 stretch vibration, C-O-C (823 to 921 cm^{-1}) vibration bands, CH_3 (1378 cm^{-1}), asymmetric CH_3 (1458 cm^{-1}) (75,76).

The FTIR analysis for the blend displays a group of similar peaks to the ones identified for mcl-PHA and PHB separately (**Figure 10** (c)). The most intense absorption peak is located near 1723 cm^{-1} and corresponds to the ester carbonyl group ($C = O$) the characteristic peak in all PHA FTIR spectrum (69). Near 2921-2847 cm^{-1} two peaks can be identified and can be attributed to the asymmetric CH_2 of the lateral monomeric chains (the peak at 2924 cm^{-1}) and to the symmetrical methyl group (the peak at 2847 cm^{-1}) (70). Between 1000 and 1500 cm^{-1}, the same group of peaks detected in mcl-PHA and PHB FTIR spectrum is identified, indicating the presence of numerous characteristic structures within both polymers. Between 1054 and 1282 cm^{-1} the peaks are related to the degree of crystallinity of PHB, with 1057 cm^{-1} peak related to C-O bonds (74,75). As it can been seen the FTIR spectrum for the blend produced combine the peaks characteristic for mcl-PHA and PHB.

2.3.3.4. Thermal properties of the biopolymers

The mcl-PHA produced by *P. citronellolis* from apple pulp waste presented a melting temperature(T_m) of 53 °C. The values are presented in **Table 10**. The T_m was in the range of 50ºC and presented an enthalpy melting (ΔH_m) of 21.3 J/g, typical values for mcl-PHAs. Indicating that the mcl-PHA produced was not completely amorphous but to some extent crystalline, since presented characteristics similar to other rubber-latex materials. For instance, mcl-PHAs produced by the same strain presented lower ΔH_m (1.9 J/g) (35) whilst other strains, such as *P. resinovorans* NRRL B-2649 presented lower ΔH_m (8.3-12.3 J/g) (35,77) implying that these mcl-PHAs were more amorphous than the mcl-PHA obtained from apple pulp waste, which was also reflected by the mcl-PHAs melting temperatures. Regarding the polymer's thermal stability, the thermogravimetric curve (**Figure 11**) shows that the decomposition of the mcl-PHA involved a fast one-step process. Its decomposition showed a single weight loss of approximately 99%, with a maximum degradation rate (T_{deg}) at 296 °C. These values, particularly the T_m and T_{deg} exhibited by the *mcl*-PHA produced from apple pulp waste, were similar to those described in literature, for the polymer produced by the same strain using saturated biodiesel fraction (48-50 °C and 296 °C, respectively) (42). The mcl-PHA produced by *P. mediterranea* CFBP 5447 from glycerol, displayed a composition similar to that of the polymer obtained from apple pulp waste, which had a significantly lower T_{deg} (283 °C) value (43).

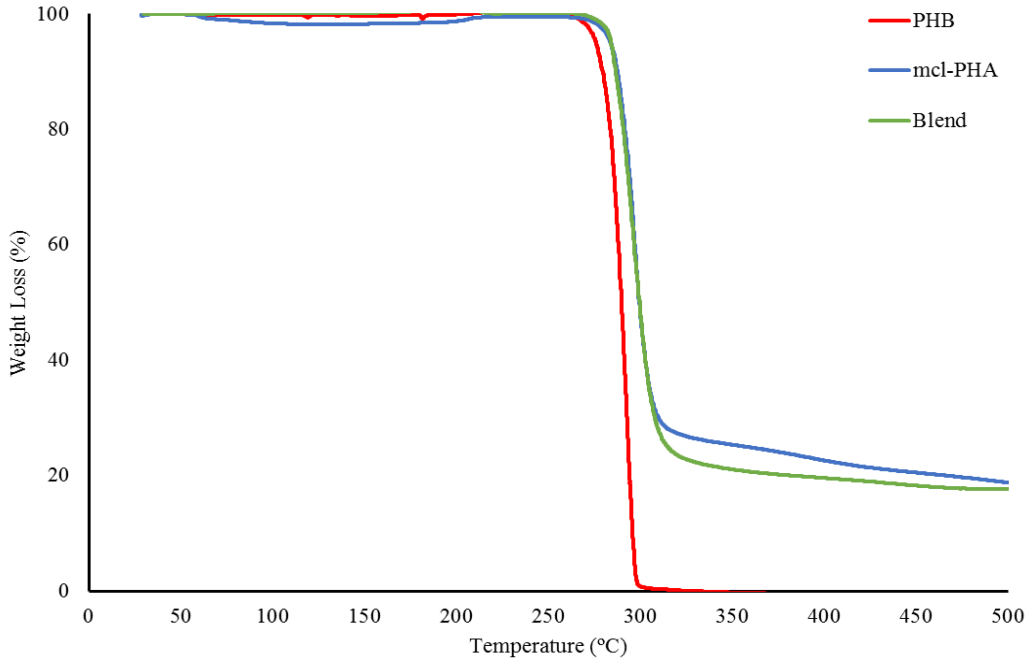

Figure 11 - Thermogravimetric analysis (TGA) curves of the PHB and mcl-PHA produced by *C. necator* DSM 428 and *P. citronellolis* NRRL B-2504, respectively, and the blend from apple pulp waste.

The observed difference may be associated with the fact that *P. mediterranea* mcl-PHA had a considerably lower Mw (0.5×10^5-0.6×10^5 Da) than that produced by *P. citronellolis* from apple pulp waste (3.7×10^5 Da).

As for the P(3HB) produced by *C. necator* from apple pulp waste, it presented a melting (T_m) temperature of 179°C (**Table 10**). The melting temperature attained was a little higher than those reported in other studies where PHB was produced by *C. necator*, with melting temperatures of approximately 172°C (35,46,50,62). The polymer presented an enthalpy melting (ΔH_m) of 63.2 J/g, a value that is below those attained for other P(3HB) produced by the same strain, where ΔH_m was in the range of 68.2 to 84.9 J/g (35,46,62), but in the same range as the PHB produced by *C. necator* NRRL B-4383, where ΔH_m presented similar values (58–67.7 J/g) (35) which also had an impact on the polymer degree of crystallinity. The fact that ΔH_m had a lower value for the other productions using the same bacteria strain may be due to the conditions in which the production occurred. As shown by the TGA curve (**Figure 11**), the decomposition of the polymer involved a fast process similar of mcl-PHA. The curve was stable up to 262 °C ($\Delta m \approx 0.50\%$ at this temperature) and exhibited a weight loss ($\Delta m \approx 99.8\ \%$) with maximum degradation rate (T_{deg}) at 293 °C (**Table 10**). Such value is higher than the one obtained for the PHB produced by the same strain and *Burkholderi. sacchari* IPT101 (50,78).

Both P(3HB) and mcl-PHA, presented thermal properties that are close to other polymers obtained from a variety of productions using other types of conditions, namely carbon sources and microorganisms. As expected, P(3HB) revealed a T_m and by extent ΔH_m much higher than those attained by mcl-PHA. The polymers demonstrate a relatively close and high degradation temperature presenting a big window to work the polymers as desired.

Concerning the thermal properties of the blend, it was determined by differential scanning calorimetry (DSC) and thermogravimetric analysis (TGA), the PHB/mcl-PHA blend produced by *P. citronellolis* and *C. necator* from apple pulp waste presented melting (T_m) temperatures of 50 and 175 °C. Regarding the polymer's sample thermal stability, the curve was stable up to 250 °C and exhibited a weight loss of approximately 80%, with a maximum degradation rate at 297 °C (**Figure 11)**.

Table 10. Thermal properties and degree of crystallinity of the mcl-PHA and P(3HB) produced from *P. citronellolis* NRRL B-2504 and *C. necator* DSM 428, respectively, as well as other PHA obtained from different bacterial strain (T_m, melting temperature; T_{deg}, degradation temperature; X_c, crystallinity fraction; ΔHm, melting enthalpy ; n. a. data not available; n. d., not detected).

Material	Bacteria	T_m (ºC)	T_{deg} (ºC)	X_c (%)	ΔHm (J g^{-1})	References
mcl-PHA	*P. citronellolis* NRRL B-2504	53	296	15	21.3	This study
	P. citronellolis NRRL B-2504	25.2	n.a.	1	1.9	(35)
	P. citronellolis DSM 50332	48.6-53.6	295-297	10.4-12.3	15.2-18.0	(42)
	P. resinovorans NRRL B-2649	35.6 – 43.3	n.a.	6-7	8.3 – 9.9	(35)
		39 – 48	n.a.	6-8	9.5-12.3	(77)
	P. chlororaphis 555	n.d.	290	n.a.	n.a.	(79)
	P. chlororaphis IMD555	38	284	n.a.	n.a.	(78)
	P. mendocina NK-01	54.9	283.94	n.a.	0.366	(72)
P(3HB)	*C. necator* DSM 428	179	293	43	63.2	This study
	C. necator DSM 428	173.4	n.a.	56.6	82.6	(46)
		172.3	n.a.	58	84.9	(62)
		164.3 – 168.6	n.a.	47 - 53	68.2 – 78.1	(35)
		172	266	n.a.	n.a.	(50)
	C. necator NRRL B-4383	164.9 – 167.2	n.a.	40-46	58 – 67.7	(35)
	P. oleovorans NRRL B-14682	156.5 – 161.7	n.a.	36-39	52.5 – 56.5	(35)
	C. necator DSM 545	173.5	n.a.	56	80.0	(63)
	B. sacchari IPT101	38.2	284	n.a.	n.a.	(78)

2.3.3.5. X-Ray Diffraction

The structural analysis achieve by XRD allowed to determine the degree of crystallinity of both mcl-PHA and PHB. Regarding the mcl-PHA, the polymer exhibited some degree of melting transition, (**Table 10**), therefore indicating it was semi-crystalline, which was also confirmed by X-ray diffraction analysis (**Figure 12**). Around 2θ = 18°, a broad hump is visible which is characteristic of the amorphous part of the polymer, while the crystalline zone displayed one diffraction peak near 21° (80,81). The polymer had a low crystallinity value (15%), which is higher than the values reported for mcl-PHA produced by *P. citronellolis* (10.4-12.3%) (**Table 10**). Mcl-PHA presents flexibility and elasticity, mainly due to its composition but also to the low crystallinity index. This parameter affects polymer properties, such as mechanical features, since polymers with higher degree of crystallinity like PHB and PHBV are more brittle and stiff whilst mcl-PHA present lower crystallinities and more elastomeric capacities (82).

Concerning the P(3HB), the X-ray diffractogram for the polymer (**Figure 12**) exhibited all main reflections of the X-ray diffraction pattern of crystalline PHB, namely, two narrow humps located around 2θ = 14 and 17°, typical for the crystalline phase of the polymer, while the amorphous phase showed a representing broad humps around 2θ = 23 and 26º (50,83). The polymer had a low crystallinity value (43%) than those reported for the same strain (47 to 58%) (**Table 10**), but within the same range of those reported by *C. necator* NRRL B-4383 (40-46%) and higher than those of *P. oleovorans* NRRL B-14682 (36-39%) (35). In comparison with the mcl-PHA, having higher crystallinity index, PHB is more stiff and rigid (84).

The PHB/mcl-PHA blend also exhibited a low degree of crystallinity (X_c) of approximately 10% (**Table 10**). The amorphous part of the polymer was characterized by the same broad hump located around 2θ= 19 and 20°, a characteristic broad for the amorphous area, whereas the crystalline zone displayed one diffraction peak near 26°, which is in accordance with the same broad present in the X-ray diffraction (**Figure 12**) for the mcl-PHA produced by *P. citronellolis*. The diffraction peaks near 14° and 17º are due to the presence of P(3HB) produced by *C. necator* which are also visible in the X-ray diffraction analysis for PHB (**Figure 12**). This is in accordance with the composition determined for the blend, proving the presence of the different PHA produced by each strain (85).

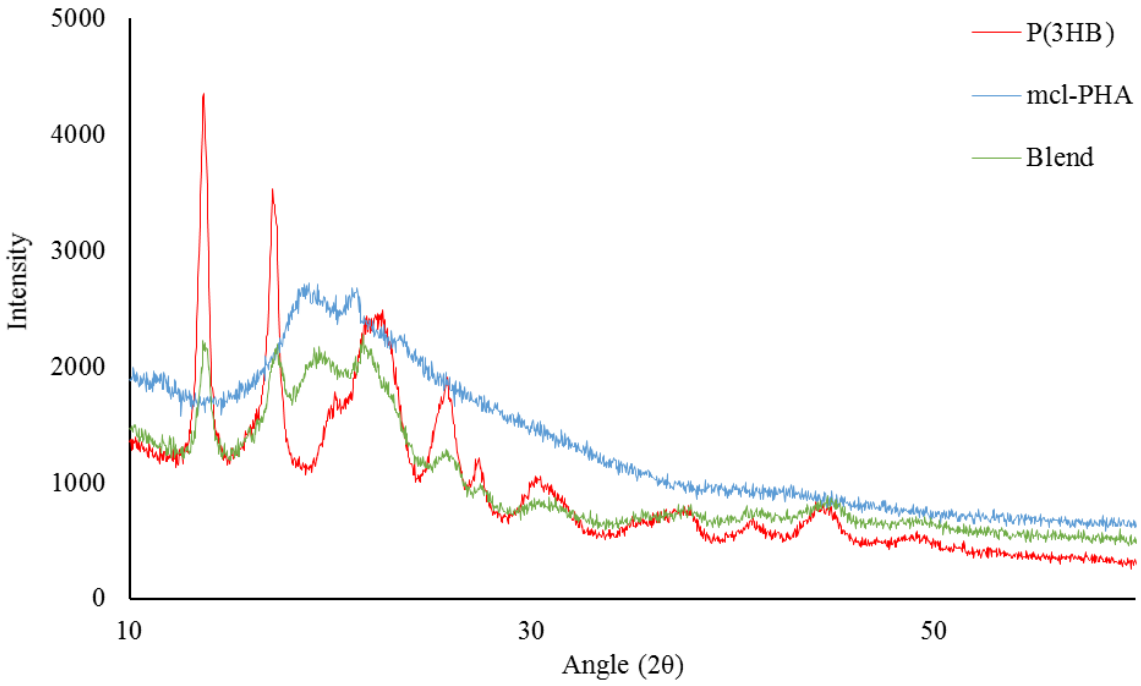

Figure 12 - X-ray diffractogram of the P(3HB), mcl-PHA and P(3Hb)/mcl-PHA blend produced by *C. necator* DSM 428, *P. citronellolis* NRRL B-2504 and co-culture, respectively, from apple pulp waste.

2.3.3.6. P(3HB), mcl-PHA and blend comparison

Overall, the cultures, using *P. citronellolis* and *C. necator*, and the co-culture presented polymers with interesting properties, especially the case of the blend (**Table 11**). The mcl-PHA and P(3HB) produced by *P. citronellolis* and *C. necator*, respectively, presented a set of physical-chemical properties similar to other polymers that were produced with a variety of feedstocks as their carbon source (**Table 11**). Interestingly, the blend produced by the *P. citronellolis* and *C. necator* co-culture, was presented as a physical mixture of the two polymers which were produced separately, mcl-PHA and P(3HB), without a bonding linking the two types of polymers. The acetone fractionation allowed to separate the two polymers that constitute the blend. Both blend components, mcl-PHA and P(3HB), were analysed and their composition as well as physical-chemical properties were determined (**Table 11**). The mcl-PHA and P(3HB) revealed the same monomeric composition as the polymers alone and the monomers that composed the blend. As for the thermal properties, the blend exhibited the T_m for mcl-PHA (50 ºC) and P(3HB) (175 ºC), those were confirmed by the components of the blend, since they attained resemblance in the values (47 and 177 ºC) (**Table 11**). As for the average molecular weight, the mcl-PHA produced by *P. citronellolis* revealed a higher value (3.7×10^5 Da) than that attained for the mcl-PHA blend component (2.9×10^5 Da) and the same occurred with P(3HB) of the blend (5.3×10^5 Da) compared to P(3HB) produced by *C. necator* (5.3×10^5 Da), this may be due to the recovery of the components during the acetone fractionation.

Table 11. Composition and physical-chemical properties of the polymers obtained from apple pulp waste (HB, 3-hydroxybutyrate; HHx, 3-hydroxyhexanoate; HO, 3-hydroxyoctanoate; HD, 3-hydroxydecanoate; HDd, 3-hydroxydodecanoate; HTd, 3-hydroxytetradecanoate; Mw, molecular weight; PDI, polydispersity index; T_m, melting temperature; T_{deg}, degradation temperature; X_c, crystallinity degree: n.a., data not available).

Culture	Polymer	Monomeric composition	T_m (ºC)	T_{deg} (ºC)	Mw ($\times10^5$ Da)	PDI	X_c (%)
P. citronellolis NRRL B-2504	mcl-PHA	HHx-HO-HD-HDd-HTd	53	296	3.7	2.1	15
C. necator DSM 428	P(3HB)	HB	179	293	5.0	2.0	43
P. citronellolis NRRL B-2504 and *C. necator* DSM 428	P(3HB)/mcl-PHA	HB-HHx-HO-HD-HDd-HTd	50 and 175	297	4.3	2.2	10
	mcl-PHA blend component	HHx-HO-HD-HDd-HTd	47	294	2.9	2.1	n.a.
	P(3HB) blend component	HB-HHx-HO-HD-HDd-HTd	177	296	5.3	1.9	n.a.

2.3. Conclusions

Apple pulp waste from the fruit processing industry demonstrated to be a suitable and prospective feedstock for the batch production of mcl-PHA by *P. citronellolis* and P(3HB) by *C. necator* and a blend by the means of a co-culture.

Under the conditions tested, the cultures were able to consume the majority of sugars that are present in the apple pulp waste, consuming preferably glucose and fructose by *P. citronellolis* and *C. necator*, respectively. The production with *C. necator* presented the highest volumetric productivity of 1.59 g/L.day, thus demonstrating that the apple pulp waste is a promising substrate for PHB production. Although the production process with *P. citronellolis* needs to be optimised to improve the polymer's volumetric productivity and yield, the results obtained in this study evidenced its potential. The interesting fact that both cultures were able to growth with the apple pomace presenting different carbon consumptions of the sugars present in the apple pulp, allowed for the third production using both *P. citronellolis* and *C. necator* to be a novelty and also presenting good results within the range of those obtained during the monocultures with *P. citronellolis* and *C. necator* productions. However, despite the fact that presented a significant volumetric productivity (0.96 g/L.day) the PHA content was low (34 wt.%), hence, the need for optimisation of the blend production.

The resulting polymers, namely mcl-PHA, P(3HB) and blend, were characterized by physical and chemical properties. Apple pulp waste served as a good source of carbon for the production of 3HB by *C. necator* and mcl-PHA by *P. citronellolis* with a rather heterogeneous composition, however, with the monomers 3HO and 3HD in the majority. On the other hand, the blend produced by the co-culture showed to be an interesting physical mixture of the two previous polymers.

This study demonstrated that apple pulp waste can successfully be used as a carbon source for the production of several types of PHA, presenting an opportunity for this waste valorisation. Future steps must proceed on the process of optimization in order to make development prove of concept and assess its economic viability. Taking into account the polymers obtained and the potentialities of the characteristics of each one, their application in films were tested and are highlighted in the following chapter.

Chapter 3

Preparation and Characterization of Films based on PHA

3.1. Introduction

Unlike fossil-fuel plastics, biopolymers, are a form of plastics derived from renewable biomass sources, bio-derived monomers (for example: polylactic acid) and microorganisms, produced during their growth (21,86). The main advantages provided by these polymers are the use of renewable resources, conserving the fossil resources, and reducing CO_2 emissions, making them important in development key to a more sustainable environment (21,87). Biopolymers have been revealing a large range of possible sources where they can be obtained and a wide range of applications in the food and pharmaceutical industries (86).

Among the biopolymers, PHAs are promising materials for numerous applications because they are natural, renewable, biocompatible and biodegradable polymers, with properties comparable to synthetic polyesters, namely thermoplastic, elastomeric and adhesive capacities, depending on the monomeric composition, the bacterial strain used, the fermentation mode, as well as the carbon source (43,88,89). PHAs are significantly influenced by their monomeric composition and chemical structure that affects the physical and material properties (88). Short chain length-PHAs (scl-PHAs) present various degrees of crystallinity, are brittle and rigid and may lack the important mechanical properties necessary for biomedical and packaging film applications. On the other hand, medium chain length-PHAs (mcl-PHAs) present low crystallinity, low glass transition temperature, low tensile strength and high elongation to break. Moreover, they are amorphous elastomers with adhesive capacities (43,88).

Given these set of encouraging characteristics, and adding the ability of PHAs to be shaped into films of a variety of forms, they present potential towards industrial applications (86). PHAs films are biodegradable making them an alternative to aluminium foil or polypropylene, for example. Besides, they present gas barrier properties, opening a window to be explored for the preparation of packaging for food, hygiene or medical film products, where the moisture barrier property is important against atmospheric gases (43,86,88,90). However, in spite of their potential, the introduction of these biopolymers onto the worldwide market is still very limited (43).

To obtain PHAs films with the desirable mechanical properties, several approaches have been suggested, such as, copolymerisation with other alkanoates and the development of new composites by blending the PHAs with other materials (89,90).

The incorporation of flexible monomers units during the PHA polymerisation, specifically of 3-hydroxyvalerate, 4-hydroxybutyrate or 3-hydroxyhexanoate, in the main chain of the polymer and the decrease of the melting point, was addressed in order to overcome thermal degradation. Some examples of PHAs copolymers are poly(3-hydroxybutyrate-co-3-hydroxyvalerate) P(HBV) and poly(3-hydroxybutyrate-co-hydroxyhexanoate) P(HBHHx). This process of copolymerisation leads to an improvement of both mechanical and thermal properties of PHAs (90).

The modification of PHA via blending is an effective approach to obtain new polymeric materials films with improved properties and can be achieved by the addition of natural raw materials or synthetic biodegradable polymers (91). PHA blends depend on the characteristics of the polymers blends like the variation of the composition of the blend and the conditions in which they are prepared. Compatibility of both parts of the blend play an important role in the final film properties, since incompatibility between both parts of PHA blend is usually a major drawback on PHA blends prepared by conventional solvent casting, commonly presented by phase separation between the PHA and the other material. It is important that PHA films maintain the integrity of the polymeric matrix by avoiding pores and cracks, or segregated drops on the surface of the polymer after its blending or during final product application (92). The addition of synthetic biodegradable polymers like the case of plasticizers onto PHAs-based films, for example, poly(lactic acid) (PLA), polyethylene glycol (PEG), polycaprolactone (PCL), natural rubber or chemical modified PHA (for example, an epoxy functionalized mcl-PHA), allowed an improvement of compatibility, mechanical strength and flexibility while handling these films (21,89,91,93).

Focusing on the PHA blending with natural raw materials, an enormous number of different approaches have been carried out to blend PHA with other natural biodegradable polymers, as the use of polysaccharide like cellulose derivatives, chitosan, lignin and starch, since they exhibited good gas barrier properties and some of these have structures that renders the films with flexibility and transparency (92). Blending with different types of PHAs have been reported to result in more unique biopolymers with more attractive thermal/mechanical behaviours. Blending PHB with several copolymers, such as PHBHV and PHBHHx, with a variety of monomer molar ratios also have been reported. PHB/PHBHHx blending films have been reported as an effective method for cell attachment and growth by improving the biocompatibility of PHB (94). Limited information is reported for the miscibility and properties of blends composed by PHB or other copolymers with mcl-PHA. A study on PHBV/mcl-PHA blend prepared by chloroform solvent casting revealed that blend was miscible in the composition range studied, along with changes on glass transition temperature and an improvement of tensile strain and decrease in the elasticity modulus (95).

The following work is focused on the preparation of several PHA-based films with the biopolymers produced using apple pulp waste by solvent casting evaporation, with the aim to improve mechanical properties of these biomaterials.

3.2. Methods

3.2.1. Films preparation

The PHA films were prepared upon the dissolution of 0.5 g polymer (mcl-PHA, PHB or the co-culture blend) in 10 mL of chloroform (Sigma-Aldrich, HPLC grade), under stirring, at room temperature, until complete dissolution. The blend films were prepared as described by Azari et al. 2014 (96), through a mixture of solvents, DMF (dimethylformamide) and chloroform (1:10 v/v) (Sigma-Aldrich, HPLC grade), under stirring, at 60ºC during 24 h. The solutions were transferred into glass petri dishes (diameter of 5 cm), which were placed in a desiccator and kept at room temperature until complete solvent evaporation. For the mechanical tests, solutions prepared with 1 g of polymer in 20 mL of solvent were used and the solvent evaporation was done in glass petri dishes (diameter of 10 cm), under the same conditions.

3.2.2. Morphology Characterization

The morphology of the obtained films was assessed by Scanning Electron Microscopy using an Energy Dispersive Spectroscopy (SEM-EDS). The PHA films were placed in a desiccator until completely dry, frozen in liquid nitrogen and fractured in small pieces followed by coating with a thin layer of Au/Pd. The films were analysed using an analytical JEOL 7001F scanning electron microscope (FEG-SEM, JEOL, USA Inc.) equipped with a field emission gun operated with an acceleration voltage of 15 kV. All samples were visualized on their surface and cross-section using different amplifications.

3.2.3. Thermal properties Analysis

Thermal analysis were performed as described in 2.2.7.4. with the PHA films (with ~40 mg for each PHA film).

3.2.4. X-Ray Diffraction Analysis

The structural analysis of the samples was performed by X-ray diffraction (XRD) using a X'Pert Pro X-ray diffractometer from PANalytical (Almelo, Netherlands), equipped with an X'Celerator detector, in a Bragg–Brentano geometry with Cu Kα line radiation (λ = 1.5406˚A). The 2θ scans were performed from 10˚ to 90˚, with a step size of 0.03˚.

3.2.5. FTIR

FTIR analysis was conducted as described in 2.2.7.2. with the PHA films (with ~100 µm of thickness) directly casted on the FTIR cells.

3.2.6. Water contact Angles

The contact angle was measured by the sessile drop method, where a drop of distilled water was manually deposited on the film's surface with a small syringe. The software acquired ten images per sample and the tangent was determined by fitting the drop shape to a known mathematical function. Multiple replicates were performed, and the mean angle was determined. All images were acquired by CAM2008 (KSV Instruments Ltd, Finland).

3.2.7. Swelling in Water

PHA film samples with a size of 1.0×1.0cm^2 were weighted and their thickness was measured (Elcometer, England). The samples were immersed in 15 mL deionized water, in a closed vial, and kept at 30 ºC during 24 h. The swelling degree of the samples was calculated with the following equation:

$$Swelling\ Degree = \frac{X2-X1}{X1} \times 100\% \quad (3)$$

where *X1* and *X2* are, respectively, initial and final mass (g), respectively, of the samples measured at a different time period. The samples thickness after immersion was also measured.

3.2.8. Gas permeation

Gas permeation tests were performed with pure CO_2 and O_2 using a gas permeation setup composed of a stainless steel cell with feed and permeate compartments that were separated by the PHA films. The experimental apparatus was placed in a thermostatic bath (Julabo GmBH ED, Germany, ± 0.1 K), at a constant temperature of 30 ºC. The experiment was initiated with both compartments pressurized with the pure gas (CO_2 or O_2), and establishing a pressure of 0.7 bar before opening the permeate valve and instantly closing it. The pressure variation in the compartments of the cell was measured by two pressure transducers (Druck PCDR 910, models 99166 and 991675, UK, ± 0.008 bar). The films' permeability (*P*, cm^3.cm/cm^2.s.cmHg) for pure CO_2 and O_2 gases was calculated according the following equation:

$$\frac{1}{\beta}\ln\frac{\Delta_{po}}{\Delta_p} = P\,\frac{t}{l} \quad (4)$$

where Δ_p (bar) corresponds to the difference of the pressures in the feed and permeate compartments, *t* (s) is the time and *l* (m) is the film's thickness. β is a geometric parameter characteristic of the cell (m^{-1}), and was obtained using equation 6:

$$\beta = A\left(\frac{1}{V_{feed}} + \frac{1}{V_{perm}}\right) \quad (5)$$

where A is the film's area (cm^2) and V_{feed} and V_{perm} are the volumes (bar) of the feed and permeate compartments, respectively. The gas permeability *P* was obtained from the slope when

representing $\frac{1}{\beta} ln \frac{\Delta_{po}}{\Delta_p}$ as a function of $\frac{t}{l}$. Gas selectivity was calculated as the ratio of the single gas permeability of each gas (CO_2 and O_2), with the following equation:

$$\alpha = \frac{P_{CO2}}{P_{O2}}$$

3.2.9. Mechanical Properties

The PHA films were cut into rectangular-shaped strips (~2.5×1.5 cm), which had an average thickness of 100 μm, measured using a digital micrometer (Mitutoyo, Japan). Tensile tests were performed at ambient temperature (22 °C) using a TA-XT plus texture analyser (Stable Micro Systems, Surrey, England) equipped with a 5 kg load cell. The films' strips were attached on tensile grips A/TG and stretched at 0.5 mm/s in tension mode until break. The stiffness of the membranes was determined by measuring the Young modulus (MPa), determined as the slope of the linear initial section of the stress-strain curve. The tensile stress at break (MPa) was calculated as the ratio of the maximum force to the films initial cross-sectional area. The elongation (strain) at break (-) was determined as the ratio of the extension of the sample upon rupture by the initial gage length. Three film replicas were analyzed.

3.3. Results and Discussion

3.3.1. Morphology and Characterization of PHA Films

The biopolymers, namely mcl-PHA, PHB and the blend, produced previously from apple pulp waste were used to prepare films (**Figure 13**) by solvent casting. Slow solvent evaporation was performed in a saturated chloroform atmosphere to avoid the formation of cracks in the films and guaranty its homogeneity. The films thus obtained were translucid and flexible for mcl-PHA, as it can been seen in **Figure 13** (A), the PHB films were very compact but still showed some level of flexibility, in **Figure 13** (B). On the other hand, the PHB/mcl-PHA blends films (**Figure 13** (C)) showed to be less compact as the PHB films and more flexible resembling mcl-PHA films, although never attaining the transparency as mcl-PHA films demonstrated to have.

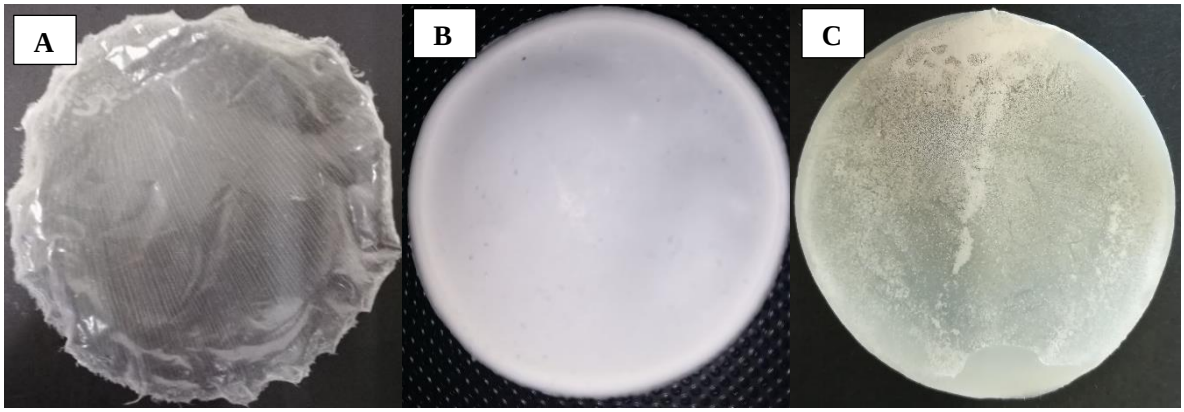

Figure 13 - mcl-PHA (A), PHB (B) and PHB/mcl-PHA blend (C) films obtained by solvent casting.

Upon the preparation of the PHB/mcl-PHA blend films with wider dimensions for the mechanical tests, the films obtained showed that homogeneity was not achieved with this method of preparation, as it can be seen in **Figure 14**.

Figure 14 - PHB/mcl-PHA blend films obtained by solvent casting using chloroform and DMF as solvents showing the PHB precipitated in the films.

Numerous attempts were made to overcome the heterogeneity of the films presented, for example the temperature and the solvent necessary to achieved a completely dissolution of the polymer sample. However, the first films prepared were obtained using only a single solvent, chloroform. This procedure showed to be inefficient since the films presented a level of heterogeneity with significant segregation between PHB and mcl-PHA that compose the blend. After, a solvent mixture of dimethylformamide (DMF) and chloroform was used in a proportion of 1:10 (v/v) to dissolve the polymer, during 24 h, at 60 ºC, a procedure adapted from the literature (96). The films were placed in the desiccator for a slow evaporation. Taking into account the results obtained (**Figure 14**), the PHB fraction present in the polymer sample used for the film was not uniformly distributed in the films. This might have occurred due to the temperature difference during the moment the polymer solution is placed in the petri dish on the desiccator to allow the solvent to evaporate. In order to obtain a blend film that is completely homogenous and is totally free from imperfections, the solvent evaporation must be slow, only then it is possible to guarantee that the PHB and mcl-PHA chains have enough time to form successive layers producing a film with a constant thickness (89,97). Since both, PHB and mcl-PHA, have different rates of solvent evaporation, with the PHB drying much faster than mcl-PHA, the films showed very different values of thickness (between 300 to 400 μm), resulting in the shrinking of the film while the solvent was evaporated. This result confirms the important role, described in the literature, of solvent evaporation rate, which is a key factor for the final blend's performance.

The films obtained by solvent casting, namely mcl-PHA, PHB and PHB/mcl-PHA blend films, were investigated using scanning electron microscopy (SEM) in order to evaluate their morphology. **Table 12** shows the surface and the cross-section of each film. The mcl-PHA films exhibited a homogeneous and rough surface, possible due to the solvent evaporation (**Table 12** (A.1.)), and were dense with no visible pores or cracks (**Table 12** (C.1.)). These findings were confirmed upon magnification (**Table 12** (B.1.) and (D.1.)) of the *mcl*-PHA films' surface and cross section images. The mcl-PHA surface morphology was very similar to those reported for PLA, PHBV, PHA + PEG (polyethylene glycol) and PHA + PVAc (polyvinyl acetate) blends (98–101). The PHB films showed a very irregular fracture surface (**Table 12** (A.2.) and (C.2.)) possible due to its crystalline structure. Upon magnification of the cross-section it is noticeable that the PHB films hold a degree of porosity in its structure which is visible in (**Table 12** (B.2.) and (D.2.).In comparison with the morphology of other PHB films, they hold a similar structure and porosity (98–100) .The PHB/mcl-PHA blend films morphology revealed a rough surface with irregular holes between the polymer junctions (**Table 12** (A.3.)), which can be attributed to a phase-separated PHA, which can be confirmed by the 5000x magnification of the film cross-section (**Table 12** (D.3.)) (102). This allowed to visualize a very low adhesion between the two phases, since the PHB fraction present in the middle area of the cross-section composed an irregular nett on the film, probably responsible for the spaces between the polymer intersections.

On the other hand, mcl-PHA existent in the sample was more dispersed in the entire film, reaching several areas but is mostly present on the film surface (**Table 12** (C.3.)).

Table 12. Surface (a, b) and cross-section (c, d) amplified 500x and 5000x, respectively images obtained by Scanning Electron Microscopy (SEM) analysis of the prepared PHA based films.

Material	*Surface*		*Cross-Section*	
mcl-PHA	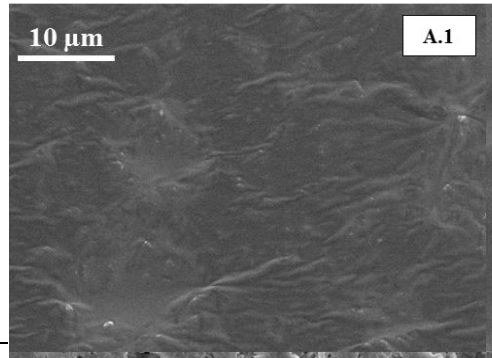	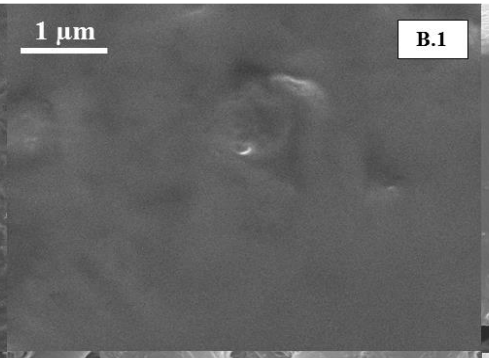	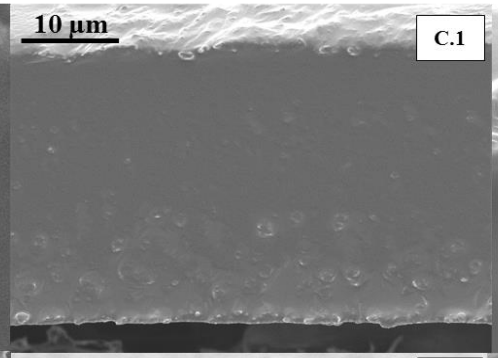	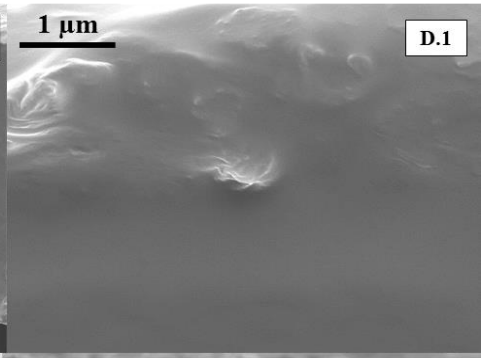
PHB	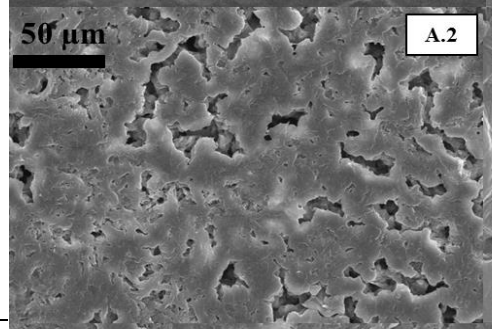	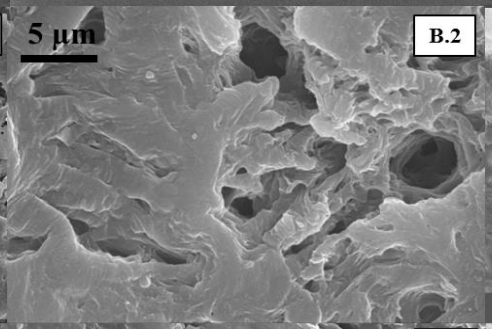	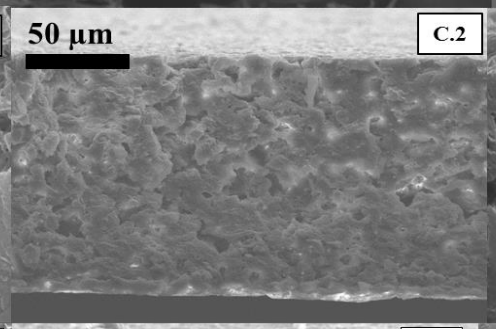	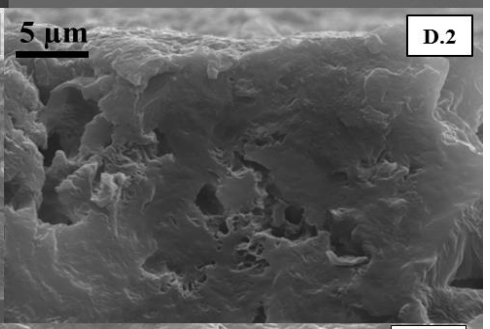
Blend	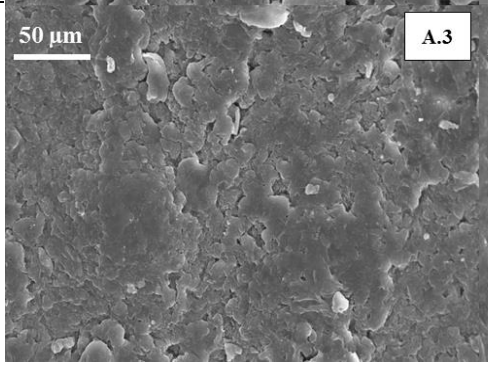	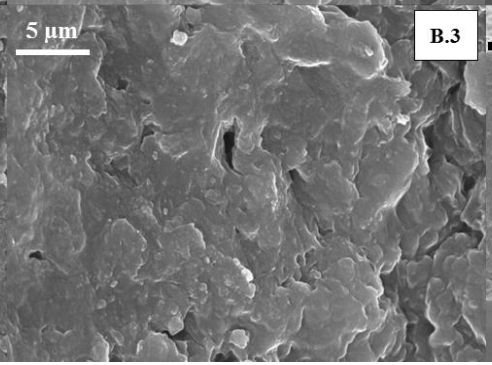	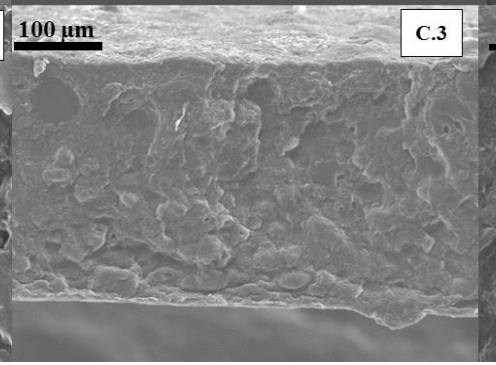	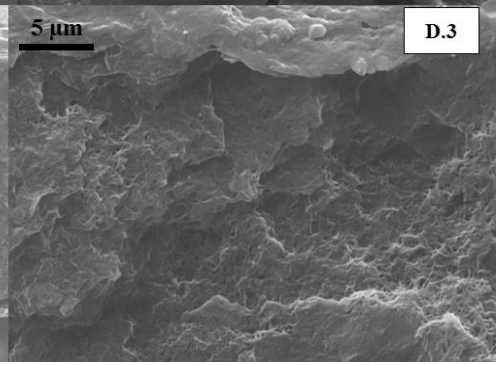

3.3.2. Thermal Properties of PHA films

The thermal properties of the PHA films prepared from mcl-PHA, PHB and PHB/mcl-PHA blend were accessed by differential scanning calorimetry (DSC) and thermogravimetric analysis (TGA).

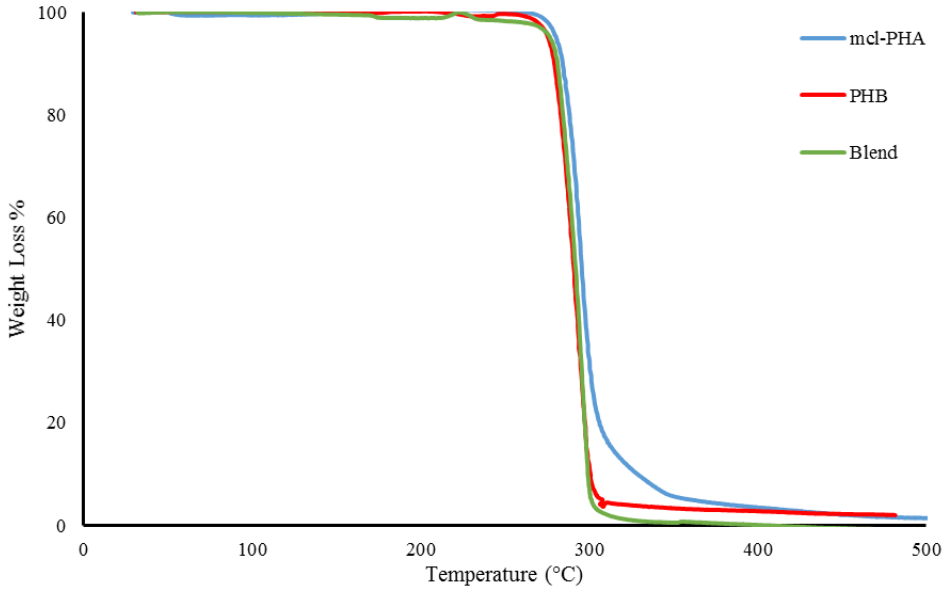

Figure 15 - Thermogravimetric analysis (TGA) curves of the PHB, mcl-PHA and the blend produced from apple pulp waste.

The film's thermal stability, the thermogravimetric curve (**Figure 15**) shows that the decomposition of the three films involved a fast one-step process. All films revealed weight loss close to the degradation temperatures (T_{deg}) characteristics of the three polymers, namely mcl-PHA (296 ºC), P(3HB) (284 ºC) and blend (297 ºC), that were characterized in **Chapter 2**. Its decomposition showed a single weight loss of approximately 92 and 97%, with a maximum degradation rate (T_{deg}) at approximately of 295 and 290 ºC for, respectively, mcl-PHA and PHB. Regarding the blend film, a maximum degradation rate (T_{deg}) at 295 ºC obtained an Δm of approximately 98 %. The PHB film revealed a T_{deg} higher than that reported in **Chapter 2**, may be due to the solvent casting technique. The mcl-PHA film presented a melting temperature (T_m) of 51 °C. As for the PHB film, a temperature of 178 ºC was determined corresponding to the melting temperature. On the other hand, the film prepared from the blend attained melting (T_m) temperatures of 52 and 174 °C, respectively.

3.3.3. X-Ray Diffraction of PHA Films

The PHA films were analysed by XRD (**Figure 16**) to determine their degree of crystallinity. The degree of crystallinity (X_c) was calculated as referred in section **2.3.3.5.** of **Chapter 2**.

The mcl-PHA film (**Figure 16**) present a degree of crystallinity of 15%.The amorphous part characterized by a broad hump located around 2θ = 19°, whereas the crystalline zone displayed one diffraction peak near 22° (80). These values are in accordance to those obtained for x-ray diffraction results attained for the polymer, mcl-PHA, thereby the solvent casting did not affect the crystallization of mcl-PHA. Regarding the PHB film (**Figure 16**), it demonstrated a degree of crystallinity of 40 %. The x-ray diffractogram demonstrated a set of peaks, namely located around 2θ = 14° and 17°, which are characteristic of the crystalline phase of PHB, whilst the humps close to 2θ = 22° and 25° where located in the amorphous zone characteristic of the PHB polymer (50,83). The PHB film demonstrated a lower degree of crystallinity (X_c = 40%) than the polymer suggesting that in this case the films preparation may have affected the crystallinity. As for the blend film, the x-ray diffractogram displayed (**Figure 16**) the main peaks identified for mcl-PHA and PHB films. Around 2θ = 19° and 22° the characteristic peaks of mcl-PHA were located, while on 2θ = 14° and 17° were the narrows peaks for PHB. This shows that the solvent casting procedure did not affect, in a considerably way, the crystalline fraction of any of the polymers that were used in the preparation of films.

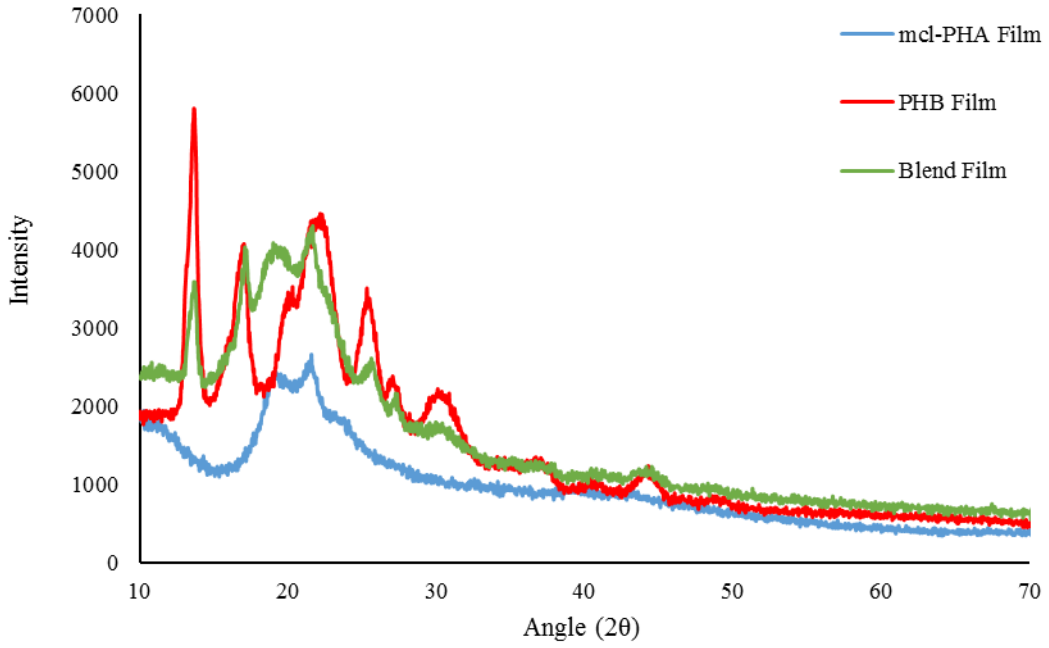

Figure 16 - X-ray diffractogram of mcl-PHA, PHB and Blend films.

3.3.4. FTIR of PHA films

FTIR spectroscopy was employed in order to examine if the solvent casting procedure had impact on the chemical interactions between the polymers (mcl-PHA, P(3HB) and blend) and the solvent, and if this interactions are reflected by characteristic changes in spectra bands. The mcl-PHA, PHB PHB/ml-PHA blend film FTIR spectra are represented in **Figure 17**. All FTIR spectrum shows an absorption peak at 1727 cm^{-1}, this band is usually the strongest peak in the spectra, corresponding to a characteristic band of PHA. The peak corresponds to the stretching band of the ester carbonyl group ($C = O$) (69). The spectra for the PHA films showed resemblance with the spectra obtained for mcl-PHA, PHB and blend polymers discussed in **2.3.3.3.** In **Figure 17** (a), is possible to identify a group of peaks indicating the presence of numerous characteristic structures within mcl-PHA, namely, asymmetric C-O-C stretching vibration (1261 cm^{-1}), C-O and C-C stretching vibration of the amorphous phase of the mcl-PHA (1019 and 1100 cm^{-1}, respectively (69,71). Regarding the PHB film (**Figure 17** (b)), spectra reveal very similar set of peaks with those found in the PHB polymers FTIR spectra. In this case, it is possible to identify peaks related to carbon bounding in CH_3 vibration (978 cm^{-1}), C-O bonds (1056 cm^{-1}), CH_3 (1377 cm^{-1}), and C-H elongation vibration (2928 cm^{-1}) (75). Lastly the blend film (**Figure 17** (c)) displayed peaks at 2908 and 2930 cm^{-1}, regarding methylene C-H vibration. This band is mostly characteristic of mcl-PHA spectra and is usually the weakest in PHB (73).Between 3000 and 3500 cm^{-1} is located a broad hump for PHB and blend films, corresponding to O-H stretch vibration (**Figure 17** (b) and (c)).

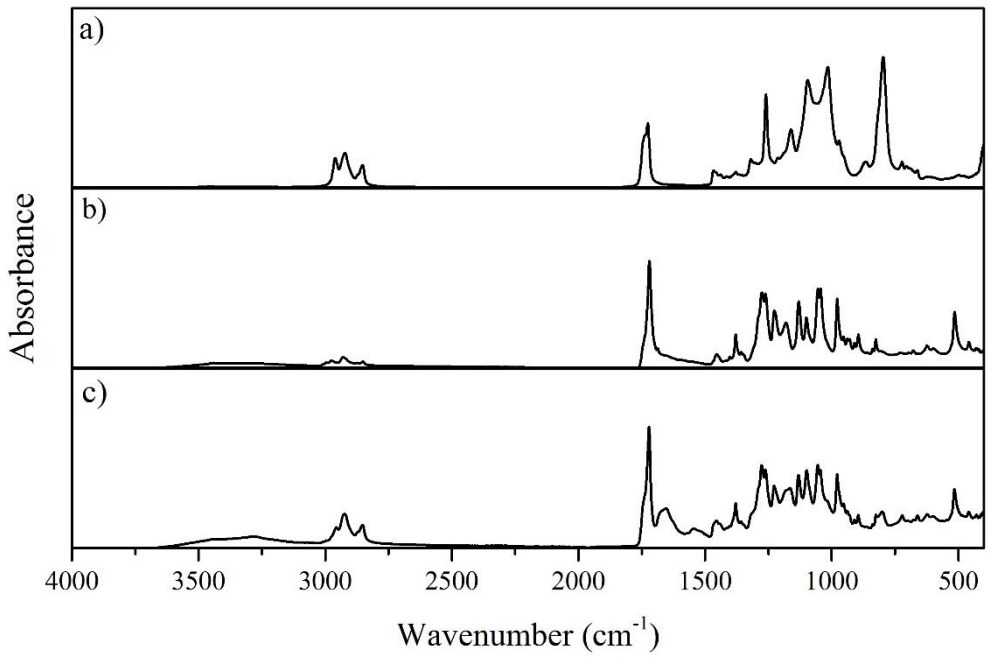

Figure 17 - FTIR-ATR spectra of the (a) mcl-PHA film, (b) PHB film and (c) PHB/ml-PHA blend film.

3.3.5. Swelling and contact angle of PHA films

With the purpose to assess the hygroscopic and hydrophobic capacities of the PHA films prepared, swelling behaviour and water contact angle were investigated. To evaluate the swelling degree of the PHA films prepared with the biopolymers produced from apple pulp waste, they were immersed in deionized water, at 30 ºC for 24 h. Altogether the films showed no significant change in the mass and in the volume of the samples after immersion. The mcl-PHA, PHB and blend films exhibited a negligible swelling degree of around, 2%, 4% and 5%, respectively. These results indicate that all PHA films showed no interaction with water, under the conditions of the test.

The water contact angle of the films was measured in the upper surface that was exposed to the atmosphere. This measurement is used as an indicator of the degree of hydrophobicity or hydrophilicity (103).This value can depend on a number of factors like, the film's roughness, and surface preparation as well as cleanliness (104). A water contact angle higher than 90° is considered hydrophobic (104). The surface water contact angles attained for the PHA films are presented on **Table 13**. The mcl-PHA films presented a surface contact angle (θ) of 101° whereas PHB films obtained a 79º on the surface. On the other hand, PHB/mcl-PHA blend attained a water contact angle of 98º (**Table 13**). Given the water contact angle, both mcl-PHA and PHB/mcl-PHA blend are considered hydrophobic, with the PHB films being hydrophilic.

The surface contact angle obtained for the mcl-PHA (**Table 13**) is similar to the one reported by PHO (θ = 98º) (105) and similar to natural rubber (θ = 92°) (106), silicone rubber (θ = 110°) (107), two known hydrophobic materials, as well as PHUA (θ = 100 to 109°) (105,108). On the other hand, the mcl-PHA film is more hydrophobic than P(HBHHx), a PHA copolymer of hydroxybutyrate (HB) with 12 mol% of hydroxyhexanoate (HHx) monomers, and the mcl-PHA synthesized by *P. putida* PGA1 from saponified palm kernel oil that has monomeric composition of HHx (9%), HO (83%), HD (5%), HDd (1%) and HTd (1%), were reported to have better wettability properties, given their lower water contact angle values (θ = 62° and 53°, for P(HBHHx) and mcl-PHA, respectively). These values may be due to the presence, in higher amount, of HHx for mcl-PHA from *P. putida* that may have contributed to a more viscous polymer compared to the mcl-PHA produced by *P. citronellolis* (94,109). Moreover, the preparation of these films was not achieved by solvent casting but instead, the polymer was dried in a vacuum oven until a thin sheet was formed which could lead to a film with less irregularities on the surface that was posteriorly measured (110).

Whilst, the contact angle attained for PHB (θ = 79º) (**Table 13**) is higher than those reported for the same polymer (θ = 63 to 68.5º) turning the films prepared from the P(3HB) produced by *C. necator* using apple pulp waste slightly more hydrophobic (36,108,111). For these materials, hydrophilicity occurs and the valleys on the surface will be penetrated by the water creating large

menisci over multiple asperities and valleys, leading to increased adhesion and friction (112). One of the ways to increase the hydrophobicity of the surface is to increase the surface roughness on a surface that is initially hydrophobic (112). Although the PHB films achieved in this study present a surface contact angle below the necessary degree to be considered hydrophobic, the SEM imaging of the films showed a certain level of roughness on the surface which might contributed to have a larger solid-liquid interface area leading to an increase of the surface contact angle relatively to other PHB films, thus proving PHB films from *C. necator* using apple pulp waste more hydrophobic. The surface contact angle is close to that of PET and PLA ($\theta = 75°$ and 74 to 84°, respectively), a known plastic with hydrophilic characteristics (106,113,114). As a result, making the PHB films is a promising option in the replacement of films mainly composed by these two plastics, since they provide a more suitable interface area. In comparison with co-polymers, namely PHBHV and PHBHHx, presented lower contact angles, since the addition of HHx and 3HV in P(3HB) results in lowering the water contact angle and thus in the increase of hydrophilicity, which will affect the rate of degradation (36).

As for the PHB/mcl-PHA blend film, presented a surface contact angle of 98º (**Table 13**) hence considered hydrophobic. The film presented an angle close to the one obtained for mcl-PHA film. Since, the SEM imaging of the blends presented a phase-separation between the PHB and mcl-PHA composing the blend, noticing that mcl-PHA was mostly present in the upper surface where solvent evaporation occurred, which coincides with the surface where the contact angle was measured. The surface presented a rough pattern, more than that of PHB, so the wettability of the blend films is higher than that of PHB and closer to mcl-PHA films. A similarity exists between the blend in study and PHO and PP, whose surface is also hydrophobic ($\theta = 98$ and 94º, respectively).

Table 13. Water contact angles for the PHA films prepared with the biopolymers produced from apple pulp waste and comparison with values reported for different materials (PET, polyethylene terephthalate; P(HBHHx), poly(3-hydroxybutyrate-*co*-3-hydroxyhexanoate); PLA, polylactic acid; PP, polypropylene; PHO, poly(hydroxyoctanoate); PHUA, poly(3-hydroxyundecanoate); P(3HB-co-4HB), poly(3-hydroxybutyrate-co-4-hydroxybutyrate); PHBHV, poly(3-hydroxybutyrate-co-3-hydroxyvalerate)).

Material	**Water Contact Angle (θ)**	**Reference**
P. citronellolis mcl-PHA	101 ± 0.9	This study
C. necator PHB	79 ± 1.6	This study
PHB/mcl-PHA Blend	98 ± 0.8	This study
P. putida mcl-PHA	53 ± 3.6	(110)
Silicone rubber	110	(107)
PET	75 ± 1.1	(113)
P(HBHHx)	62 ± 0.6	(94)
PLA	74	(106)
	84.8 ± 0.3	(114)
Natural rubber	92	(106)
PP	94	(115)
PHB	68.5	(111)
	66	(36)
	63	(108)
PHBHV	84	(108)
Polyacrylamide	25	(105)
PET	70	(105)
PHO	98 ± 2	(105)
PHUA	100 ± 2	(105)
	109	(108)

3.3.6. Gas Permeation

The pure gas permeation, CO_2 and O_2, through the different PHA films prepared were evaluated and the results obtained are presented in **Table 14**, together with the permeability values reported for several different synthetic and natural polymers.

Table 14. Oxygen and carbon dioxide permeability values for PHA films and for different natural and synthetic materials for both gases (PHB, Polyhydroxybutyrate; PHB/PEG, Polyhydroxybutyrate with 5% PEG (Polyethylene Glycol) as plasticizer ; P(HBV5), poly(3-hydroxybutyrate-*co*-3-hydroxyvalerate) with 5% valerate; P(HBHV), poly(3-hydroxybutyrate-*co*-3-hydroxyvalerate; PET, polyethylene terephthalate; LDPE, low-density polyethylene; PLA, Polylactic acid; MC/PEG, methylcellulose and poly(ethylene glycol); n.a., data not available).

Material	**Permeability ($cm^3.cm/cm^2.s.cmHg$)**		**Selectivity (α)**	**References**
	O_2	**CO_2**		
P. citronellolis mcl-PHA	1.1×10^{-09}	5.3×10^{-09}	4.69	This study
C. necator PHB	4.2×10^{-10}	2.6×10^{-09}	6.06	This study
PHB/mcl-PHA blend	2.6×10^{-10}	3.2×10^{-09}	12.25	This study
PHB	3.0×10^{-12}	n.a.	n.a.	(116)
PHB/PEG	6.0×10^{-18}	n.a.	n.a.	(117)
P(HBV5)	5.1×10^{-18}	n.a.	n.a.	(117)
P(HBHV)	2.1×10^{-11}	n.a.	n.a.	(116)
	1.3×10^{-15}	1.10×10^{-15}	0.85	(118)
PET	5.0×10^{-12}	n.a.	n.a.	(116)
	7.1×10^{-18}	2.3×10^{-17}	3.24	(119)
LDPE	6.0×10^{-16}	2.5×10^{-15}	4.17	(119)
PLA	3.0×10^{-11}	n.a.	n.a.	(116)
	8.4×10^{-18}	n.a.	n.a.	(120)
MC/PEG	n.a.	1.8×10^{-14}	n.a.	(119)
Silicone rubber	6.0×10^{-8}	3.2×10^{-7}	5.33	(121)
Natural rubber	2.4×10^{-9}	n.a.	n.a.	(121)
Polystyrene	1.2×10^{-10}	n.a.	n.a.	(121)
Nylon	7.1×10^{-18}	1.2×10^{-17}	1.69	(119)

The permeability of the mcl-PHA films was 1.1×10^{-09} $cm^3.cm/cm^2.s.cmHg$ for O_2, and 5.3×10^{-09} $cm^3.cm/cm^2.s.cmHg$, for CO_2. As for PHB films, 4.2×10^{-10} and 5.3×10^{-09} $cm^3.cm/cm^2.s.cmHg$, for O_2 and CO_2, respectively. Lastly, the PHB/mcl-PHA films presented a 2.6×10^{-10} $cm^3.cm/cm^2.s.cmHg$ permeability for O_2 and 3.2×10^{-09} $cm^3.cm/cm^2.s.cmHg$, for CO_2. The permeability of O_2 between the three tested films revealed that *P. citronellolis* mcl-PHA films are more permeable to oxygen than *C. necator* PHB or PHB / mcl-PHA films. However, between the last two, the PHB films are more susceptible to permeate oxygen than the blend films. As for the CO_2 permeability, all films presented a similar permeability with mcl-PHA films having a higher gas permeation value and *C. necator* PHB films the lowest. The mcl-PHA/mcl-PHA blend film presented a higher value than that of the PHB films, demonstrating that blending *P. citronellolis* mcl-PHA and *C. necator* PHB improved the *C. necator* PHB film permeability towards CO_2.

Regarding *P. citronellolis* mcl-PHA film (**Table 14**), the permeability to O_2 is similar to the value reported for natural rubber (2.4×10^{-09} $cm^3.cm/cm^2.s.cmHg$), which is commonly used as the principal raw material in tyre manufacturing (122). The value is higher than those described for the biodegradable polyesters PHB (3.0×10^{-12} $cm^3.cm/cm^2.s.cmHg$), P(HBHV) (2.1×10^{-11} $cm^3.cm/cm^2.s.cmHg$) and PLA (3.0×10^{-11} $cm^3.cm/cm^2.s.cmHg$) and also higher than those of the synthetic polyesters PET (5.0×10^{-12} $cm^3.cm/cm^2.s.cmHg$) and polystyrene (1.2×10^{-10} $cm^3.cm/cm^2.s.cmHg$) (Table 3). Moreover, *P. citronellolis mcl*-PHA films had lower permeability to both O_2 and CO_2 than silicone rubber (6.0×10^{-8} and 3.2×10^{-7} $cm^3.cm/cm^2.s.cmHg$, respectively), becoming a potential substitute for this material. These polymers are frequently used in the production of plastic bottles (123).

The permeability to O_2 towards the *C. necator* PHB film (**Table 14**) is higher than those reported for other PHB films (3.0×10^{-12} $cm^3.cm/cm^2.s.cmHg$) (116). Furthermore, the PHB film tested presented a higher O_2 permeability than those of P(HBHV) (2.1×10^{-11} and 1.3×10^{-15} $cm^3.cm/cm^2.s.cmHg$) and P(HBV5) (8.9×10^{-17} $cm^3.cm/cm^2.s.cmHg$) (116–118). PHB materials exhibit, per usually, low oxygen permeability values when compared with PHBV, however, when the content in 3-hydrpxyvalerate (3HV) increases, the same occurs to the material permeability towards O_2. Nevertheless, *C. necator* PHB film present an improvement regarding oxygen barrier proprieties without the presence of 3HV, since barrier properties generally decrease as HV content increases in the polymer (116,117). It was previously reported that polymers from renewable sources display significant lower permeabilities compared to common synthetic polymers from fossil resources (118). In comparison with other petroleum based conventional thermoplastics, such as PET (5.0×10^{-12} and 7.1×10^{-18} $cm^3.cm/cm^2.s.cmHg$) and polystyrene (1.2×10^{-10} $cm^3.cm/cm^2.s.cmHg$), *C. necator* PHB films revealed better oxygen permeabilities (116,119,121). The gas permeability study for the blend (**Table 14**) showed an O_2 and CO_2 permeability of 2.6×10^{-10} and 3.2×10^{-09} $cm^3.cm/cm^2.s.cmHg$, respectively. In view of the need to improve the permeability of biopolymers, the development of a film obtained from the co-production blend

allowed an improvement in the permeability of O_2 and CO_2 when compared to other synthetic materials as well as co-polymers or PHA films prepared with plasticizer agents, such as PEG. Regarding oxygen permeability of PHB/mcl-PHA blend film, it can be noted that the result obtained is close to the obtained for *C. necator* PHB film and is in line with the value reported for polystyrene (1.2×10^{-10} $cm^3.cm/cm^2.s.cmHg$) and higher that those reported for PET (5.0×10^{-12} and 7.1×10^{-18} $cm^3.cm/cm^2.s.cmHg$) (116,119,121). Usually the addition of a plasticizer, such as PEG, provides higher permeability (117). Unlike PHB/PEG and MC/PEG, the addition of PEG was not enough to contribute to improve barrier properties, since the amount that was added to PHB was very low (5% PEG) and methylcellulose (MC) is highly crystalline (117,119). In this case, the presence of mcl-PHA might have contributed for a higher O_2 permeability (**Table 14**).

The permeability coefficient of PHB/mcl-PHA blend film in CO_2 is higher than in oxygen, which is in line with gas permeability behaviour for many polymers, which is also demonstrated for both *P. citronellolis* mcl-PHA and *C. necator* PHB (118). The plasticizing effect on polymers is responsible for higher CO_2 permeabilities (118). The mcl-PHA, an amorphous polymer, present in the blend, possible acted like a plasticizing agent and improved the PHB permeability to CO_2 in the blend.

The selectivity (α) refers to ratio value attained from P_{CO2}/P_{O2}, where P_{CO2} and P_{O2} are the permeability coefficient of carbon dioxide and oxygen, respectively, in water. The resulting selectivity (α) of the films analysed (**Table 14**), reveal that the PHB/mcl-PHA blend film (α = 12.25) revealed a P_{CO2}/P_{O2} ratio double as the one for *C. necator* PHB (α = 6.06), while *P. citronellolis* mcl-PHA (α = 4.69) was the lowest. Synthetic polymers also present selectivity for carbon dioxide and oxygen, for example poly (vinylidene chloride) (PVC) (α = 5.8), polypropylene (α = 4.0) or Nylon 6 (α = 4.2) (119). Nevertheless, all films prepared, except *P. citronellolis* mcl-PHA, showed a CO_2/O_2 permeability ratio values higher than these synthetic polymers, hence, providing to be useful when both high permeability and high selectivity are required.

The gas permeability of polymers is an essential factor regarding their application, for example as barrier materials, in food packaging, as protective coatings and in a variety of biomedical materials. The gas separation of polymer membranes depends on the selectivity of a particular gas by the membrane over other gases. Gas transport properties depends on numerous factors on the membrane structure, such as the permeant size and shape, Mw, functional groups, density and polymer structure and crosslinking (124).

3.3.7. Mechanical Properties

As shown in **Table 15**, *P. citronellolis* mcl-PHA films (**Figure D** in Appendices) had a tensile strength at break of 4.9±0.68 MPa, deforming almost three times its original length until breaking (279±12%), associated with a Young Modulus of 7.8±1.58 MPa. Values of the same order of magnitude have been reported for other mcl-PHA, namely the ones synthesized by *P. mediterranea* and *P. oleovorans* from glycerol and octanoic acid, respectively (40,43) (**Table 15**). As expected, the mcl-PHA films were more ductile and less resistant to deformations than other natural polyesters, such as PHB, P(HBHV), P(HBHHx) and PLA. These materials typically have higher tensile strength at break (29.0 – 61.0 MPa) and Young Modulus (38 – 2500 MPa) values, as well as lower elongation at break (1.3 – 67.3 %), meaning they are more rigid with a higher resistance to deformation.

On the other hand, PHB films (**Figure E** in Appendices) showed a Young Modulus of 593.78 ± 32.05 MPa, a tensile strength of 19.28 ± 1.13 MPa and a strain at break of 10.44 ± 1.98 %. *C. necator* PHB films presented higher values than those reported for PHB produced by the same strain using spent coffee grounds (SCG) oils (62). The films also obtained better mechanical results compared to those attained by other films prepared by PHB (114,125). These films presented a much lower tensile strength (14.30 – 16.4 MPa) (Table 4) and a deformation at break (4.0 - 5.0 %) than *C. necator* PHB films (114,125). The same occurred when compared to a copolymer, P(3HB4HB) with 40% of 4-hydrpxybutyrate (114). Films prepared from this copolymer presented lower mechanical properties, except the deformation being significantly higher (0.30 MPa tensile strength, 62.7% of deformation and 1.9 MPa Young Modulus) when compared to *C. necator* PHB films (**Table 15**) (114). P(HBHHx) presents values of deformation at break much higher (56.5 – 67 %), this may be due to the presence of HHx, providing more flexibility to the material. However, this relationship did not extended to Young Modulus (38 – 455 MPa) or Tensile strength (10.95 – 11.3 MPa), values below those obtained for *C. necator* PHB films (114,125). In addition, other materials, such as PHA-LE (an epoxidized PHA), SBR and PP, are relatively more flexible than the PHB films tested in this study since all presented higher deformations (**Table 15**) (37,77,126).

The mechanical properties of *C. necator* PHB films are significant different than those obtained for *P. citronellolis* mcl-PHA films (**Table 15**). mcl-PHA films revealed to be flexible and resistant, whilst PHB films were more brittle and rigid. The necessity of a set of mechanical properties for PHB films, lead to the preparation of films by solvent casting using the blend of PHB and mcl-PHA attained from the production using apple pulp.

The PHB/mcl-PHA blend films presented a lack of interaction between both polymers present in the blend, PHB and mcl-PHA, as shown in **Figure 14**. This additional factor acted as a stress concentrator during the mechanical tests, facilitating the fragile behaviour of the blends. Other

studies reported in the literature show evidence that phase separation in biopolymers mixtures, such as P(HBV) and mcl-PHA or PHBHV and natural rubber (NR), affect the film structure and thus the films properties, in particular mechanical properties. The fact that the films presented irregularities on their surface, not only influenced the mechanical tests itself but also the measurement of the thickness, which, consequently, had an impact on the calculations for the mechanical features of the films. As an example of this situation, **Figure G** in Appendices, demonstrated the influence of the phase separation visible on the films.

Nevertheless, the curve for one sample of the blend films (**Figure F** in Appendices) allowed to reveal a tensile strength at break of 1.97 MPa, with a deformation of 324.20 % until breaking, associated with a Young Modulus of 6.59 MPa. Taking these values into account, the PHB/mcl-PHA blend films revealed more similarity to *P. citronellolis* mcl-PHA than *C. necator* PHB. The PHB/mcl-PHA revealed to be more prone to deformations close to some values obtained for P(HBHV) (212.1 %) and P(HBHHx) (380.0 %) (89,127). For instance, the bends revealed to have matching mechanical features to PHHxHO, which presented a similarity with the strain at break (380.00 %) and Young Modulus (8.00 MPa), although it revealed higher tensile strength (9.00 MPa) (127). Despite the fact that the blend showed closer deformation values with PP (375 %), the tensile strength (32.3 MPa) and Young Modulus (1222 MPa) are still very high (37).

It is possible to observe that *P. citronellolis* mcl-PHAs and Tissucol, a commercialized synthetic fibrin sealant used in surgery, have features in common, due to low Young Modulus values (7.80 MPa and 0.04 MPa, respectively) and higher deformations (279.20 % and 363 %, respectively) (128). These mechanical features demonstrate that mcl-PHAs films are flexible and susceptible to elastic and plastic deformations. On the other hand, *C. necator* PHB and PHB films in general, show opposite characteristics, with higher tensile strength at break (19.28 MPa and 14.30 to 37 MPa) and higher Young Modulus (583.78 MPa and 400 to 1500 MPa, respectively). Despite the fact that the blends were not completely approved for mechanical tests, it was possible to see with one sample that the presence of mcl-PHA had influence by decreasing tensile strength and Young Modulus and raising strain at break.

Table 15. Mechanical properties of films prepared by solvent casting and comparison with other natural and synthetic polymers (PHB, polyhydroxybutyrate; P(HBHV), poly(3-hydroxybutyrate-*co*-3-hydroxyvalerate); P(HBHHx), poly(3-hydroxybutyrate-*co*-3-hydroxyhexanoate); P(3HB4HB), poly(3-hydroxybutyrate-*co*-4-hydroxybutyrate); PHHxHO, poly(3-hydroxyhexanoate-*co*-3-hydroxyoctanoate); PHA-LE, epoxidized PHA from lineseed oil; PLA, Polylactic acid; SBR, styrene butadiene rubber; PP, polypropylene; n.a., data not available).

Material	Tensile strenght at break (MPa)	Strain at break (%)	Young Modulus (MPa)	Reference
P. citronellolis mcl-PHA(1)	4.86 ± 0.68	279.20 ± 12.01	7.80 ± 1.58	This study
C. necator PHB(2)	19.28 ± 1.13	10.44 ± 1.98	583.78 ± 32.05	This study
PHB/mcl-PHA blend(3)	1.97	324.20	6.59	This study
P. mediterranea mcl-PHA	6.5 ± 0.35	195 ± 46	5.3 ± 1.14	(43)
P. oleovorans mcl-PHA	n.a.	n.a.	100 ± 4.00	(40)
PHB	16.4	4.0	1317	(125)
	16.0	1.3	1000	(62)
	14.30	5.0	1500	(114)
	37	21.6	400	(36)
P(HBHV)	28.0-29.0	3-14	2500 ± 0.20	(99,129)
	15.1	212.1	1344.4	(89)
P(HBHV)/NR	7.3	547.7	7333.2	(89)
P(HBHHx)	11.3	67	38	(125)
	10.95	56.5	455	(114)
PHHxHO	9.00	380.00	8.00	(127)
P(3HB4HB)	0.30	62.7	1.9	(114)
PHA-LE	4.8 ± 0.5	54.2 ± 6.4	12.9 ± 1.6	(77)
PLA	61.0	5	1904	(101)
SBR	2.1±0.05	450 ± 0.0	1.8 ± 0.05	(126)
PP	32.3	375	1222	(37)
Tissucol	0.14 ± 0.02	363.10 ± 30.58	0.04 ± 0.01	(128)

(1) *P. citronellolis* mcl-PHA mechanical properties were calculated from an average of 3 samples. Tensile-Deformation curve is available in **Figure D** in appendices.
(2) *C. necator* PHB mechanical properties were calculated from an average of 3 samples. Tensile-Deformation curve is available in **Figure E** in appendices.
(3) PHB/mcl-PHA blend mechanical properties were calculated from one sample. Tensile-Deformation curve is available in **Figure F** in appendices.

3.4. Conclusions

PHAs, namely mcl-PHA, PHB and the blend produced from apple pulp waste in the previous chapter, showed interesting features, hence they were used in the development of PHA based films.

The analysis performed for the PHA films revealed that the blend films (containing mcl-PHA and PHB) were not miscible, showing signs of phase separation between the PHB and the mcl-PHA. From SEM analysis, the films presented a compact structure, nevertheless it is possible to see that the blend is not miscible in the preparations. TGA experiments showed that all PHA films present one single step of weight loss. DSC measurements for mcl-PHA and PHB showed films with only one T_m, while for the blend, it was revealed that the blend hold two melting temperatures corresponding to the mcl-PHA and PHB of 52 and 174 °C, respectively. The same occur for T_{deg}, where mcl-PHA and PHB presented 296 and 284 °C, respectively. Thus the T_{deg} for the blend film showed temperature close to the one for mcl-PHA of 295 °C.

The solvent casting procedure did not affect significantly the polymers features, since all films displayed similar chemical interactions through the FTIR spectra as well as similar degree of crystallinity. Altogether, the PHA films tested for swelling and contact angle were characterized by their hydrophobicity, which allowed to produce films that are expected to be resistant to water. The film's permeability was also tested for oxygen and carbon dioxide. From all films, *P. citronellolis* mcl-PHA film revealed to be most permeable, 1.1×10^{-09} and 5.3×10^{-09} $cm^3.cm/cm^2.s.cmHg$, to O_2 and CO_2, respectively. mcl-PHA, PHB and the blend films revealed higher permeabilities to oxygen and carbon dioxide than other synthetic materials from petroleum-based sources, confirming the potential applicability of these materials to be used for films in applications such as wound dressing and clinical sutures or as carrier for control release drugs.

Moreover, the mechanical tests for the blend revealed an improvement on the strain at break (324.20 %) and Young Modulus (6.59 MPa) compared to the PHB film alone. The presence of mcl-PHA may have act as plasticizer on PHB mechanical features. However, the tensile strength at break attained was too low (1.97 MPa) when compared to mcl-PHA film (4.86 MPa) which means the sample might needed a larger amount of PHB to display more strength at break.

The films presented a set of characteristics that are attractive due to the flexibility, a required feature, namely in the biomedical area, where high permeabilities provided by films are important for gases exchanges. Therefore, it can be anticipated that *P. citronellolis mcl*-PHA, *C. necator* PHB and a blend of both polymers, might developed into a material useful for applications ranging from commodity packaging products to high-value biomaterials.

Chapter 4

Conclusions and Future Work

4.1. Conclusions and Future Work

Apple pulp waste demonstrated to be an interesting and highly potential carbon source for microbial biopolymers production, turning into a suitable waste to be valorised. The work developed in this thesis allowed to demonstrate the versatility of the feedstock to be used by different bacteria while producing different polymers compared to other carbon sources. Meanwhile, it was evident that all the bacterial strains tested have the ability to use apple pulp for the production of biopolymers, being the results obtained in this work an indicative of their potential towards the production for mcl-PHA and PHB. However, the process still needs to be improved or optimized regarding PHA accumulation, especially for the new blend biopolymer. Different strategies may be applied in the future such as using a different set of conditions regarding the oxygen, pulse feed to achieve higher biomass content and different inoculations percentages for each strain used in the production, in order to understand if the blend is be able to produce more content in mcl-PHA than PHB, or vice-versa, and the possible impact on the mechanical and gas barrier properties.

PHB, mcl-PHA and the blend produced from apple pulp waste from fruit processing industry demonstrated to have physical-chemical properties to be used as suitable materials in the development of PHA based films with interesting properties, comparable to those of other synthetic polymers, with the advantage of being biodegradable and biocompatible.

The development of PHA films using the biopolymers that were produced using apple pulp waste by means of solvent casting is also a focus for future work, namely for the blend films. These showed signs of high segregation between the PHB and mcl-PHA that constitute the blend. The need to test other solvents or mixtures for the films preparation as well as to use different evaporation conditions (drying step) are important for further future works regarding the optimization of the blend films process.

Besides the problem showed by the films preparation, it stays clear that the polymer produced by the co-culture is able to rearrange into a polymeric structure in the form of a film. However, one of the advantages that the tests performed with the films is that the presence of mcl-PHA contributed for gas permeation. The PHA films revealed similar high permeabilities, another aspect to be considered, taking into account that most applications require the need for gas exchanges in wound management applications like the case of bandages for surgical applications. The characteristic defects of scl-PHA confine the processing and stability of this type of polymer, as well as the application of its products. Many efforts have been focused on the modification of scl-PHA to improve the mechanical properties and the applicability of obtained scl-PHA products. This feature was evident upon the mechanical tests and results for the PHB films prepared during this work. Therefore, the blend allowed to understand that by producing a

polymer that already had the presence of mcl-PHA would improve the properties of PHB. The results attained for the mechanical tests for the all PHA films showed this evidence. The blend films, regardless of the phase separation problem revealed better mechanical features than PHB itself.

At the end, there are still many tests that remain to be done, especially regarding the optimization for the polymers production, the films preparation, particularly the case of the blend, confirmation of the potential of the blend films by producing blends using mcl-PHA and PHB that were produced in batch using apple pulp waste. Moreover, puncture tests would be important to perform in order to understand the films resistance to perforation for package applicability, adhesive tests also would allow to understand if prepared PHA films would provide adhesion to the skin for its application in the medicine field.

References

1. Mirabella, N., Castellani, V., Sala, S., (2014). Current options for the valorization of food manufacturing waste: A review. *Journal of Cleaner Production*, (65), 28–41.
2. Nielsen, C., Rahman, A., Rehman, A.U., Walsh, M.K., Miller, C.D., (2017). Food waste conversion to microbial polyhydroxyalkanoates. *Microbial Biotechnology*, 10 (6), 1338–1352.
3. Fava, F., Totaro, G., Diels, L., Reis, M., Duarte, J., Carioca, O.B., Poggi-Varaldo, H. M., Ferreira, B. S. (2015). Biowaste biorefinery in Europe: Opportunities and research & development needs. *New Biotechnology*, 32 (1), 100–108.
4. Federici, F., Fava, F., Kalogerakis, N., Mantzavinos, D. (2009). Valorisation of agro-industrial by-products, effluents and waste: Concept, opportunities and the case of olive mill waste waters. *Journal of Chemical Technology & Biotechnology: International Research in Process, Environmental & Clean Technology*, 84(6), 895–900.
5. Carreira, P., Mendes, J.A.S., Trovatti, E., Serafim, L.S., Freire, C.S.R., Silvestre, A.J.D., Neto, C.P. (2011). Utilization of residues from agro-forest industries in the production of high value bacterial cellulose. *Bioresource Technology*, 102(15), 7354–7360.
6. Antunes, S., Freitas, F., Sevrin, C., Grandfils, C., Reis, M.A.M. (2017) Production of FucoPol by Enterobacter A47 using waste tomato paste by-product as sole carbon source. *Bioresource Technology*, 227, 66–73.
7. Yates, M., Gomez, M.R., Martin-Luengo, M.A., Ibañez, V.Z., Martinez Serrano, A.M. (2017). Multivalorization of apple pomace towards materials and chemicals. Waste to wealth. *Journal of Cleaner Production*, 143, 847–53.
8. Saheed, O.K., Jamal, P., Karim, M.I.A., Alam, M.Z., Muyibi, S.A. (2016). Utilization of fruit peels as carbon source for white rot fungi biomass production under submerged state bioconversion. *Journal of King Saud University-Science*, 28(2), 143–151.
9. Bhushan, S., Kalia, K., Sharma, M., Singh, B., Ahuja, P.S. (2008). Processing of apple pomace for bioactive molecules. *Critical Reviews in Biotechnology*, 28(4), 285–96.
10. Wang, X. & Lu, X. (2014). Characterization of pectic polysaccharides extracted from apple pomace by hot-compressed water. *Carbohydrate Polymers*, 102, 174–184.
11. Vendruscolo, F., Albuquerque, P.M., Streit, F., Esposito, E., Ninow, J.L. (2008). Apple pomace: A versatile substrate for biotechnological applications. C*ritical Reviews in Biotechnology*, 28 (1), 1–12.
12. Nicolas, J.J., Richard-Forget, F. C., Goupy, P. M., Amiot, M. J., & Aubert, S.Y. (1994). Enzymatic browning in Apple and Apple Products. *Critical Reviews in Food Science and Nutrition*, 34(2), 109-157.
13. Madrera, R.R., Bedriñana, R.P., & Valles, B.S. (2015). Production and characterization of aroma compounds from apple pomace by solid-state fermentation with selected yeasts. *LWT - Food Science and Technology*, 64(2), 1342–53.

14. Castilho, L.R., Mitchell, D.A., & Freire, D.M.G. (2009). Production of polyhydroxyalkanoates (PHAs) from waste materials and by-products by submerged and solid-state fermentation. Bioresource technology.100(23), 5996–6009.
15. Keshavarz, T., & Roy, I. (2010). Polyhydroxyalkanoates: bioplastics with a green agenda. *Current Opinion Microbiology*, 13(3), 321–326.
16. Kunasundari, B., & Sudesh, K. (2011) Isolation and recovery of microbial polyhydroxyalkanoates. Express Polymer Letters, 5(7), 620–634.
17. Reddy, C.S.K., Ghai, R., & Kalia, V.C. (2003). Polyhydroxyalkanoates : an overview. *Bioresource technology*, 87(2), 137–146.
18. Pouton, C.W., & Akhtar, S. (1996). Biosynthetic polyhydroxyalkanoates and their potential in drug delivery. *Advanced Drug Delivery Reviews*, 18(2), 133–162.
19. Verlinden, R.A.J., Hill, D.J., Kenward, M.A., Williams, C.D., & Radecka, I. (2007). Bacterial synthesis of biodegradable polyhydroxyalkanoates. *Journal of applied microbiology*, 102(6), 1437–1449.
20. Serafim, L.S., Lemos, P.C., Albuquerque, M.G.E., & Reis, M.A.M.(2008). Strategies for PHA production by mixed cultures and renewable waste materials. *Applied microbiology and biotechnology*,81(4), 615–628.
21. Bugnicourt, E., Cinelli, P., Lazzeri, A., & Alvarez, V. (2014). Polyhydroxyalkanoate (PHA): Review of synthesis, characteristics, processing and potential applications in packaging. *Express Polymers Letters*, 8(11), 791–808.
22. Laycock, B., Halley, P., Pratt, S., Werker, A., & Lant, P. (2014). The chemomechanical properties of microbial polyhydroxyalkanoates. Progress in Polymer Science, 39(2), 536–583.
23. Salehizadeh, H., & Van Loosdrecht, MCM. (2004). Production of polyhydroxyalkanoates by mixed culture: Recent trends and biotechnological importance. *Biotechnology Advances*, 22(3), 261–279.
24. Albuquerque, M.G.E., Martino, V., Pollet, E., Avérous, L., & Reis, M.A.M. (2011). Mixed culture polyhydroxyalkanoate (PHA) production from volatile fatty acid (VFA)-rich streams: Effect of substrate composition and feeding regime on PHA productivity, composition and properties. *Journal Biotechnology*, 151(1), 66–76.
25. Martinez, G. A., Bertin, L., Scoma, A., Rebecchi, S., Braunegg, G., & Fava, F. (2015). Production of polyhydroxyalkanoates from dephenolised and fermented olive mill wastewaters by employing a pure culture of Cupriavidus necator. *Biochemical engineering journal*, 97, 92–100.
26. Lee, S.Y. (1996). Plastic bacteria? Progress and prospects for polyhydroxyalkanoate production in bacteria. *Trends in Biotechnology*, 14(11), 431–438.
27. Elain, A., Le Grand, A., Corre, Y.M., Le Fellic, M., Hachet, N, Le Tilly, V., Loulergue,

P., Audic, J., & Bruzaud, S. (2016). Valorisation of local agro-industrial processing waters as growth media for polyhydroxyalkanoates (PHA) production. *Industrial Crops and Products*, 80, 1–5.

28. Tan, G.Y.A., Chen, C.L., Li, L., Ge, L., Wang, L., Razaad, I.M.N., Li, Y., Zhao, L., Mo, Y., & Wang, J. (2014). Start a research on biopolymer polyhydroxyalkanoate (PHA): A review. *Polymers from Biomass*, 6(3), 706–754.
29. Madkour, M.H., Heinrich, D., Alghamdi, M.A., Shabbaj, I.I., & Steinbüchel, A. (2013) PHA recovery from biomass. *Biomacromolecules*, 14(9), 2963–2972.
30. Koller, M., Niebelschütz, H., & Braunegg, G. (2013). Strategies for recovery and purification of poly[(R)-3-hydroxyalkanoates] (PHA) biopolyesters from surrounding biomass. *Engineering in Life Sciences*, 13(6), 549–562.
31. Anjum, A., Zuber, M., Zia, K.M., Noreen, A., Anjum, M.N., & Tabasum, S. (2016). Microbial production of polyhydroxyalkanoates (PHAs) and its copolymers: A review of recent advancements. *International journal of biological macromolecules*,89, 161–174.
32. Ashby, R.D., & Solaiman, D.K.Y. (2008). Poly(hydroxyalkanoate) biosynthesis from crude alaskan pollock (theragra chalcogramma) oil. *Journal of Polymers and the Environment*, 16(4), 221–229.
33. Wang, S., Chen, W., Xiang, H., Yang, J., Zhou, Z., Zhu, M. (2016). Modification and potential application of short-chain-length polyhydroxyalkanoate (SCL-PHA). *Polymers*, 8(8), 273.
34. Roy, I., & Visakh, P.M. (Eds.). (2014). Polyhydroxyalkanoate (PHA) Based Blends , Composites and Nanocomposites (Vol. 30). *Royal Society of Chemistry*.
35. Cruz, M. V., Freitas, F., Paiva, A., Mano, F., Dionísio, M., Ramos, A.M., & Reis, M. A. (2016). Valorization of fatty acids-containing wastes and byproducts into short- and medium-chain length polyhydroxyalkanoates. *New Biotechnology*, 33(1), 206–215.
36. Misra, S., Valappil, S., Roy I., & Boccaccini, A. R. (2006). Polyhydroxyalkanoate (PHA) / inorganic phase composites for tissue engineering applications. *Biomacromolecules*, 7(50), 2249–2258.
37. Villaluenga, J.P.G., Khayet, M., López-Manchado, M.A., Valentin, J.L., Seoane, B., & Mengual, J.I. (2007). Gas transport properties of polypropylene/clay composite membranes. *European Polymer Journal*, 43(4), 1132–1143.
38. Kang, D.K., Lee, C.R., Lee, S.H., Bae, J.H., Park, Y.K., Rhee, Y.H., Sung, B. H., Sohn, J. (2017). Production of polyhydroxyalkanoates from sludge palm oil using pseudomonas putida S12. Journal of microbiology and biotechnology, 27(5), 990–994.
39. Muhr, A., Rechberger, E.M., Salerno, A., Reiterer, A., Malli, K., Strohmeier, K., Schobber, S., Mittelbach, M., & Koller, M. (2013). Novel Description of mcl-PHA Biosynthesis by Pseudomonas chlororaphis from Animal-Derived Waste. *Journal of*

Biotechnology, 165(1), 45–51.

40. Chardron, S., Bruzaud, S., Lignot, B., Elain, A., & Sire, O. (2010). Characterization of bionanocomposites based on medium chain length polyhydroxyalkanoates synthesized by Pseudomonas oleovorans. *Polymer Testing*, 29(8), 966–971.
41. Rai, R., Keshavarz, T., Roether, J.A., Boccaccini, A.R., & Roy, I. (2011). Medium chain length polyhydroxyalkanoates, promising new biomedical materials for the future. *Materials Science and Engineering: R: Reports*,72(3), 29–47.
42. Muhr, A., Rechberger, E.M., Salerno, A., Reiterer, A., Schiller, M., Kwiecień, M., Adamus, G., Kowalczuk, M., Strohmeier, K., Schober, S., Mittelbach, M., & Koller, M. (2013). Biodegradable latexes from animal-derived waste: Biosynthesis and characterization of mcl-PHA accumulated by Ps. citronellolis. *Reactive and Functional Polymers*, 73(10), 1391–1398.
43. Pappalardo, F., Fragalà, M., Mineo, P.G., Damigella, A., Catara, A.F., Palmeri, R., & Rescifina, A. (2014). Production of filmable medium-chain-length polyhydroxyalkanoates produced from glycerol by Pseudomonas mediterranea. *International Journal of Biological Macromolecules*, 65, 89–96.
44. Woolnough, C.A., Yee, L.H., Charlton, T., & Foster, L.J.R.(2010). Environmental degradation and biofouling of "green" plastics including short and medium chain length polyhydroxyalkanoates. *Polymer International*, 59(5), 658–667.
45. Wang, Y., Yi,n J., & Chen, G.Q. (2014) Polyhydroxyalkanoates, challenges and opportunities. *Current Opinion in Biotechnology*, 30, 59–65.
46. Morais, C., Freitas, F., Cruz, M. V., Paiva, A., Dionísio, M., & Reis, M.A.M. (2014). Conversion of fat-containing waste from the margarine manufacturing process into bacterial polyhydroxyalkanoates. *International Journal of Biological Macromolecules*, 71, 68–73.
47. Cruz, M.V., Araújo, D., Alves, V.D., Freitas, F., & Reis, M.A.M. (2016). Characterization of medium chain length polyhydroxyalkanoate produced from olive oil deodorizer distillate. *International Journal of Biological Macromolecules*, 82, 243–248.
48. Follonier, S., Goyder, M.S., Silvestri, A.C., Crelier, S., Kalman, F., Riesen, R., & Zinn, M. (2014). Fruit pomace and waste frying oil as sustainable resources for the bioproduction of medium-chain-length polyhydroxyalkanoates. *International Journal of Biological Macromolecules*, 71, 42–52.
49. Fall, R.R., Brown, J.L., Schaeffer, T.L. (1979). Enzyme recruitement allows the biodegradation of recalcitrant branched hydrocarbons by Pseudomonas citronellolis. *Applied and Environmental Microbiology*, 38(4), 715–722.
50. Martino, L., Cruz, M.V., Scoma, A., Freitas, F., Bertin, L., Scandola, M., & Reis, M. A. (2014). Recovery of amorphous polyhydroxybutyrate granules from Cupriavidus necator

cells grown on used cooking oil. *International Journal of Biological Macromolecules*, 71, 117–123.

51. He, W., Tian, W., Zhang, G., Chen, G-Q., & Zhang, Z. (1998). Production of novel polyhydroxyalkanoates by *Pseudomonas stutzeri* 1317 from glucose and soybean oil. *FEMS Microbiology Letters*, 169(1), 45–49.
52. Mothes, G., Schnorpfeil, C., & Ackermann, JU. (2007). Production of PHB from crude glycerol. *Engineering in Life Sciences*, 7(5), 475–479.
53. Ashby, R.D., Solaiman, D.K.Y., & Foglia, T.A. (2005). Synthesis of Short- /Medium-Chain-Length Poly (hydroxyalkanoate) blends by mixed culture fermentation of glycerol. *Biomacromolecules*, 6(4), 2106–2112.
54. Brandl, H., Gross, R. A., Lenz, R.W., & Fuller, R.C. (1988). Pseudomonas oleovorans as a Source for novel Poly(beta-Hydroxyalkanoates). *Applied and Environmental Microbiology*, 54(8), 1977–1982.
55. Lagunes, F.G, & Winterburn, J.B. (2016). Bioresource Technology Effect of limonene on the heterotrophic growth and polyhydroxybutyrate production by Cupriavidus necator H16. *Bioresource Technology*, 221, 336–343.
56. Cromwick, A.M., Foglia, T., & Lenz, R. W. (1996). The microbial production of poly (hydroxyalkanoates) from tallow. *Applied Microbiology and Biotechnology*, 46(5-6), 464–469.
57. Kahar, P., Tsuge, T., Taguchi, K., & Doi, Y. (2004). High yield production of polyhydroxyalkanoates from soybean oil by Ralstonia eutropha and its recombinant strain. *Polymer degradation and stability*, 83(1), 79–86.
58. Park, D.H., & Kim, B.S. (2011). Production of poly (3-hydroxybutyrate) and poly (3-hydroxybutyrate-co-4- hydroxybutyrate) by Ralstonia eutropha from soybean oil. *New Biotechnology*, 28(6), 719–724.
59. Ng, K., Ooi, W., Goh, L., Shenbagarathai, R., Sudesh, K.(2010). Evaluation of jatropha oil to produce poly (3-hydroxybutyrate) by Cupriavidus necator H16. *Polymer Degradation and Stability*, 95(8), 1365–1369.
60. Fuchtenbusch, B., Wullbrandt, D., & Steinbuchel, A. (2000). Production of polyhydroxyalkanoic acids by Ralstonia eutropha and Pseudomonas oleovorans from an oil remaining from biotechnological rhamnose production. *Applied microbiology and biotechnology*, 53(2), 167–72.
61. Zahari, M.A.K.M., Zakaria, M.R., Ariffin, H., Mokhtar, M.N., Salihon, J., Shirai, Y., & Hassan, M.A. (2012). Renewable sugars from oil palm frond juice as an alternative novel fermentation feedstock for value-added products. *Bioresource Technology*, 110, 566–571.
62. Cruz, M.V., Paiva, A., Lisboa, P., Freitas, F., Alves, V.D., Simões, P., Barreiros, S. & Reis, M.A.M. (2014). Production of polyhydroxyalkanoates from spent coffee grounds oil

obtained by supercritical fluid extraction technology. *Bioresource Technology*,157, 360–363.

63. Fiorese, M.L., Freitas, F., Pais, J., Ramos, A.M., De Aragão, G.M.F., & Reis, M.A.M. (2009). Recovery of polyhydroxybutyrate (PHB) from Cupriavidus necator biomass by solvent extraction with 1,2-propylene carbonate. *Engineering in Life Science*s, 9(6), 454–461.
64. Guo-Qiang, C., Jun, X., Qiong, W., Zengming, Z., & Kwok-Ping, H. (2001). Synthesis of copolyesters consisting of medium-chain-length β-hydroxyalkanoates by Pseudomonas stutzeri 1317. *Reactive and Functional Polymers*, 48(1–3),107–112.
65. Miura, T., Ishii, D., & Nakaoki, T.. Production of Poly(3-hydroxyalkanoate)s by Pseudomonas putida Cultivated in a Glycerol/Nonanoic Acid-Containing Medium. *Journal of Polymers and the Environment*, 21(3), 760–765.
66. Haas, C., Steinwandter, V., Diaz de Apodaca, E., Maestro Madurga, B., Smerilli, M., Dietrich, T., & Neureiter, M. (2015). Production of PHB from Chicory Roots – Comparison of Three Cupriavidus necator Strains. *Chemical and biochemical engineering quarterly*, 29(2), 99–112.
67. Taniguchi, I., Kagotani, K., & Kimura, Y. (2003). Microbial production of poly (hydroxyalkanoate) s from waste edible oils. *Green Chemistry*, 5(5), 545–548.
68. Hahn, S.K., Chang, Y.K., Kim, B.S., Lee, K.M., & Chang, H.N. (1993). The recovery of poly (3-hydroxybutyrate) by using dispersions of sodium hypochlorite solution and chloroform, *Biotechnology Techniques*,7(3), 209–212.
69. Ouyang, S., Luo, R.C., Chen, S., Liu, Q., Chung, A., Wu, Q., & Chen, G. Q. (2007). Production of Polyhydroxyalkanoates with High 3-Hydroxydodecanoate Monomer Content by fadB and fadA Knockout Mutant of Pseudomonas putida KT2442. *Biomacromolecules*, 8(8) 2504–2511.
70. Gumel, A.M., Annuar, M. S. M., & Heidelberg, T. (2014). Growth kinetics , effect of carbon substrate in biosynthesis of mcl-PHA by Pseudomonas putida Bet001. *Brazilian Journal of Microbiology*,45(2), 427–438.
71. Xu, J., Guo, B.H., Yang, R., Wu, Q., Chen, G.Q., & Zhang, Z.M. (2002). In situ FTIR study on melting and crystallization of polyhydroxyalkanoates. *Polymer*, 43(25), 6893–6899.
72. Guo, W., Duan, J., Geng, W., Feng, J., Wang, S., & Song, C. (2013). Comparison of medium-chain-length polyhydroxyalkanoates synthases from Pseudomonas mendocina NK-01 with the same substrate specificity. *Microbiological Research*, 168(4), 231–237.
73. Hong, K., Sun, S., Tian, W., Chen, G.Q., & Huang, W. (1999). A rapid method for detecting bacterial polyhydroxyalkanoates in intact cells by Fourier transform infrared spectroscopy. *Applied Microbiology and Biotechnology*, 51(4),523–526.

74. Randriamahefa, S., Renard, E., Gue, P., & Langlois, V. (2003). Fourier Transform Infrared Spectroscopy for Screening and Quantifying Production of PHAs by Pseudomonas Grown on Sodium Octanoate, *Biomacromolecules*, 4(4), 1092–1097.

75. Rech, C. R., Martelli, S.M., & Brabes, K.C.D.S.(2018). Antimicrobial Analysis and Characterization of P(3HB) Films Containing Essential Oils, *Orbital: The Electronic Journal of Chemistry*, 10(1),9–13.

76. Tănase, E.E., Popa, M.E., Râpă, M., & Popa, O. (2015). PHB/Cellulose Fibers Based Materials: Physical, Mechanical and Barrier Properties. *Agriculture and Agricultural Science Procedi*a, 6, 608–615.

77. Ashby, R.D., Foglia, T.A., Solaiman, D.K.Y., Liu, C. K., Nuñez, A., & Egging, G. (2000). Viscoelastic properties of linseed oil-based medium chain length poly(hydroxyalkanoate) films: effects of epoxidation and curing. *International Journal of Biological Macromolecules*, 27(5), 355–361.

78. Cerrone, F., Davis, R., Kenny, S.T., Woods, T., O'Donovan, A., Gupta, V.K., Tuohy, M., Babu, R. P., O'Kiely, P., & O'Connor, K. (2015). Use of a mannitol rich ensiled grass press juice (EGPJ) as a sole carbon source for polyhydroxyalkanoates (PHAs) production through high cell density cultivation. *Bioresource Technology*, 191, 45–52.

79. Walsh, M.., O'Connor, K., Babu, R., Woods, T., & Kenny, S. (2015) Plant Oils and Products of Their Hydrolysis as Substrates for Polyhydroxyalkanoate Synthesis. *Chemical and Biochemical Engineering Quarterly*, 29(2), 123–133.

80. Dufresne, A., Kellerhals, M.B., & Witholt, B. (1999). Transcrystallization in Mcl-PHAs/Cellulose Whiskers Composites. *Macromolecules*, 32 (22) 7396–7401.

81. Sánchez, R.J., Schripsema, J., Da Silva, L.F., Taciro, M.K., Pradella, J.G.C., & Gomez J.G.C. (2003). Medium-chain-length polyhydroxyalkanoic acids (PHAmcl) produced by Pseudomonas putida IPT 046 from renewable sources. *European Polymer Journal*, 39(7), 1385–1394.

82. Noda, I., Lindsey, S.B., & Caraway, D. (2010). Nodax™ Class PHA Copolymers: Their Properties and Applications. Plastics from Bacteria (pp 237–255). Vol.14. Springer, Berlin, Heidelberg.

83. Barham, P.J., Keller, A., Otun, E.L., & Holmes, P.A. (1984). Crystallization and morphology of a bacterial thermoplastic: poly-3-hydroxybutyrate. Journal of Materials Science, 19(9), 2781–2794.

84. Sato, H., Nakamura, M., Padermshoke, A., Yamaguchi, H., Terauchi, H., Ekgasit, S.,Noda, I., & Ozaki, Y.(2004). Thermal Behavior and Molecular Interaction of Poly (3-hydroxybutyrate- co -3-hydroxyhexanoate) Studied by Wide-Angle X-ray Diffraction. Macromoleucles, 37 (10), 3763–3769.

85. Furukawa, T., Sato, H., Murakami, R., Zhang, J., Noda, I., Ochiai, S., & Ozaki, Y. (2007).

Comparison of miscibility and structure of poly(3-hydroxybutyrate-co-3-hydroxyhexanoate)/poly(l-lactic acid) blends with those of poly(3-hydroxybutyrate)/poly(l-lactic acid) blends studied by wide angle X-ray diffraction, differential scanning calorimetry, and FTIR microsocopy. *Polymer*, 48(6), 1749–1755.

86. Vijayendra, S.V.N., & Shamala, T.R. (2014). Film forming microbial biopolymers for commercial applications - A review. Critical Reviews in Biotechnology, 34(4), 338–357.
87. Yu, L,, Dean, K., & Li, L. (2006) Polymer blends and composites from renewable resources. Progress in Polymer Science, 31(6), 576–602.
88. Hazer, D.B., Kiliçay, E., & Hazer, B. (2012). Poly(3-hydroxyalkanoate)s: Diversification and biomedical applications: A state of the art review. *Materials Science and Engineering: C*, 32(4), 637–647.
89. Coelho, J.F.J., Góis, J.R., Fonseca, A.C., & Gil, M.H. (2010). Modification of Poly(3-hydroxybutyrate)-co-Poly (3-hydroxyvalerate) with Natural Rubber. *Journal of Applied Polymer Science*, 116(7), 718–726.
90. Gonzalez, A., Iriarte, M., Iriondo, P.J., & Iruin, J.J. (2002). Miscibility and carbon dioxide transport properties of blends of bacterial poly(3-hydroxybutyrate) and a poly(vinylidene chloride-co-acrylonitrile) copolymer. *Polymer*, 43(23), 6205–6211.
91. Li, Z., Yang, J., & Loh, X.J. (2016). Polyhydroxyalkanoates: Opening doors for a sustainable future. *NPG Asia Materials*, 8(4), e265.
92. Vieira, M.G.A., Da Silva, M.A., Dos Santos, L.O., & Beppu, M.M. (2011). Natural-based plasticizers and biopolymer films: A review. *European Polymer Journal*, 47(3), 254–263.
93. Nerkar, M., Ramsay, J.A., Ramsay, B.A., & Kontopoulou, M. (2014). Melt Compounded Blends of Short and Medium Chain-Length Poly-3-hydroxyalkanoates. *Journal of Polymers and the Environment*, 22(2), 236–243.
94. Zheng, Z., Bei, F., Tian, H., & Chen, G. (2005). Effects of crystallization of polyhydroxyalkanoate blend on surface physicochemical properties and interactions with rabbit articular cartilage chondrocytes. *Biomaterials*, 26(17), 3537–3548.
95. Martelli, S.M., Sabirova, J., Fakhoury, F.M., Dyzma, A., de Meyer, B., & Soetaert, W.. (2012). Obtention and characterization of poly(3-hydroxybutyricacid-co-hydroxyvaleric acid)/mcl-PHA based blends. *LWT - Food Science and Technology*, 47(2), 386–392.
96. Azari, P., Yahya, R., Wong, C.S., Gan, S.N. (2014). Improved processability of electrospun poly[(R)-3-hydroxybutyric acid] through blending with medium-chain length poly(3-hydroxyalkanoates) produced by Pseudomonas putida from oleic acid. *Materials Research Innovations*, 18(sup6),S6-345-S6-349.
97. Ha, C., & Cho, W. (2002). Miscibility , properties , and biodegradability of microbial polyester containing blends. *Progress in Polymer Science*, 27(4), 759–809.
98. Weng, Y.X., Wang, Y., Wang, X.L., & Wang, Y.Z. (2010). Biodegradation behavior of

PHBV films in a pilot-scale composting condition. Polymer Testing, 29(5), 579–587.

99. Shamala, T.R., Divyashree, M.S., Davis, R., Kumari, K.L., Vijayendra, S.V.N., & Raj, B. (2009). Production and characterization of bacterial polyhydroxyalkanoate copolymers and evaluation of their blends by fourier transform infrared spectroscopy and scanning electron microscopy. *Indian Journal of Microbiology*, 49(3), 251–258.
100. Abdelwahab, M.A., Flynn, A., Chiou, B. S., Imam, S., Orts, W., & Chiellini, E. (2012). Thermal, mechanical and morphological characterization of plasticized PLA-PHB blends. Polymer Degradation and Stability, 97(9), 1822–1888.
101. Botta, L., Mistretta, M.C., Palermo, S., Fragalà, M., & Pappalardo, F. (2015). Characterization and Processability of Blends of Polylactide Acid with a New Biodegradable Medium-Chain-Length Polyhydroxyalkanoate. *Journal of Polymers and the Environment*, 23(4), 478–486.
102. Takagi, Y., Yasuda, R., Yamaoka., M., & Yamane, T. (2004). Morphologies and Mechanical Properties of Polylactide Blends with Medium Chain Length Poly (3-Hydroxyalkanoate) and Chemically Modified Poly (3- Hydroxyalkanoate). Journal of applied polymer science, 93(5), 2363-2369.
103. Abreu, A.S., Oliveira, M., De Sá, A., Rodrigues, R.M., Cerqueira, M.A., Vicente, A.A., & Machado, A. V. (2015). Antimicrobial nanostructured starch based films for packaging. Carbohydrate Polymers, 129, 127–134.
104. Jung, Y.C., & Bhushan, B. (2006). Contact angle, adhesion and friction properties of micro-and nanopatterned polymers for superhydrophobicity. *Nanotechnology*, 17(19), 4970–4980.
105. Mauclaire, L., Brombacher, E., Bünger, J.D., & Zinn, M. (2010). Factors controlling bacterial attachment and biofilm formation on medium-chain-length polyhydroxyalkanoates (mcl-PHAs). *Colloids and Surfaces B: Biointerfaces*, 76(1), 104–111.
106. Bitinis, N., Verdejo, R., Maya, E.M., Espuche, E., Cassagnau, P., & Lopez-Manchado, M.A. (2012). Physicochemical properties of organoclay filled polylactic acid/natural rubber blend bionanocomposites. *Composites Science Technology*, 72(2), 305–313.
107. Busscher, H.J., Geertsema-Doornbusch, G.I., & Van der Mei, H.C. (1997). Adhesion to silicone rubber of yeasts and bacteria isolated from voice prostheses: Influence of salivary conditioning films. *Journal of Biomedical Materials Research: An Official Journal of The Society for Biomaterials and The Japanese Society for Biomaterials*, 34(2), 201–210.
108. Rathbone, S., Furrer, P., Lubben, J., Zinn, M., & Cartmell, S. (2010). Biocompatibility of polyhydroxyalkanoate as a potential material for ligament and tendon scaffold material. *Journal of Biomedical Materials Research Part A: An Offical Journal of the Society for Biomaterials, The Japanese Society for Biomaterials, and The Australian Society for*

Biomaterials and the Korean Society for Biomaterials, 93(4), 1391-1403.

109. Tan, I.K.P., Kumar K. S. K, Theanmalar, M., Gan, S.N., & Gordon B. (1997). Saponified palm kernel oil and its major free fatty acids as carbon substrates for the production of polyhydroxyalkanoates in *Pseudomonas putida* PGA1. *Applied Microbiology and Biotechnology*, 47(3), 207–211.
110. Naveen, S.V., Tan, I.K.P., Goh, Y.S., Raghavendran, H.R.B., Murali, M.R., & Kamarul, T. (2015). Unmodified medium chain length polyhydroxyalkanoate (uMCL-PHA) as a thin film for tissue engineering application - Characterization and in vitro biocompatibility. *Materials Letters*, 141, 55–58.
111. Zhang, D.M., Cui, F.Z., Luo, Z.S., Lin, Y.B., Zhao, K., & Chen, G.Q. (2000) Wettability improvement of bacterial polyhydroxyalkanoates via ion implantation. Surface and Coatings Technology, 131(1-3), 350–354.
112. Burton, Z., & Bhushan, B. (2005). Hydrophobicity, adhesion, and friction properties of nanopatterned polymers and scale dependence for micro- and nanoelectromechanical systems. *Nano Letters*, 5(8), 1607–1613.
113. Donelli, I., Taddei, P., Smet, P.F., Poelman, D., Nierstrasz, V.A., & Freddi, G. (2009). Enzymatic surface modification and functionalization of PET: A water contact angle, FTIR, and fluorescence spectroscopy study. Biotechnology and Bioengineering, 103(5), 845–856.
114. Chen, Z., Cheng, S., Li, Z., Xu, K., & Chen, G.Q. (2009). Synthesis, characterization and cell compatibility of novel poly(ester urethane)s based on poly(3-hydroxybutyrate-co-4-hydroxybutyrate) and poly(3-hydroxybutyrate-co-3-hydroxyhexanoate) prepared by melting polymerization. Journal of Biomaterials Science, Polymer Edition, 20(10), 1451–1471.
115. Cui, N.Y., & Brown, N.M. (2002). Modification of the surface properties of a polypropylene (PP) film using an air dielectric barrier discharge plasma. *Applied surface science*, 189(1-2), 31–38.
116. Sanchez-Garcia, M.D., Gimenez, E., & Lagaron, J.M. (2007). Novel PET nanocomposites of interest in food packaging applications and comparative barrier performance with biopolyester nanocomposites. *Journal of Plastic Film & Sheeting*, 23(2), 133–148.
117. Fabra, M.J., Lopez-Rubio, A., & Lagaron, J.M. (2014). Nanostructured interlayers of zein to improve the barrier properties of high barrier polyhydroxyalkanoates and other polyesters. *Journal of Food Engineering*, 127, 1–9.
118. Kovalcik, A., Machovsky, M., Kozakova, Z., & Koller, M. (2015). Designing packaging materials with viscoelastic and gas barrier properties by optimized processing of poly(3-hydroxybutyrate-co-3-hydroxyvalerate) with lignin. *Reactive and Functional Polymers*, 94, 25–34.

119. Gontard, N., Thibault, R., Cuq, B., & Guilbert, S. (1996). Influence of Relative Humidity and Film Composition on Oxigen and Carbon Dioxide Permeabilities of Edible Films. *Journal of Agricultural and Food Chemistry*, 44(4), 1064–1069.

120. Cabedo, L., Luis Feijoo, L., Pilar Villanueva, M., Lagarón, J.M., & Giménez, E. (2006, February). Optimization of Biodegradable Nanocomposites Based on aPLA / PCL Blends for Food Packaging Applications. In *Macromolecules Symposia* (Vol.233, No. 1, pp 191–197). Weinheim: WILEY-VCH Verlag.

121. Zhang, H., & Cloud, A. (2006, November). The permeability characteristics of silicone rubber. In P*roceedings of 2006 SAMPE Fall Technical Conference*, 72–75.

122. Fernández-Berridi, M.J., González, N., Mugica, A., & Bernicot, C. (2006). Pyrolysis-FTIR and TGA techniques as tools in the characterization of blends of natural rubber and SBR. *Thermochimica Acta*, 444(1), 65–70.

123. Boutroy, N., Pernel, Y., Rius, J.M., Auger, F., Von Bardeleben, H.J., Cantin, J.L., Abel, F., Zeinert, A., Casiraghi, C., Ferrari, A.C., & Robertson, J. (2006). Hydrogenated amorphous carbon film coating of PET bottles for gas diffusion barriers. *Diamond and Related Material*s, 15(4–8), 921–927.

124. Stephen, R., Thomas, S., & Joseph, K. (2005) Gas permeation studies of natural rubber and carboxylated styrene-butadiene rubber latex membranes. *Journal of Applied Polymer Science*, 98(3), 1125–1134.

125. Liu, W., & Chen, G.Q. (2007). Production and characterization of medium-chain-length polyhydroxyalkanoate with high 3-hydroxytetradecanoate monomer content by fadB and fadA knockout mutant of Pseudomonas putida KT2442. *Applied Microbiology and Biotechnology*, 76(5), 1153–1159.

126. Tripathi, L., Wu, L.P., Chen, J., & Chen, G.Q. (2012). Synthesis of Diblock copolymer poly-3-hydroxybutyrate -block-poly-3-hydroxyhexanoate [PHB-b-PHHx] by a β-oxidation weakened Pseudomonas putida KT2442. *Microbial Cell Factories*, 11(1), 44.

127. Koller, M., Atlic, A., Dias, M., Reiterer, A., & Braunegg, G.(2010). Microbial PHA Production from Waste Raw Materials. In *Plastic from bacteria* (pp. 85-119). Springer, Berlin, Heidelberg.

128. Kull, S., Martinelli, I., Briganti, E., Losi, P., Spiller, D., Tonlorenzi, S., & Soldani, G. (2009). Glubran2 Surgical Glue: In Vitro Evaluation of Adhesive and Mechanical Properties. *Journal of Surgical Research*, 157(1), e15–e21.

129. Chea, V., Angellier-Coussy, H., Peyron, S., Kemmer, D., & Gontard, N. (2016). Poly(3-hydroxybutyrate-co-3-hydroxyvalerate) films for food packaging: Physical-chemical and structural stability under food contact conditions. *Journal of Applied Polymer Science*, 133(2), 1–8.

130. Koller, M., Gasser, I., Schmid, F., & Berg, G. (2011). Linking ecology with economy:

Insights into polyhydroxyalkanoate-producing microorganisms. *Engineering in Life Sciences*, 11(3), 222–237.

131. Patricia Freitas (2017), Valorization of food processing wastes into the fucose-rich polysaccharide FucoPol. Masters in Biotechnology by FCT/UNL

Appendices

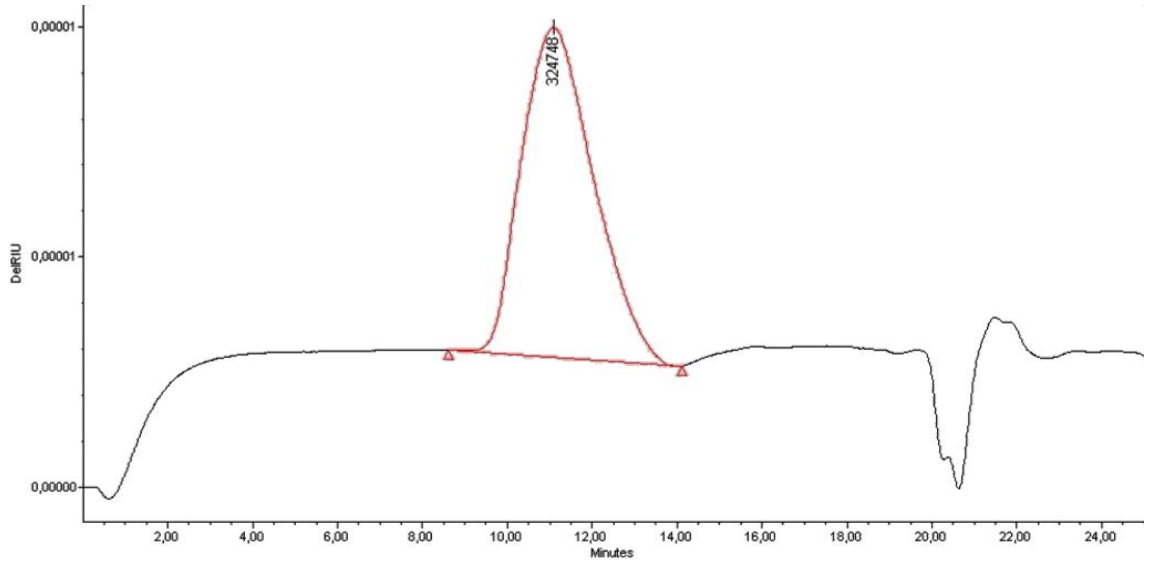

Figure A - Size exclusion chromatograms (SEC) of the mcl-PHA polymer produced by *P. citronellolis* NRRL B-2504 from apple pulp waste.

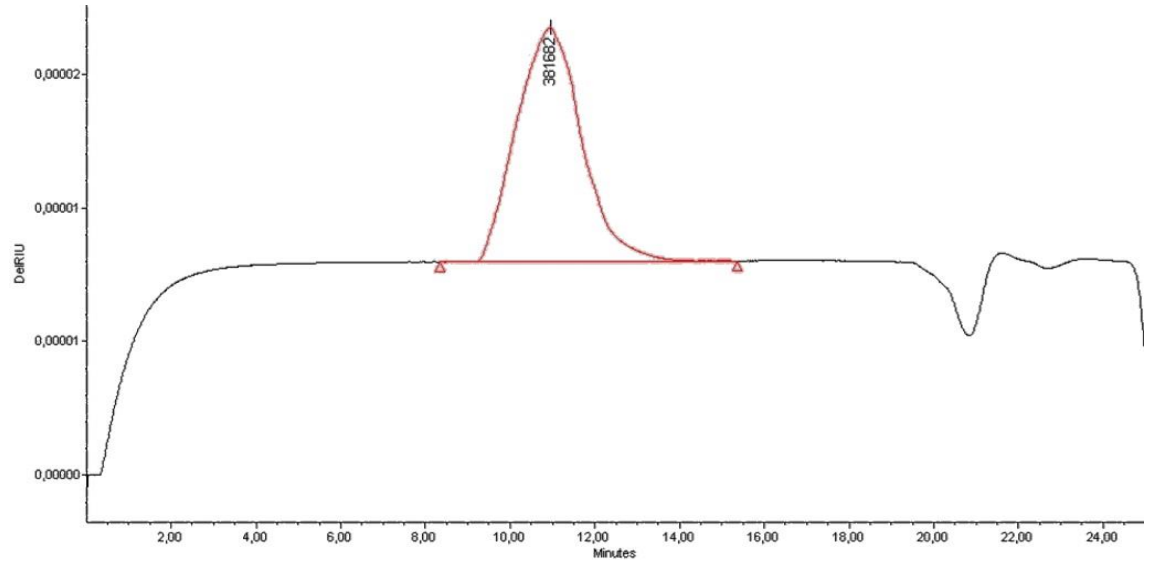

Figure B - Size exclusion chromatograms (SEC) of the PHB polymer produced by *C. necator* DSM 428 from apple pulp waste.

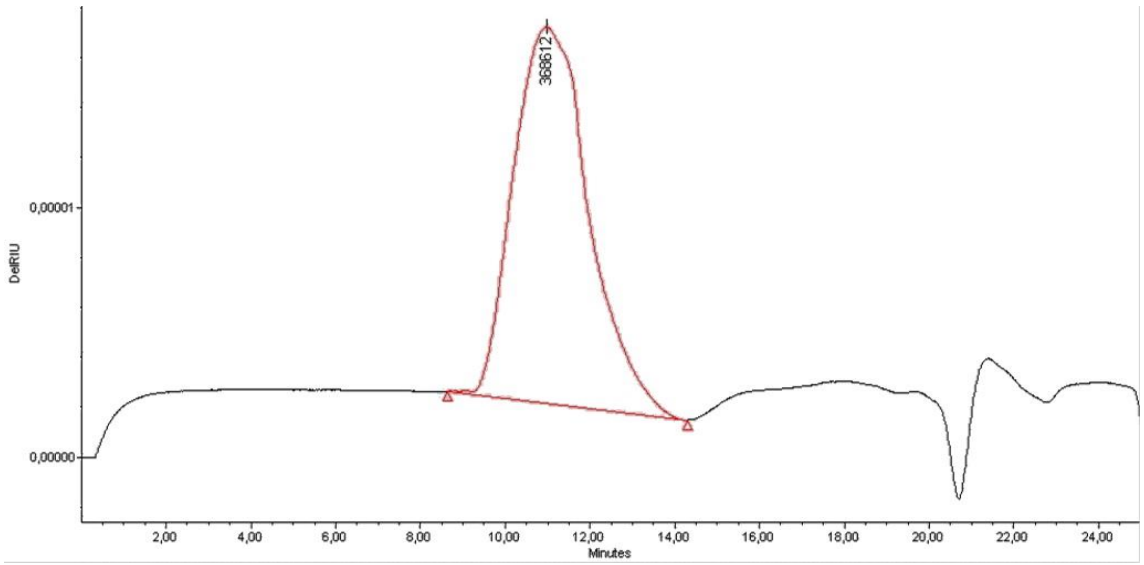

Figure C - Size exclusion chromatograms (SEC) of the PHB/mcl-PHA polymer produced by a mixed culture fermentation of *P. citronellolis* NRRL B-504 and *C. necator* DSM 428 from apple pulp waste.

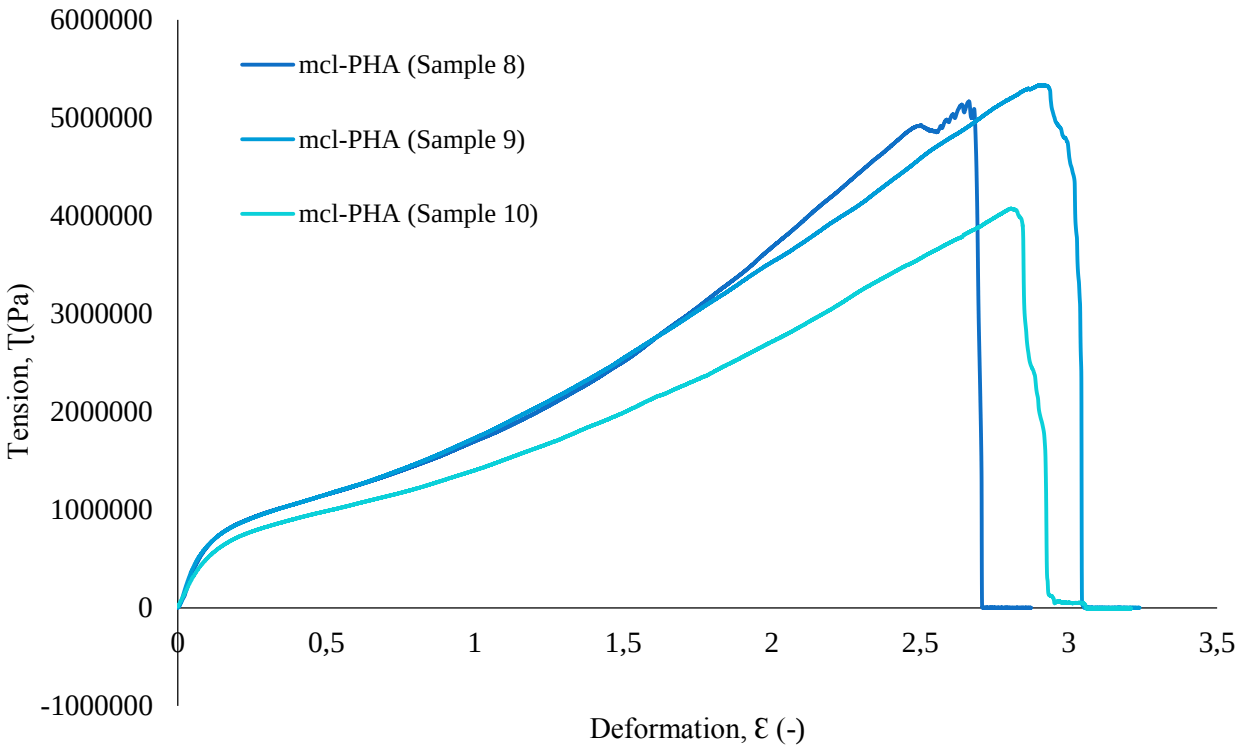

Figure D – Tensile- deformation curve for *P. citronellolis* mcl-PHA films.

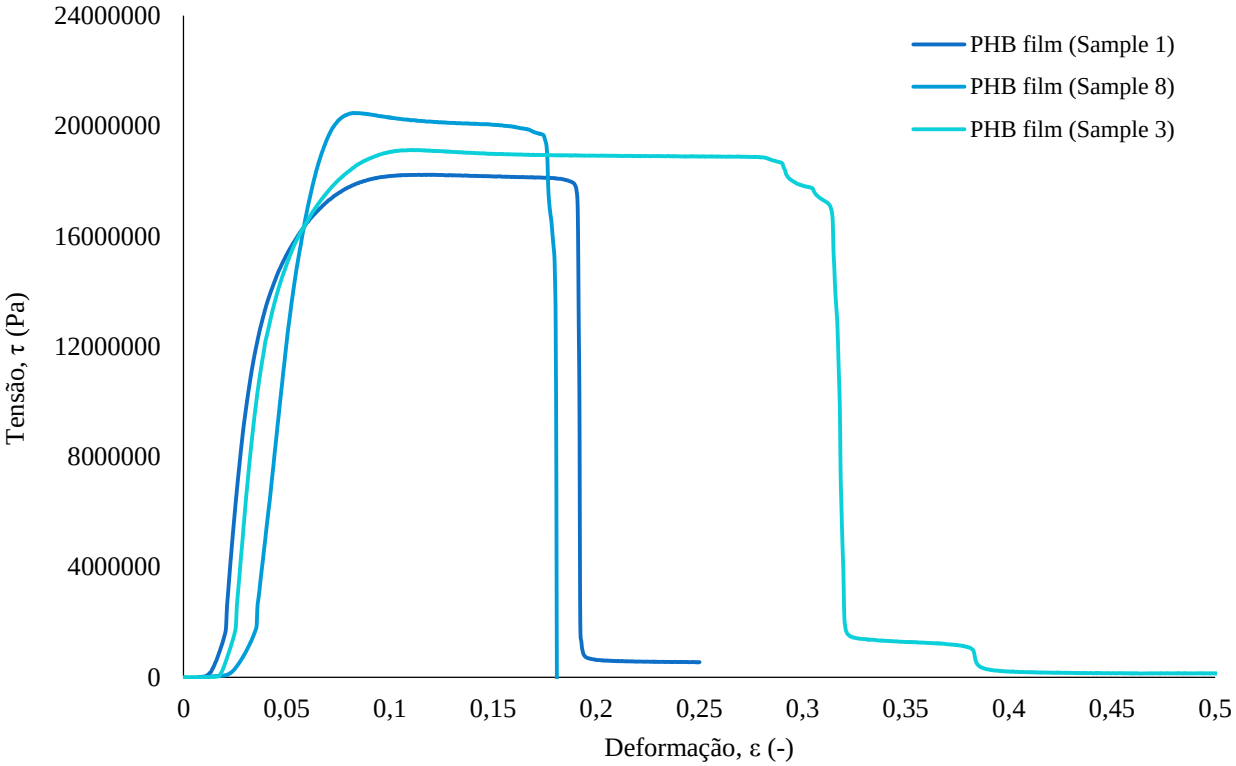

Figure E – Tensile- deformation curve for *C. necator* PHB films.

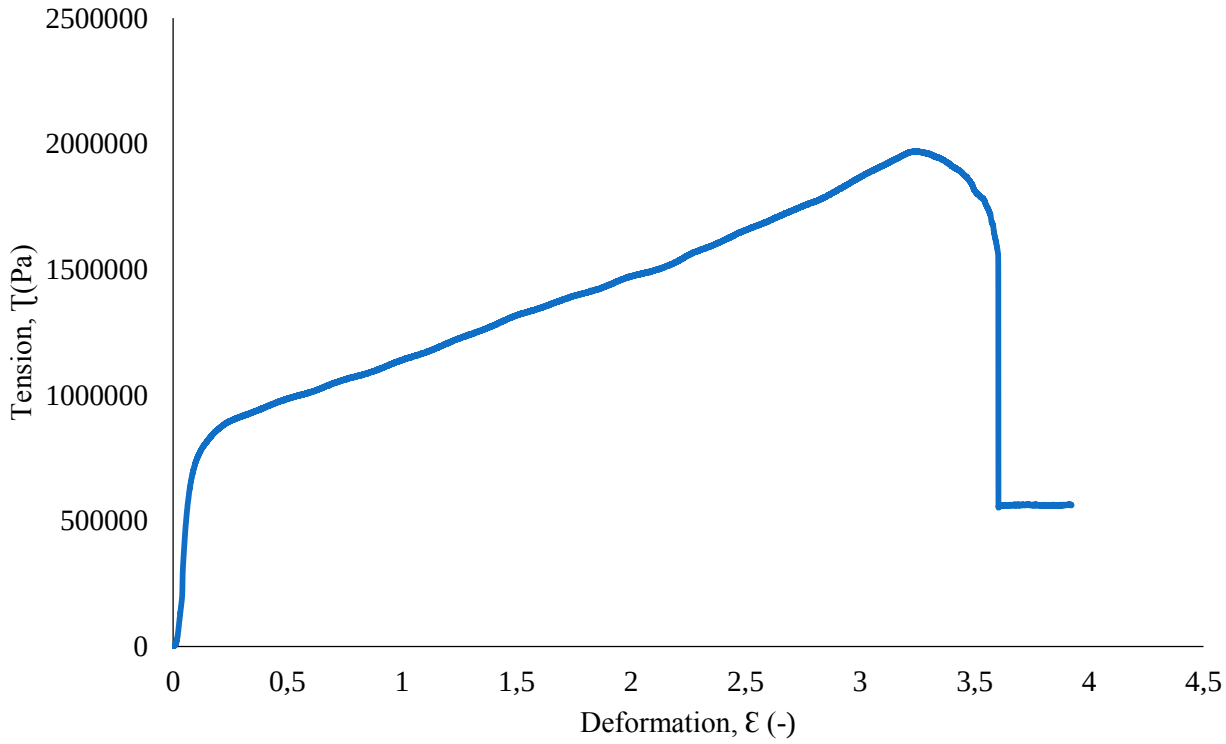

Figure F – Tensile- deformation curve for PHB/mcl-PHA blend films.

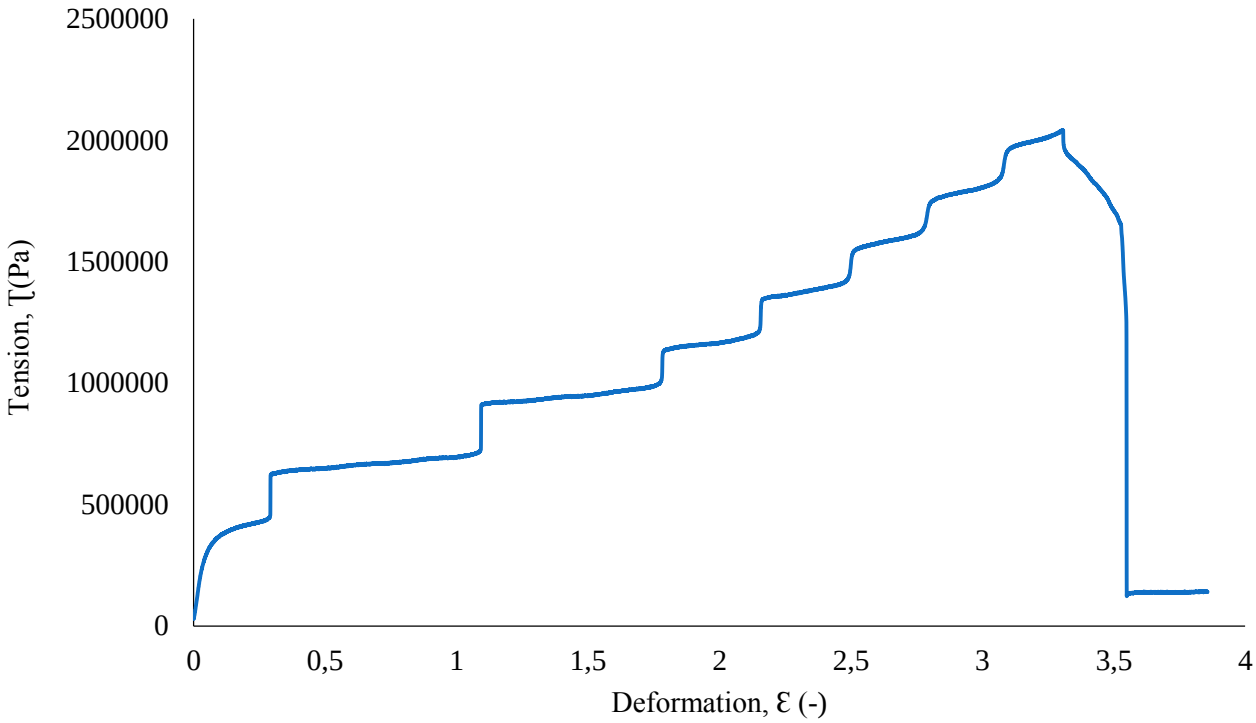

Figure G – Tensile-Deformation curve for PHB/mcl-PHA film that presented a significant segregation of the polymers presented in the blend.